

VALIDATION OF RAT MESENTERY CULTURE MODEL FOR
TIME-LAPSE DRUG EVALUATION AND CELL LINEAGE STUDIES

AN ABSTRACT

SUBMITTED ON THE TWENTIETH DAY OF JULY 2017
TO THE DEPARTMENT OF BIOMEDICAL ENGINEERING
IN PARTIAL FULFILLMENT OF THE REQUIREMENTS
OF THE SCHOOL OF SCIENCE AND ENGINEERING

OF TULANE UNIVERSITY

FOR THE DEGREE

OF

DOCTOR OF PHILOSOPHY

BY

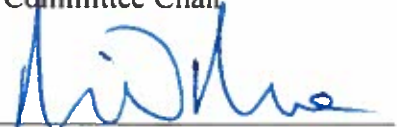


Mohammad Sadegh Azimi

APPROVED:



Walter Lee Murfee, Ph.D.
Committee Chair



Michael Moore, Ph.D.



Bruce Bunnell, Ph.D.

ABSTRACT

An emerging need in the microcirculation research is the development of biomimetic angiogenesis models that recapitulate the complexity of a real tissue. Angiogenesis, defined as the growth of new vessels from pre-existing vessels, involves multiple cell types, such as endothelial and perivascular cells, in a multi-system setting since blood vessel networks are usually accompanied by lymphatic and nervous systems. Therefore, a need exists for a model of angiogenesis from intact microvascular networks that more closely reflects an in vivo scenario for the investigation of underlying mechanisms and the pre-clinical development of therapies. While other approaches have proven useful in identifying mechanistic signaling information, they are often limited in their complexity and capability to mimic physiologically relevant scenarios in one way or another and do not fully recapitulate the in vivo scenario.

The first aim of this study was to demonstrate the ability for time-lapse comparisons of microvascular networks in angiogenesis scenarios to investigate the fate of vascular islands and investigate the endothelial cell plasticity. We developed a time-lapse angiogenesis model based on our previously introduced rat mesentery model. We demonstrated that time-lapse rat mesentery culture model is a powerful tool to study multi-cell, multi-system dynamics in microvascular networks.

For the second aim of this study, we used the method developed in aim one to establish rat mesentery culture model as a novel anti-angiogenic drug screening tool. Using time-lapse model enabled tissue-specific comparisons before and after drug treatment to investigate its effects on entire microvascular networks. Validation of this method for anti-angiogenic drug testing was demonstrated using known angiogenesis inhibitor. Next, we showcased a potential application of the model for evaluating unknown effects of drug repositioning based on FDA-approved drug combinations. The results demonstrated the ability to identify concentration-dependent effects in an intact network scenario.

The objective of the third aim was to showcase the capability of the rat mesentery culture model to study stem cell fate. We developed a protocol to deliver mesenchymal stem cells to mesentery tissues and culture for a period of time in a controlled environment. We confirmed the perivascular location of a subset of stem cells within capillaries, with morphologies resembling pericytes, and expressing pericyte markers. We also demonstrated that tracking stem cells within the microvascular networks is possible using the rat mesentery culture model. Furthermore, we reported a high variability in perivascular incorporation among cells from different donors.

This work establishes for the first time, to the best of our knowledge, an *ex vivo* model to look at microvascular networks before and after growth. We confirmed, for the first time, vascular island incorporation as a new mode of angiogenesis using a novel method for time-lapse imaging of microvascular networks *ex vivo*. The results also establish this method for drug testing and stem cell tracking in a microvascular setting.

VALIDATION OF RAT MESENTERY CULTURE MODEL FOR
TIME-LAPSE DRUG EVALUATION AND CELL LINEAGE STUDIES

A DISSERTATION

SUBMITTED ON THE TWENTIETH DAY OF JULY 2017
TO THE DEPARTMENT OF BIOMEDICAL ENGINEERING
IN PARTIAL FULFILLMENT OF THE REQUIREMENTS
OF THE SCHOOL OF SCIENCE AND ENGINEERING

OF TULANE UNIVERSITY

FOR THE DEGREE

OF

DOCTOR OF PHILOSOPHY

BY

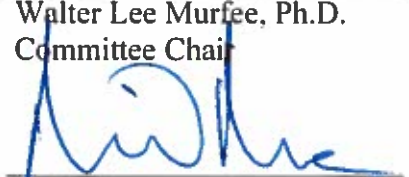


Mohammad Sadegh Azimi

APPROVED:



Walter Lee Murfee, Ph.D.
Committee Chair



Michael Moore, Ph.D.



Bruce Bunnell, Ph.D.

ACKNOWLEDGEMENTS

I would like to start by thanking Dr. Walter Lee Murfee for advising me throughout my years in the Microvascular Dynamics Laboratory, teaching me new things almost every day, and sharing his wisdom with me. I feel lucky to have such an excellent mentor and I am forever grateful to him. I would like to thank my committee, Dr. Michael Moore, and Dr. Bruce Bunnell, for advising me throughout my projects and providing me with constructive feedback. I would also like to thank my lab mates, especially Dr. Ming Yang, Dr. Peter Stapor, Dr. Richard Sweat, Molly Kelly-Goss, Scott Stewart, Chris Sloas, Jessica Motherwell, Nicholas Hodges, Ariana Suarez-Martinez, Jim Brault, Ryan Fishel, and Matt Nice, with whom I have spent my last six years, and made great friends. I learned a lot from them, and this work would not have been accomplished without their help and support. My hope is that I've been as good of a colleague to them as they have been to me. I would also like to offer my sincere gratitude to the faculty, staff, and students of the Department of Biomedical Engineering, including Dr. Donald Gaver, Dr. Ronald Anderson, Dr. Lars Gilbertson, Dr. Taby Ahsan, Dr. Michael Dancisak, Dr. Annette Oertling, Dr. Quincy Brown, Dr. Ming Li, Cindy Stewart, Lorrie McGinly, John Sullivan, Megan Ohar, Anne Nguyen, and Rebecca Derbes for accepting me with open arms, helping me in tough times, and supporting me every step of the way. I have also been very fortunate to have collaborated with some of the most amazing

people across different disciplines at Tulane University, including Dr. Debasis Mondal, Dr. Prasad Katakam, Dr. Matt Burow, Dr. Theresa Phamduy, Dr. Hope Burks, Dr. Amy Strong, Maria Dutreil, and Jayant Saksena. I would like to thank them for their guidance and contribution to my projects.

I'm also lucky to have been surrounded by great friends, back home, and here in New Orleans. Whenever I felt tired or down, they were always there to cheer me up and support me. My life has been touched by so many great friends, including Dr. Parastoo Khoshakhlagh, Dr. Mohammad Reza Gaeini, Dr. Armin Darvish, Khashayar Misaghian, Shannon Sparrow, Dr. Will Glindmeyer, Lina Quijano, Federico Segura, Devon Bowser, Mitchell Fullerton, Jason Ryans, Ashwin Sivakumar, Pete Lawson, and Ali Enami. I will cherish our friendship forever as *those friends thou hast, and their adoption tried, grapple them unto thy soul with hoops of steel.*

I'm beyond grateful to my family for the values they have instilled in me, and their constant vigilance and kindness since I was a little kid. I would not have been here today without their undying love and support. Lastly, I would like to dedicate this work to my parents, who have always pushed me to strive for excellence, and ingrained in me a sense of compassion, and a drive for problem solving. I'm always proud to bear their names and indebted to have them on my side.

TABLE OF CONTENTS

ACKNOWLEDGMENTS	II
TABLE OF CONTENTS	IV
LIST OF FIGURES	VII
CHAPTER 1: BACKGROUND	1
1.1. Introduction	1
1.2. Motivation: Microvascular Networks Form and Function	6
1.2.1. Blood Vessels, Lymphatic Vessels, and Nerves	6
1.2.2. Angiogenesis	9
1.2.3. Angiogenesis in Pathological Conditions	10
1.2.4. Endothelial Cell Dynamics during Angiogenesis	12
1.2.5. Endothelial Cell Plasticity	15
1.2.6. Importance of Pericytes During Angiogenesis	16
1.3. Stem Cell Therapy in Microvascular Networks	19
1.4. Current Angiogenesis Models	21
CHAPTER 2: AN <i>EX VIVO</i> TISSUE CULTURE MODEL CAPABLE OF TIME-LAPSE EVALUATION OF MICROVASCULAR NETWORK GROWTH.....	24
2.1. Introduction	24
2.2. Materials and Methods	26
2.2.1. Rat Mesentery Culture Model	26
2.2.2. Time-Lapse Imaging of Blood Vessels for Angiogenesis Study	28
2.2.3. Immunohistochemistry	29
2.2.4. Vascular Island Lineage Study	30
2.2.5. Time-Lapse Imaging of Blood and Lymphatic Vessels	31
2.2.6. Lymphatic Marker Coverage Studies	31
2.2.7. Image Acquisition	32
2.2.8. Statistical Analysis	32

2.3. Results	34
2.3.1. Time-Lapse Imaging Enables Tissue Specific Quantification of Microvascular Network Growth	34
2.3.2. Time-Lapse Imaging Enables Lineage Studies for Vascular Island Incorporation During Angiogenesis	38
2.3.3. Time-Lapse Imaging Enables Tracking of Blood and Lymphatic Vessel Remodeling	41
2.3.4. Lymphatic Endothelial Switch Phenotype Under Serum Stimulation	43
2.4. Discussion	47
2.5. Future Studies	51
CHAPTER 3: VALIDATING THE RAT MESENTERY CULTURE MODEL FOR ANTI-ANGIOGENIC DRUG TESTING	53
3.1. Introduction	53
3.2. Materials and Methods	56
3.2.1 Rat Mesentery Culture Model	56
3.2.2 Drug Testing Studies	56
3.2.3. Image Acquisition	58
3.2.4 Statistical Analysis	58
3.3. Results	59
3.3.1 Time-Lapse Imaging Enables Evaluation of Anti-Angiogenic Drugs	59
3.3.2 Time-Lapse Imaging Enables Kinetic Evaluation of Anti- angiogenic Drugs	64
3.4 Discussion	67
3.5 Future Studies	70
CHAPTER 4: INVESTIGATING STEM CELL FATE USING RAT MESENTERY CULTURE MODEL	72
4.1. Introduction	72
4.2. Materials and Methods	75
4.2.1. Rat Mesentery Culture Model	75
4.2.2. Stem Cell Isolation and Expansion	75
4.2.2.1. ASCs Preparation	75
4.2.2.2. BMSCs Preparation	76
4.2.2.3. Cell Culture	77
4.2.3. Stem Cell Seeding on Mesentery Tissues	77

4.2.4. Printing Stem Cells by Laser-Direct Write Method (LDW) .	79
4.2.5. Stem Cell Location Investigation	82
4.2.6. Immunohistochemistry	82
4.2.7. Quantification of Angiogenesis	83
4.2.8. Image Acquisition	84
4.2.9. Statistical Analysis	84
4.3. Results	85
4.3.1. Rat Mesentery Culture Model Enables Tracking of MSCs ...	85
4.3.2. MSCs Can Differentiate into Pericytes After 5 Days in Rat Mesentery Culture Model	88
4.3.3. Age or Type Is Not a Deciding Factor in MSCs Differentiation to Vascular Pericytes.....	92
4.3.4. Angiogenic Response to MSCs	95
4.4. Discussion	97
4.5. Future Studies	103
CHAPTER 5: CONCLUSIONS	105
LIST OF REFERENCES	107
BIOGRAPHY	120

LIST OF FIGURES

Chapter 1

Figure 1.1 Microvascular Network Schematic	12
Figure 1.2 Angiogenesis in physiological vs. pathological conditions.....	16
Figure 1.3 Angiogenesis and the role of pericytes.....	18
Figure 1.4 Pericyte roles in angiogenesis.....	22
Figure 1.5 Rat mesentery culture model	27

Chapter 2

Figure 2.1 Illustration of the rat mesentery culture model.....	31
Figure 2.2 Microvascular networks in the rat mesentery culture model before and after angiogenesis.....	39
Figure 2.3 Angiogenic response in rat mesentery tissues following stimulation.....	40
Figure 2.4 Presence of vascular pericytes, viable cells, and proliferative cells in angiogenic microvascular networks in the rat mesentery culture model.....	41
Figure 2.5 Tracking endothelial cell segments during angiogenesis.	43
Figure 2.6 Vascular island incorporation occurs during growth factor stimulation.....	44
Figure 2.7 Time-lapse imaging of blood and lymphatic vessel remodeling following stimulation by serum	46
Figure 2.8 Lymphatic endothelial cell mis-patterning by serum stimulation .	48
Figure 2.9 Loss in LYVE-1 coverage of lymphatic vessels after 5 days.....	49
Figure 2.10 Quantification of lymphatic-to-blood endothelial cell phenotype switch by serum stimulation	50

Chapter 3

Figure 3.1 Inhibition of angiogenic response in microvascular networks by sunitinib	64
Figure 3.2 Quantification of angiogenesis inhibition following sunitinib treatment	65

Figure 3.3 Inhibition of angiogenic response in microvascular networks by bevacizumab	66
Figure 3.4 Quantification of angiogenesis inhibition following bevacizumab treatment	67
Figure 3.5 Time-lapse imaging of rat mesentery culture for drug testing combination of Nelfinavir/curcumin.....	69
Figure 3.6 Quantification of angiogenesis for the drug testing study in untreated (Control), Low Dose and High Dose experimental groups	70
Figure 3.7 Example of a lymphatic/blood vessel connection at day 3 in a microvascular network stimulated by 100 ng/mL VEGF-C	61

Chapter 4

Figure 4.1 Schematic of stem cell seeding on mesentery tissue.	82
Figure 4.2 Schematic of stem cell printing on mesentery tissue using laser-direct write (LDW) method	85
Figure 4.3 Tracking seeded MSCs within mesentery tissue for 5 days	90
Figure 4.4 Tracking printed MSCs within mesentery tissue for 3 day	91
Figure 4.5 MSCs differentiation into vascular pericytes	93
Figure 4.6 NG2 expression of MSCs in vascular pericyte locations	94
Figure 4.7 Alpha-SMA expression of MSCs in vascular pericyte locations ..	95
Figure 4.8 Incorporation of stem cells from different donors into microvascular networks	97
Figure 4.9 Average percent incorporation of stem cells from experimental groups into microvascular networks	98
Figure 4.10 Angiogenic response to presence of stem cells	100
Figure 4.11 Regions of interest for MSCs in mesentery tissues	106

CHAPTER 1: BACKGROUND

1.1. INTRODUCTION

Microvascular network growth and remodeling are common denominators for tissue function, wound healing, and multiple pathologies. Inhibition of microvascular remodeling hinders the growth and will lead to cell death and tissue loss. On the other hand, excessive microvascular growth is usually associated with cancerous tumors. Whether for tissue engineering applications and stem cell therapy, or the design of therapies for cancer treatment, understanding how and where angiogenesis, defined as the growth of new blood vessels from pre-existing vessels, occurs within a network is critical.

Angiogenesis involves multiple cells types, including endothelial cells, pericytes, smooth muscle cells, nerves, and immune cells across multiple systems within the microvascular network. To advance our knowledge about the multi-cellular/multi-system interactions during angiogenesis, experimental models are needed that are capable of mimicking *in vivo* scenarios.

Current models of angiogenesis such as 2- and 3- dimensional cell cultures, tissue cultures, microfluidic models, and integrated computational approaches have been instrumental in identifying different inter-cellular signaling pathway, cell-cell interactions, mechanical and chemical driving forces, and remodeling patterns in

angiogenesis. Their ability to address complicated, inter-systemic interactions underlying angiogenesis mechanisms, however, has been limited by the lack of blood and lymphatic vessels in the same setting. Often, there are gaps in our knowledge about the interactions between blood vessels, lymphatic vessels, and nerves that cannot be investigated because the current experimental models lack the complexity to contain one or more of these systems. Moreover, the ability to study microvessels in real time could offer invaluable information about the underlying mechanisms by which angiogenesis is promoted and initiated, and answer some of the questions proposed about angiogenesis: What is the fate of disconnected endothelial cell segments present within microvascular networks? Can the effects of anti-angiogenic drugs be monitored closely in a real network scenario with high reproducibility for pre-clinical trials? Is it possible to select and track stem cell therapy candidates within a microvascular network in real time? Answering these questions is crucial to better understand the dynamics that guide vessel remodeling, and could give us insights into developing new platforms aimed at therapies involving microvascular networks. That served as the motivation for

Specific Aim 1: To develop an *ex vivo* model capable of time-lapse evaluation of microvascular network growth

As our first aim, we developed the rat mesentery culture model capable of time-lapse imaging, and validated the use of this model for studying angiogenesis and various cells and systems present in the tissue. Using immunolabeling, we showed that vascular cells, such as endothelial cells, and pericytes, remain functional and alive during tissue culture. Next, a robust angiogenic response was induced in the samples and was

quantified to showcase the ability to use the rat mesentery culture model for angiogenesis studies. Using our new model, we also showed that vascular islands can connect to their nearby vascular networks and play a role in angiogenesis, and identified vascular incorporation as a possible new mode of angiogenesis. Furthermore, we studied how lymphatic endothelial cells could change their identity under serum stimulation and switch their phenotypes to one of a blood endothelial cell.

(Published: Azimi et al., Methods in Molecular Biology, 2016, 1464:85-95)

Specific Aim 2: To validate the use of the rat mesentery culture model for evaluating anti-angiogenic drug effects on intact microvascular networks

For the second aim, we utilized the rat mesentery culture model for investigation of microvascular remodeling in response to anti-angiogenic drugs. The *proof-of-concept* studies were carried out by evaluating the angiogenic response to serum stimulation in control vs. established anti-angiogenic formulations. The vascular density and capillary sprouting was quantified and compared across different groups to confirm media supplementation with sunitinib (SU11248), a tyrosine kinase inhibitor targeting VEGFR-2, and bevacizumab, a known VEGF-A inhibitor, hindered the network angiogenic responses. After the drug testing application feasibility was confirmed, we showcased the use for evaluating unknown effects of potential repositioning based on FDA-approved drug combinations. Different combinations of nelfinavir, a drug that causes endothelial dysfunction, and curcumin, an antioxidant and NF- κ B inhibitory dietary supplement known to have anti-angiogenic effects, were tested to determine if the dose specific anti-tumor effect of the combination was associated with anti-angiogenesis.

(Published: Azimi, et al., PLOS ONE, 2015,10(3):e0119227)

Specific Aim 3: To demonstrate that the rat mesentery culture model can be used as a novel tool to evaluate stem cell fate within intact microvascular networks

The third aim of this study was to explore the possibility of using the rat mesentery culture model for stem cell fate investigation. We developed a protocol to deliver mesenchymal stem cells (MSCs) to mesentery tissues and culture for a period of time in a controlled environment. The protocol enabled the stem cells to adhere to the tissue and migrate to regions of interest. We confirmed the perivascular location of a subset of stem cells within capillaries, with morphologies resembling pericytes, and expressing pericyte markers. We also demonstrated that tracking stem cells within the microvascular networks is possible using the rat mesentery culture model. Furthermore, we reported a high variability in perivascular incorporation among cells from different donors. Cells derived from different tissues, adipose and bone marrow, were used to investigate the effects of cell source on stem cell differentiation. We also used stem cells from different age groups to study the effects of aging on differentiation. Although significantly different across individual donors, we did not report a significant difference in pericyte differentiation between the groups.

This body of work introduces a novel angiogenesis model capable of time-lapse imaging of microvascular networks and establishes the model as a platform for anti-angiogenic drug testing and stem cell therapy. It also offers a powerful tool to further advance studies into microvascular dynamics, such as angiogenesis, endothelial cell

phenotype plasticity, and the relationship between multiple cells and systems across a vascular network.

In this document, we will elaborate on some of the motivations driving our work. In this chapter, we will discuss the fundamentals of microvascular networks, angiogenesis, and the current models of angiogenesis. In the second chapter, we will introduce our model, and share some of the basic discoveries we have made by taking advantage of this model. Expanding upon our discoveries, in the third chapter, the drug testing capabilities of our model will be presented, and in chapter four, we will show that our model is a powerful platform for tracking stem cell fate within a microvascular network.

1.2. MOTIVATION: MICROVASCULAR NETWORKS FORM AND FUNCTION

1.2.1. Blood Vessels, Lymphatic Vessels, and Nerves

The circulatory system is one of the most remarkable systems in the body. With the responsibility of carrying food, oxygen, leukocytes, hormones, growth factors, and other soluble factors such as drugs to virtually every single cell on the blood side, and collecting nutrition waste, leukocytes, and interstitial fluid on the lymphatic side, it stretches throughout the body for 60 thousand miles, and carries 1800 gallons of blood each day. On the lymphatic side, the network is a one-way system that drains lymph, formed from the by-products of tissue metabolism as well as remnants of the defense capillaries grow larger to become collecting lymphatics, and continue to carry the lymph through lymph nodes and lymphatic ducts before emptying it into the venous circulation. On the blood side, however, the vascular system is a closed-loop system of an ever-branching tree-like network, starting with larger arteries leaving the heart, followed by smaller arterioles and subsequently capillary beds. After spreading inside the tissues, these capillary beds come back to form draining venules and eventually become larger veins returning deoxygenated blood to the heart. The third system interacting with blood vessels is the nervous system. These nerves run alongside blood vessels and oversee carrying neural signals to blood vessels. It has been shown that nerves follow the alignment of microvessels, and their growth is dependent on chemical factors that promote angiogenesis as well [1-3]. The collection of small arterioles, capillaries, and small venules, put together with lymphatic vessels and nerves create the microvascular network. As a result, the microvascular remodeling is dependent on the interactions and the dynamics present between multiple cell types and systems (Fig 1.1). This compels us

to study angiogenesis in the context of endothelial cell dynamics, the endothelial cell plasticity, and the role of pericytes and their relation to stem cells, to have a better understanding of how microvascular growth happens.

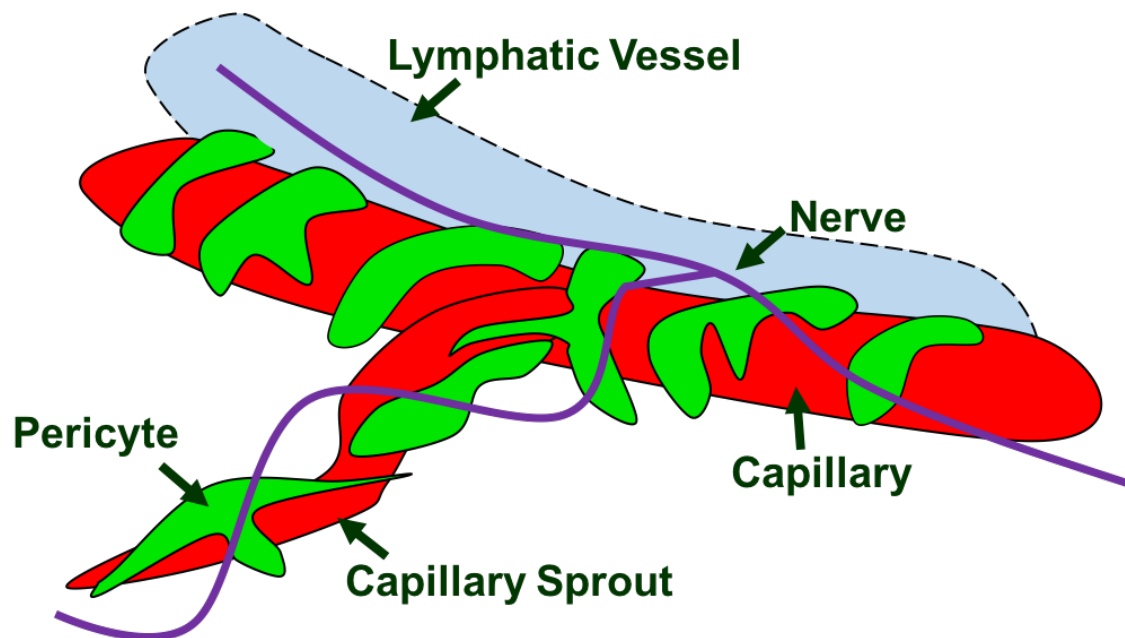


Figure 1.1 Microvascular Network Schematic. Blood capillary vessels are covered with vascular pericytes, which stabilize the vessels. The lymphatic vessels run throughout most tissues and are in charge of trafficking waste and cells from the interstitial space. Nerves run alongside vessels and carry neuronal signals. The interaction between different cells and systems determines microvascular remodeling scenarios in a network.

1.2.2. Angiogenesis

Since the microvascular network is where the exchange between blood and tissue happens, it has been a major point of focus in medicine. Understanding how the microvascular structure is formed and remodeled, and how different cell types interact with each other in the microvascular setting can help to identify the dynamics involved in microvascular growth, and that knowledge can be applied to create better therapeutic treatments. Formation of blood vessels is one of the most crucial steps in organogenesis during development. Endothelial progenitor cells create an endothelial cell plexus, by a process called vasculogenesis, that acts as a primitive vascular network, which in turn branches out and grows, becomes more organized, and creates a mature vascular network. This process of building new blood vessels and expanding vascular networks is known as angiogenesis. The maturation of blood vessels is accompanied by pericyte and smooth muscle cell recruitment to vessels. New blood vessel formation, however, is not limited to the developmental stage. After birth, as the human body goes through the growth periods, the demand for oxygen and nutrients increases. Physical growth in tissues and organs calls for angiogenesis to create enough blood vessels capable of carrying fresh blood throughout the body. Angiogenesis also plays an important role when it comes to wound healing and tissue repair [4,5]. During the proliferative phase, recently recruited macrophages, endothelial cells, and fibroblasts speed up the invasion of blood vessels by secreting pro-angiogenic cytokines, and contribute to angiogenesis as building blocks. These newly formed vessels then become mature and are necessary for supplying the new tissue with oxygenated blood [6,7].

1.2.3. Angiogenesis in Pathological Conditions

As it was described in the previous section, angiogenesis plays a vital role in tissue growth repair. The process usually starts with a VEGF gradient induced by hypoxia that is followed by endothelial cell proliferation and migration, forming capillaries, and recruiting pericytes that eventually stabilize the vessels. However, in pathological conditions such as cancer, this process is manipulated to sustain cancerous cells and speed up the growth of the tumor.

The onset of pathological angiogenesis is initiated by tumor growth. As tumor cells proliferate and increase in number, the demand for oxygen and nutrients grows, to the point that the existing capillaries are unable to provide enough oxygen. This leads to a hypoxic environment, which in turn triggers the secretion of proangiogenic growth factor VEGF [8,9]. This process is exacerbated by signaling and recruitment of other cells such as Tumor-Associated Fibroblasts (TAF), monocytes, macrophages, and mast cells and leads to what is called the resolution failure [10,11] (Fig. 1.2). Moreover, the abnormal growth caused by rapid proliferation in tumors keeps the demand for new blood vessels high. This also leads to a lack in pericyte coverage and leaky vessels [12,13] in tumors. On top of that, it has been shown that in some types of cancer such as melanoma, the cancer cells have the capability to undergo a process called, genetic reversion and directly contribute to the construction of new blood vessel, termed vasculogenic mimicry [14]. Without an external intervention, these factors combined create an environment in which angiogenesis never stops. Considering that, new proposed methods of anti-angiogenic

therapies aimed at stopping microvascular growth in tumor cells will have great implications in treating cancer.

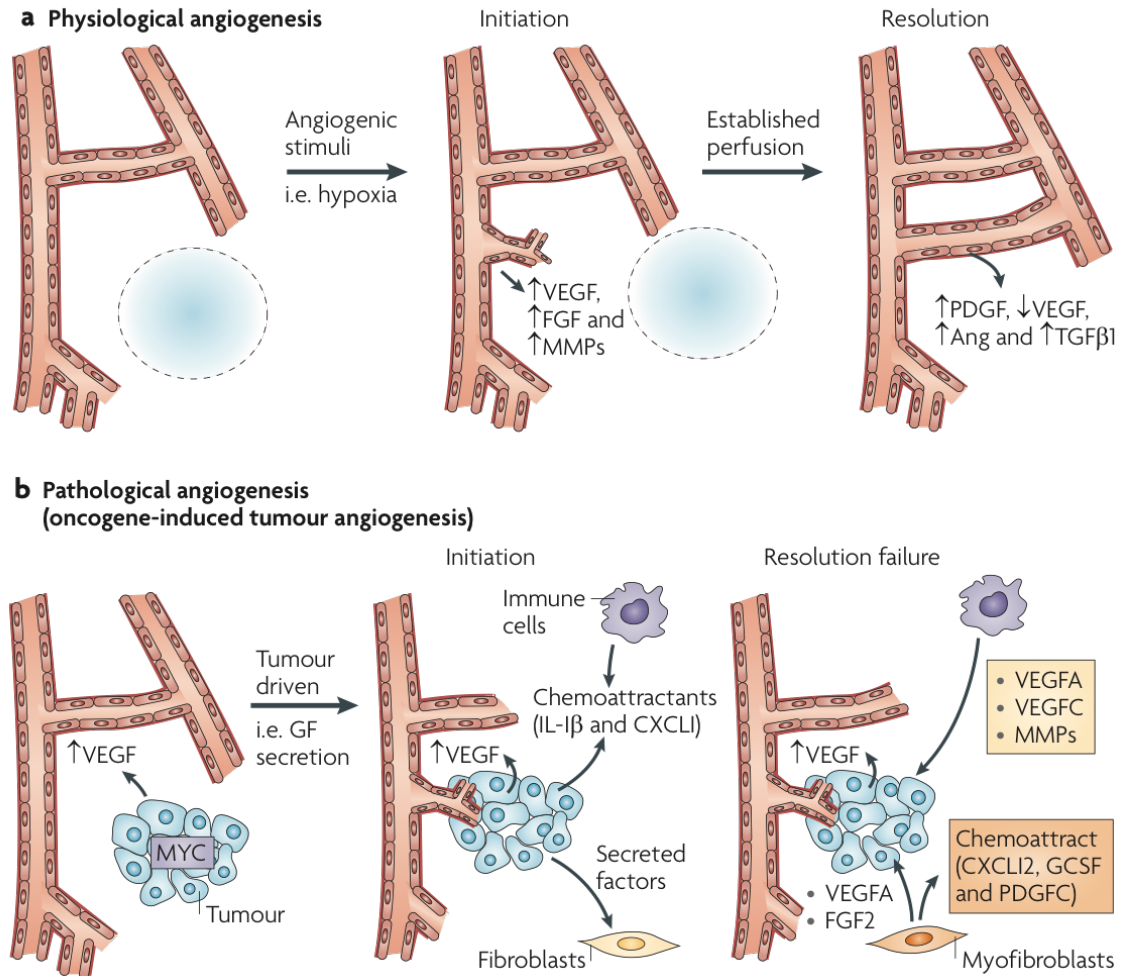


Figure 1.2 Angiogenesis in physiological vs. pathological conditions. The biggest difference between the two scenarios is the resolution happening in physiological angiogenesis. After cytokine signaling, endothelial cells become mobilized, create capillary sprouts and eventually connect to another segment, mature and get perivascular coverage. In pathological scenarios, such as cancer, the maturation does not happen. Adopted from [10].

1.2.4. Endothelial Cell Dynamics during Angiogenesis

So far, there are two major angiogenesis mechanisms that have been identified, namely intussusception and sprouting (Fig. 1.3). Intussusception happens by proliferation of endothelial cells in a vessel, leading to the creation of a wide lumen. The subsequent growth of the lumen results in partitioning of the vessel and an increase in the vascular network coverage [5]. Sprouting, the second mode of angiogenesis, starts by basement membrane degradation of the vessel and continues by migration of endothelial cells away from the lumen guided by either tip cells or sometimes pericytes towards a VEGF gradient [15]. The endothelial cell proliferation in these newly formed sprouts eventually stops behind the migration zone, sprouts adhere to each other, and form a new mature vessel with the help of chemical and cellular cues from pericytes and the surrounding environment [12]. However, previous work by our lab has identified a potential third mode for angiogenesis. There is evidence of endothelial cell segments in the vicinity of microvascular networks that are disconnected from the nearby vessels [16]. It has been shown that these disconnected segments, or vascular islands, are connected to the nearby networks by a trail of collagen IV, usually found in blood vessel basement membrane [17]. More studies are needed to analyze these vascular islands and investigate their relationship with the nearby microvascular networks.

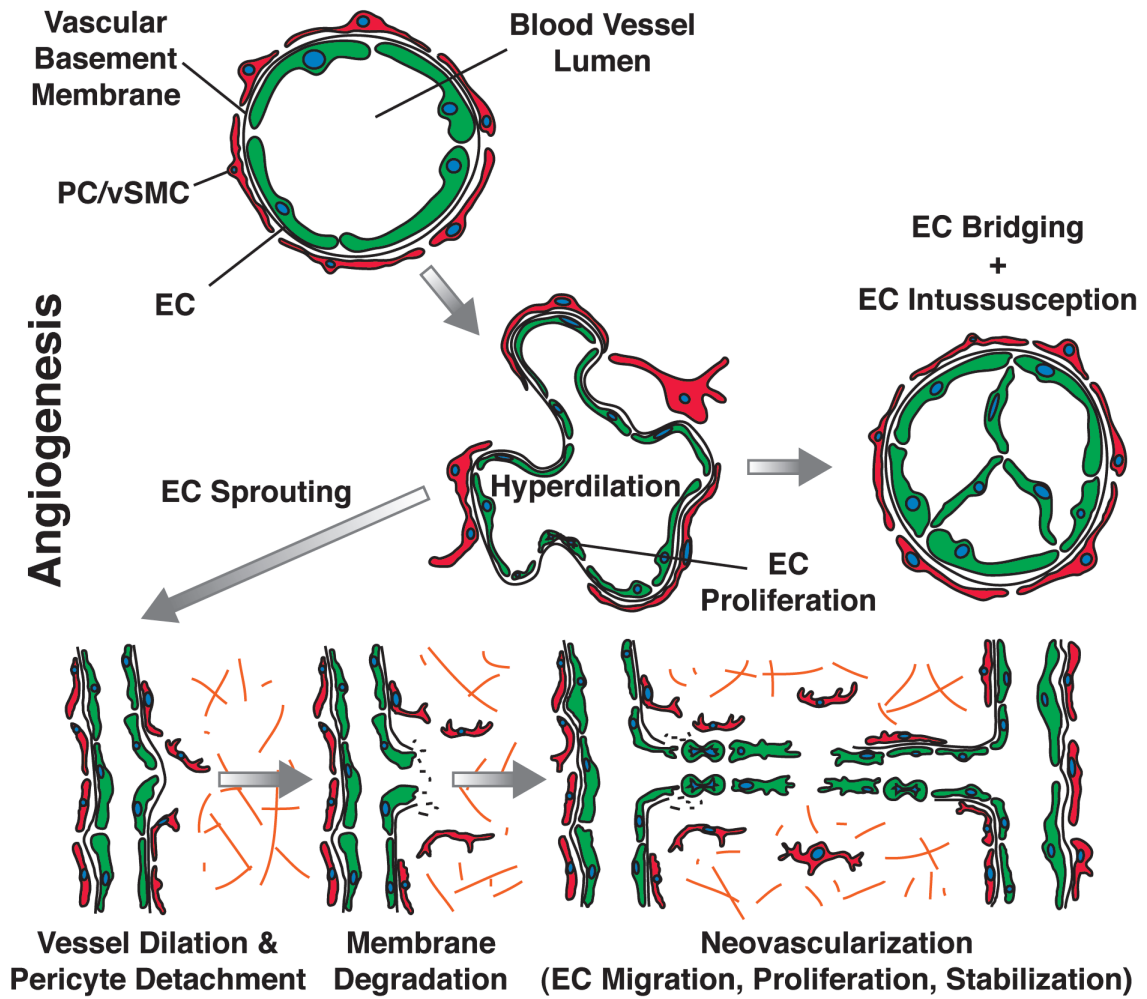


Figure 1.3 Angiogenesis and the role of pericytes. During angiogenesis, the vascular basement membrane is degraded to facilitate the migration of endothelial cells into the extracellular matrix towards angiogenic signals. Endothelial cells can be either guided by tip cells or by pericytes. After creating a newly formed vessel, endothelial cells meet each other and mature with the help of pericyte signaling [12].

1.2.5. Endothelial Cell Plasticity

During embryogenesis, progenitor endothelial cells create the primary capillary plexus that eventually turns into the blood vessel network. A subset of the endothelial cells transdifferentiates from the cardinal vein into lymphatic endothelial cells and create the lymphatic vessels. Since the origin of both cell types is the same, it's not unusual for blood and lymphatic endothelial cells to display similar flat morphologies, and express common markers. However, some of their functions are different from each other. Lymphatic endothelial cells, in comparison to blood endothelial cell characteristics mentioned in the previous section, are not covered by perivascular cells and have incomplete basement membranes. At the initial lymphatic vessel level, endothelial cells are connected to the extracellular matrix with strands of fibrin anchoring filaments to help the drainage process [18,19]. Lymphatic endothelial cells also often display overlapping junctions which is absent in blood endothelial cells [20]. Although there is a great deal of similarity in their respective genetic profiles, there is a meaningful difference in the level of expression and the number of genes between blood and lymphatic endothelial cells. A report by Podgrabinska et al. showed that out of 5,789 genes present in either blood or lymphatic endothelial cells, 9% were present only in blood endothelial cells and 14% were present only in lymphatic endothelial cells, whereas 67% were mutually expressed at comparable levels. The report also showed that the remaining 10% of the genes were expressed by the two cell types at different levels [21]. Studies like this highlight the importance of investigating endothelial cell dynamics, such as the possibility of phenotypic change under different circumstances. Deciphering

the relationship between blood and lymphatic endothelial cells can be achieved using more physiologically relevant models of angiogenesis.

1.2.6. Importance of Pericytes During Angiogenesis

First identified more than 100 years ago by French scientist Charles Rouget [22], pericytes, also known as Rouget cells or mural cells, are perivascular cells that wrap around endothelial cells in blood capillaries and are present in virtually every vascularized tissue in the body. Although occasionally seen in larger vessels, pericytes are most commonly associated with microvascular networks, and their functions include vascular maturation [23,24], endothelial cell proliferation and survival [12], vessel stabilization and permeability [25], capillary diameter control, and constriction through paracrine and direct cell contact signaling [26,27]. The relationship between endothelial cells and pericytes is however interdependent since endothelial cells also play a major role in pericyte recruitment and differentiation through PDGF-B/PDGFR- β signaling as well. Pericytes are considered major regulators of angiogenesis (Fig. 1.4) since they can both promote angiogenesis by secreting VEGF and signal endothelial sprouting and growth, and stop angiogenesis by stabilizing endothelial cells through Ang1/Tie2 signaling [12,28,29]. This role is more apparent when faced with pathological conditions such as diabetic retinopathy and cancer. For instance, in diabetic patients, unmanaged glucose levels are higher than normal and recent findings have shown that pericytes particularly have a high sensitivity towards elevated glucose levels, which have been linked to pericyte malfunction and apoptosis [30]. Therefore, pericyte loosening is identified as a major cause of abnormal vascular growth in retinas of diabetic patients. To

this end, there has been an effort to identify therapies aimed at resupplying pericytes to microvascular networks present in the retina [31-33]. In cancer, high microvascular density regions are often found in tumors since tumor cells show aggressive behaviors and proliferate at a faster rate than healthy cells, which is suggested to be partially caused by pericyte loosening. Therefore, altering pericyte recruitment to the endothelium can cause microvascular dysfunction, change vascular patterning, and hinder the formation of new sprouts and subsequently microvascular growth during pathological angiogenesis [34-36]. In both cases, the loosening of pericytes from endothelial cells results in excessive angiogenesis in microvascular networks present in the tissue, which leads to pathological conditions. Therefore, understanding the mechanisms of these pathologies, as well as proposing novel therapies aimed at restoring pericytes to the microvasculature are crucial. One of the proposed solutions to restore pericyte coverage to networks has been stem cell therapy [32,33,37]. So far, however, there have been a small number of candidates used for these experiments. Moreover, it is still relatively unclear how to manipulate the stem cells for them to differentiate to pericytes more efficiently.

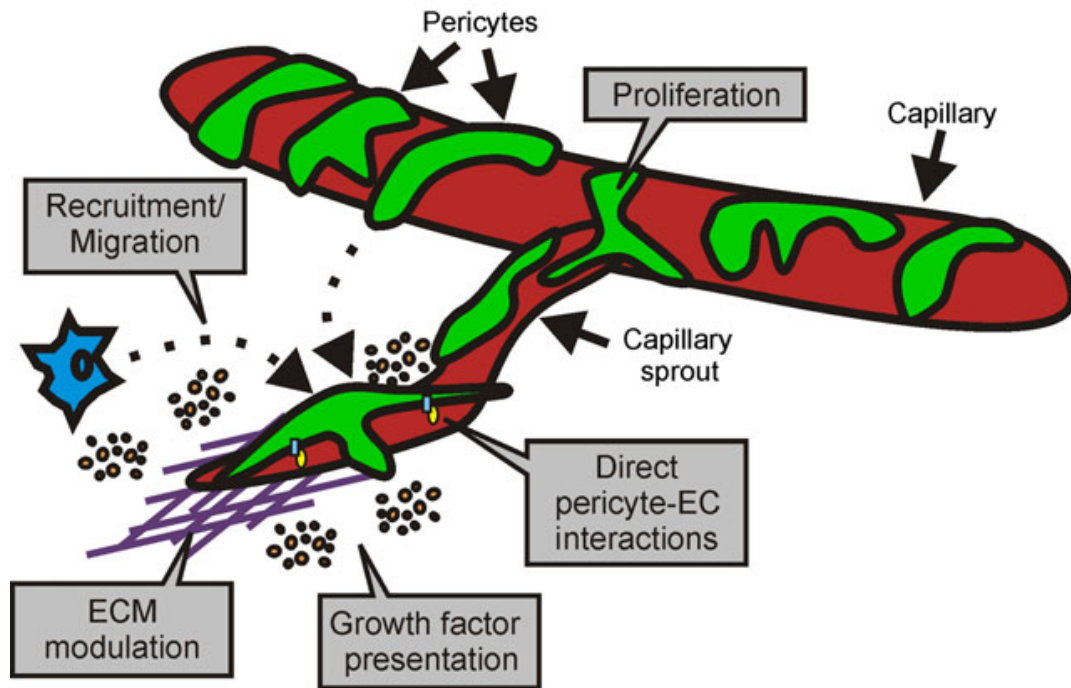


Figure 1.4 Pericyte roles in angiogenesis. Pericytes promote angiogenesis through paracrine and direct cell contact signaling. They also play a role in guiding endothelial cells to form capillary sprouts. Adopted from [28].

1.3. STEM CELL THERAPY IN MICROVASCULAR NETWORKS

Stem cell therapy has emerged as a promising method to combat a wide range of diseases in recent years, such as myocardial ischemia [38], cancer [39], peripheral artery disease [40], and Parkinson's [41]. In most of these applications, stem cells are introduced to the abnormal tissue to replace the dead cells, or to maintain and support the tissue. The use of stem cells to promote angiogenesis offers a promising approach towards future therapies for multiple pathological conditions, such as diabetic retinopathy. Diabetic retinopathy is the most common complication in patients who suffer from diabetes. It usually starts with macular edema, followed by pericyte loss, endothelial dysfunction, and consequently loss of microvascular networks in the retina [42]. Romeo et al. showed that high levels of glucose in diabetes lead to the activation of NF- κ B in pericytes, but not the endothelial cells, which in turn triggers a pro-apoptotic response in pericytes [30]. This means the loss of pericyte coverage, or pericyte dropout, can be the onset of pathologic angiogenesis in diabetic retinopathy. Considering that, one could propose the use of stem cell therapy as a potential treatment to replace the apoptotic cells. Taking advantage of the signals present in a microvascular setting, the introduction of suitable stem cells to the retina could lead to differentiation of stem cells into pericytes which could incorporate into the microvascular network and restore the normal network structure. While MSCs derived from bone marrow [43] and adipose tissue [33] have been shown to enhance angiogenesis via paracrine signaling and direct cell incorporation, our understanding of how to manipulate them or target where they go within a tissue still remains relatively unclear. Previous studies have shown the incorporation of Adipose-derived Stem Cells (ASCs) into the retinal microvascular network as new pericytes [33],

but choosing the best candidate requires screening different cell types, preferably in the presence of a microvascular network. New models can help answer these questions and add to our knowledge about the cell fate and its function within intact microvascular networks.

1.4. CURRENT ANGIOGENESIS MODELS

As it's often the case with biological models, angiogenesis models can be divided into *in vitro* and *in vivo* assays, each presenting advantages and disadvantages when applied. *In vivo* models represent angiogenesis in normal and pathological scenarios within real vascular networks, but they are often more complicated, and the analysis of specific mechanisms is difficult or sometimes impossible. While animal based models, for that matter, cannot substitute for human clinical trials for understanding the mechanisms present during physiological events, they have proved to play a crucial role in pre-clinical testing. Indeed, *in vivo* animal studies are identified as a crucial step between *in vitro* studies and clinical trials [44,45], since they offer a less expensive method for screening responses. On the other hand, *in vitro* models are easier to control and more accessible to use, but they do not match the level of complexity present in *in vivo* models. However, as *in vitro* and *ex vivo* models try to mimic the complexity of *in vivo* scenarios more closely, they too have become a useful pre-clinical alternative. Cell culture models can be divided into two- and three-dimensional culture systems [46,47]. Culturing endothelial cells within ECM-mimicking materials such as Matrigel or Puramatrix resulted in developing tubular structures resembling capillary networks. The majority of these models, however, use endothelial cells or endothelial progenitor cells as the cell source and ignore perivascular cells. Recently, there have been attempts to culture endothelial cells with MSCs as precursors for pericytes [48], but it is still unclear how effective these methods are in creating functional pericytes. Furthermore, other systems involved in microvascular dynamics, such as lymphatic and neural systems are absent from these models. *Ex vivo* tissue explants have proven extremely useful for

studying angiogenesis. Nicosia et al. first introduced the aortic ring model as an assay to investigate angiogenic sprouting from aortic segments embedded in a collagen gel [49]. While sprouting in the aortic ring involves multiple cell types, a limitation is that the sprouting occurs from macrovessels, atypical of the *in vivo* process. Also, while these sprouts are associated with perivascular wrapping cells, the vessels do not typically form networks with a hierarchical structure. More recently, the retina culture model has been introduced in which angiogenesis does occur from intact microvascular networks [50,51]. In these models, culturing tissues harvested from GFP-transgenic mice strains offers the ability for observing endothelial sprouting over time, yet it's a technically difficult and expensive model. Moreover, the microvascular network in retina lacks the lymphatic system, contrary to most of the tissues found in the body. The value of more realistic 3-dimensional microfluidic environments that integrate tumor spheroids and endothelial monolayers have been highlighted by others. Compared to less complicated 2-dimensional assays, the more realistic environment influences the effective dose required for inhibiting cancer cell dispersion [52]. Yet in microfluidic models single channels are typically lined with only endothelial cells and the pattern of an intact network is lost. Compared to already commonly used tissue culture models and *in vitro* cell systems, the rat mesentery culture model is unique because blood and lymphatic vessel growth occur within an intact microvascular network. This offers an excellent opportunity to investigate the endothelial cell dynamics across blood and lymphatic vessels (Fig. 1.5). Moreover, the presence of vascular pericytes enables us to examine the relationship between pericyte and endothelial cells in the context of an intact microvascular network.

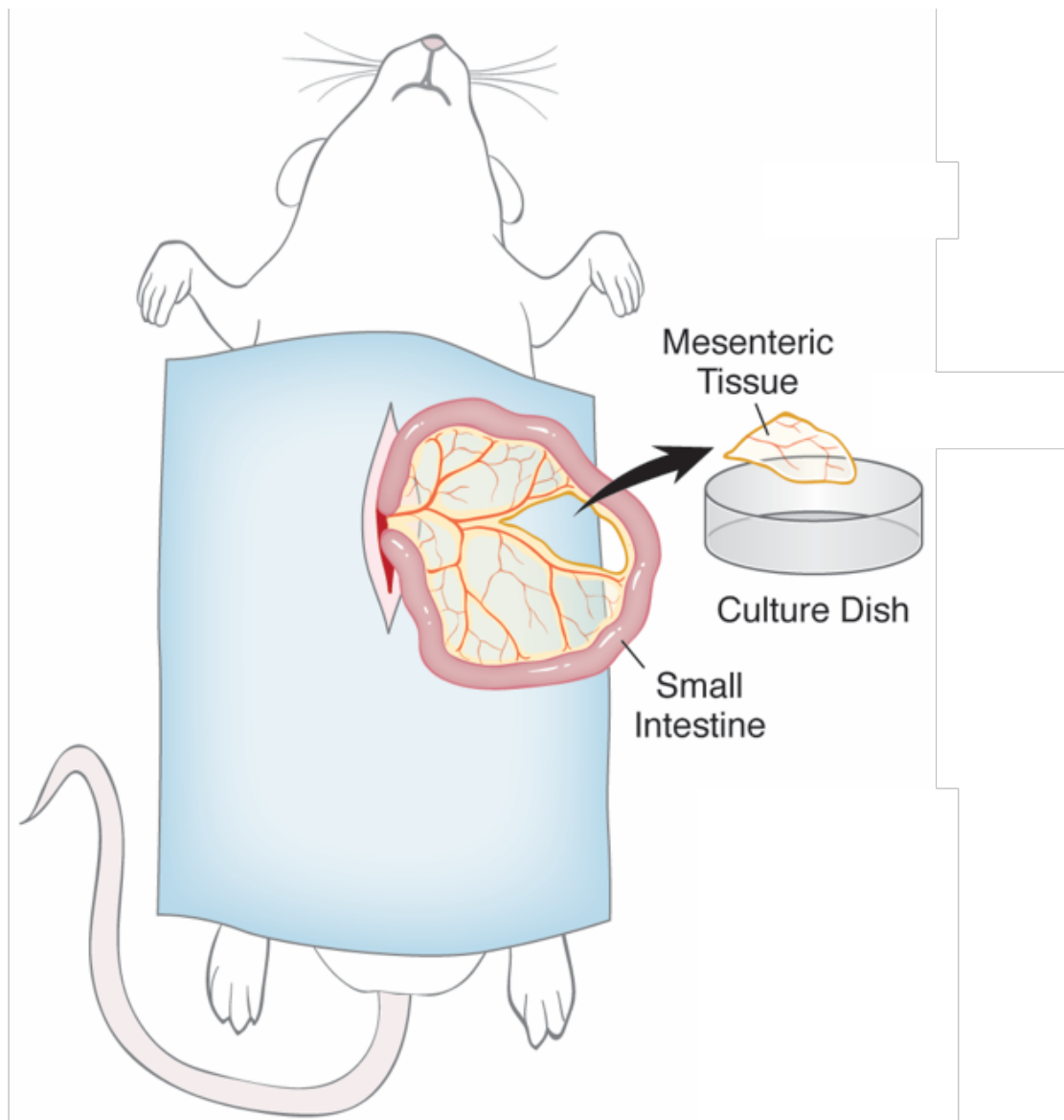


Figure 1.5 Rat mesentery culture model. The rat mesentery culture model is unique because blood and lymphatic vessel growth occur within an intact microvascular network. Mesentery's optical and physical properties make it an excellent model to study angiogenesis in real time and track the developments within a microvascular network.

CHAPTER 2: AN *EX VIVO* TISSUE CULTURE MODEL CAPABLE OF TIME-LAPSE EVALUATION OF MICROVASCULAR NETWORK GROWTH

(Published: Azimi et al., Methods in Molecular Biology, 2016, 1464:85-95)

2.1. INTRODUCTION

Microvascular network growth and remodeling are common denominators for tissue function, wound healing, and multiple pathologies [53,54]. Whether for tissue engineering applications or the design of therapies, understanding how and where angiogenesis, defined as the growth of new blood vessels from existing ones, occurs within a network is critical. Angiogenesis involves multiple cell types and is related to the growth of other systems, like lymphatic networks [29,55]. To advance our knowledge about the multi-cellular/multi-system interactions during angiogenesis, new experimental models are needed.

In vitro models have proven extremely valuable for mechanistic investigations of intra-cellular signaling and cell-cell interactions associated with angiogenesis [46]. Two-dimensional culture or co-culture systems, however, are limited in their complexity and the physiological relevance can be unclear. Recognition of the need to incorporate the multi-scale complexity of a real microvascular scenario, i.e. cells, vessels, networks, and systems, has motivated the development of three-dimensional culture systems [46], *ex vivo* tissue explant models [49], microfluidic platforms [47,56], and the use of integrated

computational approaches to study angiogenesis [57]. Still, a need exists for a model that enables time-lapse investigation of angiogenesis in intact microvascular networks *ex vivo*. Previously, our laboratory showed that the rat mesentery culture model could be such a tool, and used this model to 1) investigate pericyte-endothelial cell interactions during angiogenesis, and 2) investigate the spatial relationships between lymphatic and blood endothelial cells [58].

The objective of aim 1 was to develop a method for time-lapse quantification of network growth in the rat mesentery culture model. An advantage of using rat mesentery tissue is that it is self-contained and does not require embedding into a matrix. The thickness of the mesentery (20 - 40 μm) [44] enables observation of single cells across the branching hierarchy of intact networks. By simply securing the tissue on the bottom of a culture well, labeling live endothelial cells with BSI-lectin and epifluorescent imaging, we demonstrated that vessel density and capillary sprouting can be quantified in a network before, during, and after angiogenesis. Application of this method is supported by 1) the confirmation that vascular islands, defined as endothelial cell segments initially disconnected from nearby networks, connect to networks during angiogenesis under various culture conditions, and 2) observation of endothelial cell plasticity. Our results suggest that the rat mesentery culture model offers an environment for cell lineage monitoring during angiogenesis and lymphangiogenesis. The time-lapse quantification of network growth is not possible with typical animal models and with any of the other currently available *ex vivo* tissue culture models.

2.2. MATERIALS AND METHODS

2.2.1. Rat Mesentery Culture Model

All animal experiments were approved by Tulane University's Institutional Animal and Care Use Committee. Rat mesenteric tissues were harvested and cultured according to our previous description [58]. Adult male Wistar rats (325 - 349 g) were anesthetized via intramuscular injection with ketamine (80 mg/kg body weight) and xylazine (8 mg/kg body weight). The mesentery was aseptically exteriorized [59] and euthanized by intracardiac injection of 0.2 ml Beuthanasia. Then, mesenteric windows, defined as the thin, translucent connective tissues found between artery/vein pairs feeding the small intestine, were harvested from the ileum section. Tissues were immediately rinsed in sterile phosphate-buffered saline (PBS; Gibco; Grand Island, NY) with CaCl_2 and MgCl_2 at 37 °C, and immersed in sterile medium essential medium (MEM; Gibco) containing 1% penicillin-streptomycin (PenStrep; Gibco). They were then transferred to individual wells in either a 6-well or 12-well culture plate. Each tissue was quickly spread out on the bottom of a well and secured in place with a commercially available insert (CellCrown; Sigma-Aldrich; St. Louis, MO) with 1- μm polycarbonate filter and covered with 2 ml of MEM containing 1% PenStrep. Tissues were cultured in standard incubator conditions (5% CO_2) (Fig. 2.1).

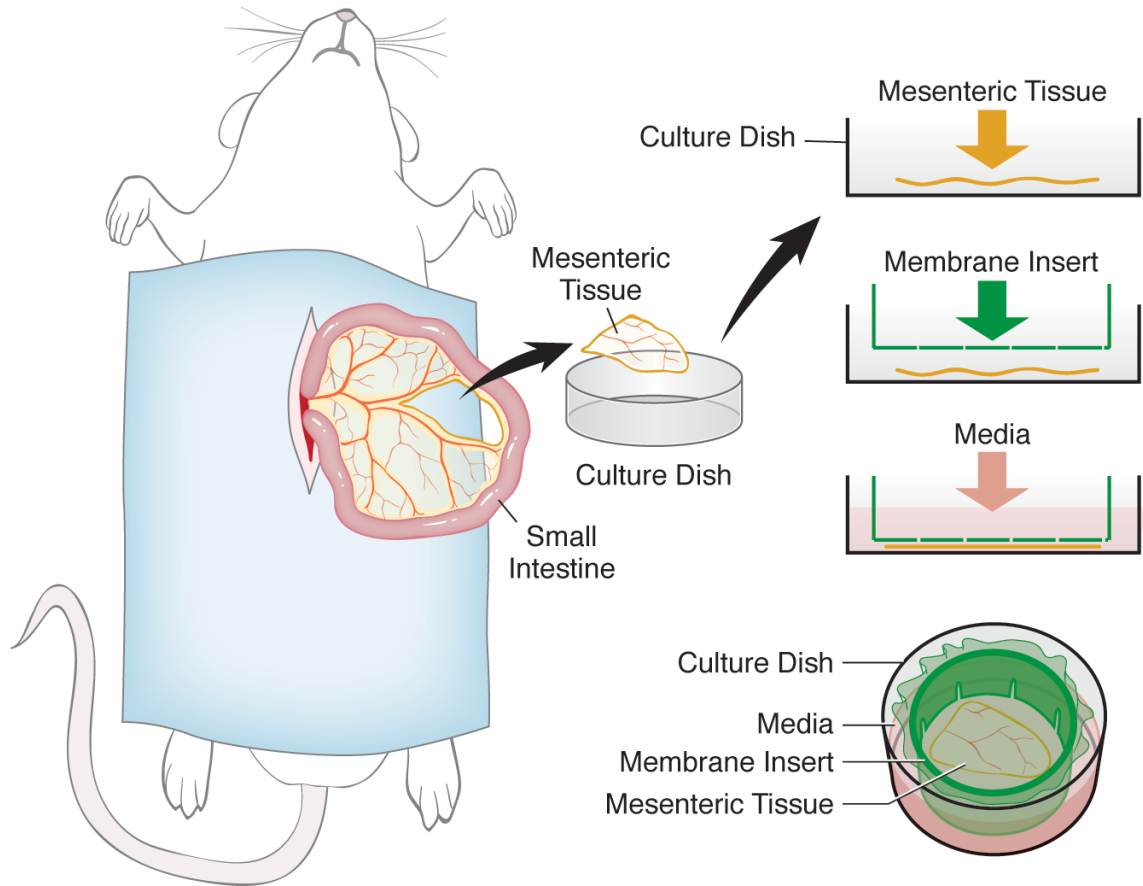


Figure 2.1 Illustration of the rat mesentery culture model. The mesenteric tissue, harvested from the small intestine of an adult Wistar rat, is transferred into a culture dish, quickly spread out on the bottom of a well, secured in place with a membrane insert, and covered with media. Tissues are cultured in standard conditions (37 °C, 5% CO₂).

2.2.2. Time-Lapse Imaging of Blood Vessels for Angiogenesis Study

Tissues (n= 16 tissues; 4 tissues harvested from 4 rats) were cultured in media supplemented with 10% fetal bovine serum (FBS; Gibco). On day 0, the media in each well was supplemented with BSI-Lectin conjugated to FITC (1:40; Sigma-Aldrich). Tissues were then incubated for 30 min under standard culture conditions. After the incubation, the lectin-supplemented media was removed, and tissues were washed with lectin-free media. Labeling with BSI-Lectin identified all blood and lymphatic vessels. “Before” images of the microvascular networks were obtained per tissue. Tissues were then returned and cultured according to their experimental group for 3 days. On day 3, tissues were again labeled with BSI-lectin and imaged. Positioning of the motorized microscope stage ensured that the same microvascular network region was re-imaged.

The number of vessels per vascular area and the number of capillary sprouts per vascular area were quantified per tissue from 4x images of randomly selected network regions per tissue. Two to four fields of view were arbitrarily selected to be representative of the microvascular networks and to minimize imaging time. Blood vessels were defined as lectin-positive blood endothelial cell segments present between two branch points and capillary sprouts were defined as blind ended segments originating from a host vessel. Lectin labeling identified the hierarchy of both blood and lymphatic microvascular networks. Blood vessels were distinguished from lymphatic vessels based on smaller vessel diameters, network structure, and their morphology [60,61,58]. This morphological method was confirmed by classification of lymphatics via lymphatic vessel endothelial hyaluronan receptor 1 (LYVE-1) labeling.

2.2.3. Immunohistochemistry

Additional tissues were harvested, cultured and labeled according to the following steps.

Lectin/NG2: 1) 1:100 rabbit polyclonal neural/glial antigen 2 (NG2) antibody (Millipore; Billerica, MA); 2) 1:100 goat anti-rabbit (GAR) CY3-conjugated antibody (Jackson ImmunoResearch Laboratories; West Grove, PA) and 5% normal goat serum (NGS; Jackson ImmunoResearch Laboratories)

Lectin/BrdU: 1) 2 h incubation in 1mg/ml Bromodeoxyuridine (BrdU; Sigma-Aldrich) supplemented media; 2) 6 M HCl for 1 h at 37°C to denature the DNA; 3) 1:100 mouse monoclonal anti-BrdU (Dako; Carpinteria, CA); 4) 1:100 goat anti-mouse (GAM) CY3-conjugated Fab fragments (Jackson ImmunoResearch Laboratories).

Live/Dead: 1) 1:400 Calcein AM and 1:200 Ethidium Homodimer-1 (EthD-1; Molecular Probes; Grand Island, NY) for 10 min at 37 °C.

PECAM/LYVE1: 1) 1:200 mouse biotinylated monoclonal Platelet endothelial cell adhesion molecule (PECAM) antibody (BD Pharmingen; San Diego, CA) + 1:100 rabbit polyclonal LYVE-1 antibody (AngioBio; Del Mar, CA); 2) 1:500 CY2-conjugated Streptavidin secondary (Strep-CY2; Jackson ImmunoResearch Laboratories) + 1:100 GAR-CY3 antibody and 5% NGS.

PECAM/Podoplanin: 1) 1:100 mouse monoclonal Podoplanin antibody (AngioBio); 2) 1:100 GAM-CY3 antibody and 5% NGS; 3) 5% normal mouse serum (NMS; Jackson ImmunoResearch Laboratories) for 1 hour at room temperature and overnight in refrigerator; 4) 1:200 mouse biotinylated monoclonal PECAM antibody (BD Pharmingen); 5) 1:500 Strep-CY2.

Lectin/Prox1/DAPI: 1) 1:100 mouse monoclonal Prospero homeobox protein 1 (Prox1) antibody (Novus Biologicals; Littleton, CO) for 2 hours; 2) 1:100 Alexa Fluor 594-conjugated GAM antibody (Jackson ImmunoResearch Laboratories), 3) 1:3000 4',6-diamidino-2-phenylindole (DAPI) Nucleic Acid Stain for 10 min.

Lectin labeling was performed as described above. Tissues were fixed with methanol fixation at -20 °C for 30 min. All antibodies were diluted in PBS + 0.1% saponin + 2% bovine serum albumin (BSA; Jackson ImmunoResearch Laboratories), and placed on tissues for 1 hour at room temperature unless specified otherwise. Between each step, tissues were rinsed with PBS + 0.1% saponin for 10 min three times.

2.2.4. Vascular Island Lineage Study

Vascular islands were defined as lectin-positive endothelial segments disconnected from a nearby microvascular network and have been previously characterized by our group [16,17]. To demonstrate that the time-lapse imaging method could be used to determine the fate of vascular islands during angiogenic scenarios, tissues were cultured in MEM supplemented with 10% serum (n = 16 tissues from 4 rats). Time-lapse imaging was performed as described above on days 0, 3, and 5 for additional tissues. To ensure that vascular islands were captured and to minimize cumulative exposure time during imaging, entire tissues were imaged using an automated mosaic tiling program. In addition, other groups of tissues were cultured in A) MEM + 400 ng/ml Basic fibroblast growth factor (bFGF; Life Technologies; Carlsbad, CA), and B) MEM + 200 ng/ml Vascular endothelial growth factor (VEGF; R&D Systems; Minneapolis, MN) + 200 ng/ml Platelet-derived growth factor (PDGF; R&D Systems). bFGF and

VEGF/PDGF supplement concentrations were selected based on previous evidence for their stimulation of angiogenesis [62] [Hao 2007].

2.2.5. Time-Lapse Imaging of Blood and Lymphatic Vessels

Tissues (n= 24 tissues; 6 tissues harvested from 4 rats each) were cultured in media + 10% serum. On hour 0, the media in each well was supplemented with BSI-lectin conjugated to FITC (1:40; Sigma-Aldrich). Tissues were then incubated for 30 min under standard culture conditions. After the incubation, the lectin-supplemented media was removed, and tissues were washed with lectin-free media. Labeling with BSI-lectin identified all blood and lymphatic vessels and blood vessels were identified from lymphatics based on their morphology, network structure [61], and the intensity of lectin labeling. The culture plates were then placed into a culture chamber mounted on the microscope stage to ensure maintaining the temperature at 37 °C. 3-4 microvascular networks were imaged per tissue using an inverted epifluorescent microscope. Tissues were then returned to the incubator and cultured for 48 hours. After that, tissues were again labeled with BSI-lectin and imaged every 8 hours. Positioning of the motorized microscope stage ensured that the same microvascular network region was re-imaged. After hour 120 imaging, tissues were spread on microscopic slides and immunolabeled for lymphatic markers.

2.2.6. Lymphatic Marker Coverage Studies

To quantify the endothelial cell mis-patterning of the lymphatic vessels, tissues were harvested from adult male Wistar rats were divided into two experimental groups:

1) Control group: Tissues were immediately mounted on slides, fixed, and labeled for lymphatic and endothelial cell markers (n= 16 tissues from 4 rats), and 2) Culture group: Tissues were cultured in media supplemented with 10% serum for 5 days as previously described without imaging during culture (n= 16 tissues from 4 rats). After 5 days, tissues were mounted on slides, fixed, and labeled for lymphatic and endothelial cell markers.

To quantify the lymphatic marker coverage of lymphatic vessels, the number of lymphatic vessel segments with full LYVE-1 expression per total number of lymphatic vessels was calculated in the whole tissue. Tissues without lymphatic vessels were eliminated from the study.

2.2.7. Image Acquisition

Images were acquired using 4x (dry, NA = 0.1), 10x (dry, NA = 0.3), and 20x (oil, NA = 0.8) objectives on an inverted microscope (Olympus IX70) coupled with a Photometrics CoolSNAP EZ camera. Confocal microscopy images were acquired using 40x (oil, NA = 1.3) objective captured on a Nikon A1 confocal microscope equipped with 405, 488, and 561 nm diode laser lines, coupled with an ECLIPSE Ti Nikon inverted microscope. Image analysis and quantification were done using ImageJ 2.0.0-rc-54 (U.S. National Institutes of Health, Bethesda, MD).

2.2.8. Statistical Analysis

For the angiogenic response, data was analyzed in terms of change in number of vessel segments and number of capillary sprouts between day 0 and day 3. Mixed model regression methods were used to determine whether the change from day 0 to day 3 was

significant. Mixed model methods were used to control the non-independence of change scores measured on the same subject; reported means are adjusted for this correlation.

Where possible, alternative nonparametric analyses were used to confirm the findings.

Comparison of LYVE-1 coverage of lymphatic vessels was made using two-tailed Student's t-test to compare between hour 0 and hour 120. Results were considered statistically significant when $P < 0.05$. Statistical analyses were conducted using SAS version 9.3, and Prism version 7 (Graphpad Software; La Jolla, CA). Values are presented as mean \pm standard error of the mean (SEM).

2.3. RESULTS

2.3.1. Time-Lapse Imaging Enables Tissue Specific Quantification of Microvascular Network Growth

Lectin labeling at day 0 and day 3 identified endothelial cells along the hierarchy of intact rat mesenteric microvascular networks (Fig. 2.2). Mesenteric tissues stimulated in culture for 3 days with 10% FBS displayed dramatic increases in microvascular network growth. Qualitative comparison of network regions before and after stimulation revealed increases in vessel density and capillaries sprouting from pre-existing vessels (Fig. 2.2). Increases in both the number of vessel segments per vascular area and the number of capillary sprouts per vascular area were evident and statistically significant ($p < 0.05$ for both measures) (Fig. 2.3). Consistent with our previous characterization of the model, angiogenic networks at day 3 contained NG2-positive pericytes along the microvessels confirming that vascular pericytes remain present along endothelial cells during angiogenesis after *ex vivo* culture (Figure 2.4 A-C). In addition, vessel growth was associated with vascular cell viability (Figure 2.4 D-F) and proliferation (Figure 2.4 G-I).

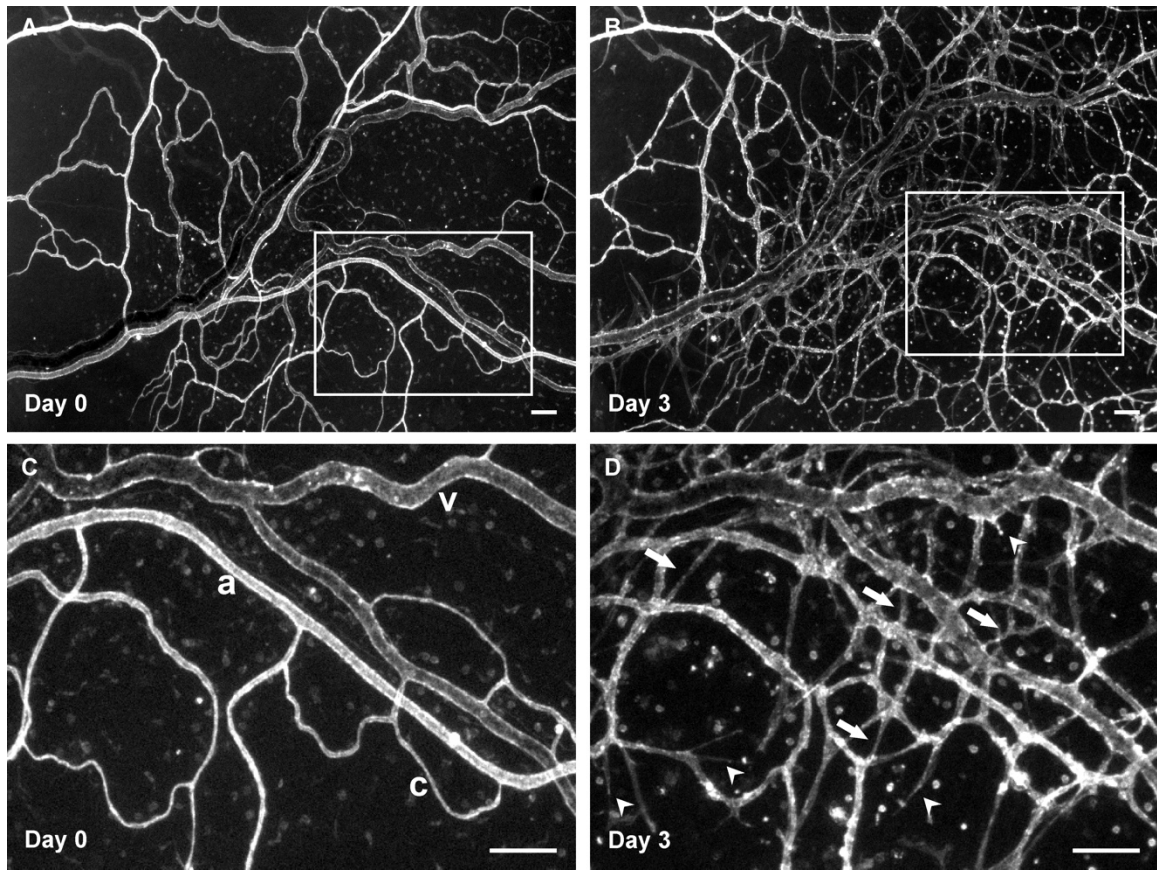


Figure 2.2 Microvascular networks in the rat mesentery culture model before and after angiogenesis. A, B) Comparison of the same network labeled with BSI-lectin on day 0 (before) and day 3 (after) post-stimulation with 10% serum identifies new vessels. C, D) Higher magnification images of the same region indicated by the above squares. Examples of arterioles, venules, and capillaries are marked by letters “a,” “v,” and “c,” respectively. Increased blood capillary sprouting is evident by day 3 (arrowheads). The new vessel segments (arrows) are indicative of increased vessel density. Lectin also labels a population of unidentified interstitial cells. Scale bars = 100 μm .

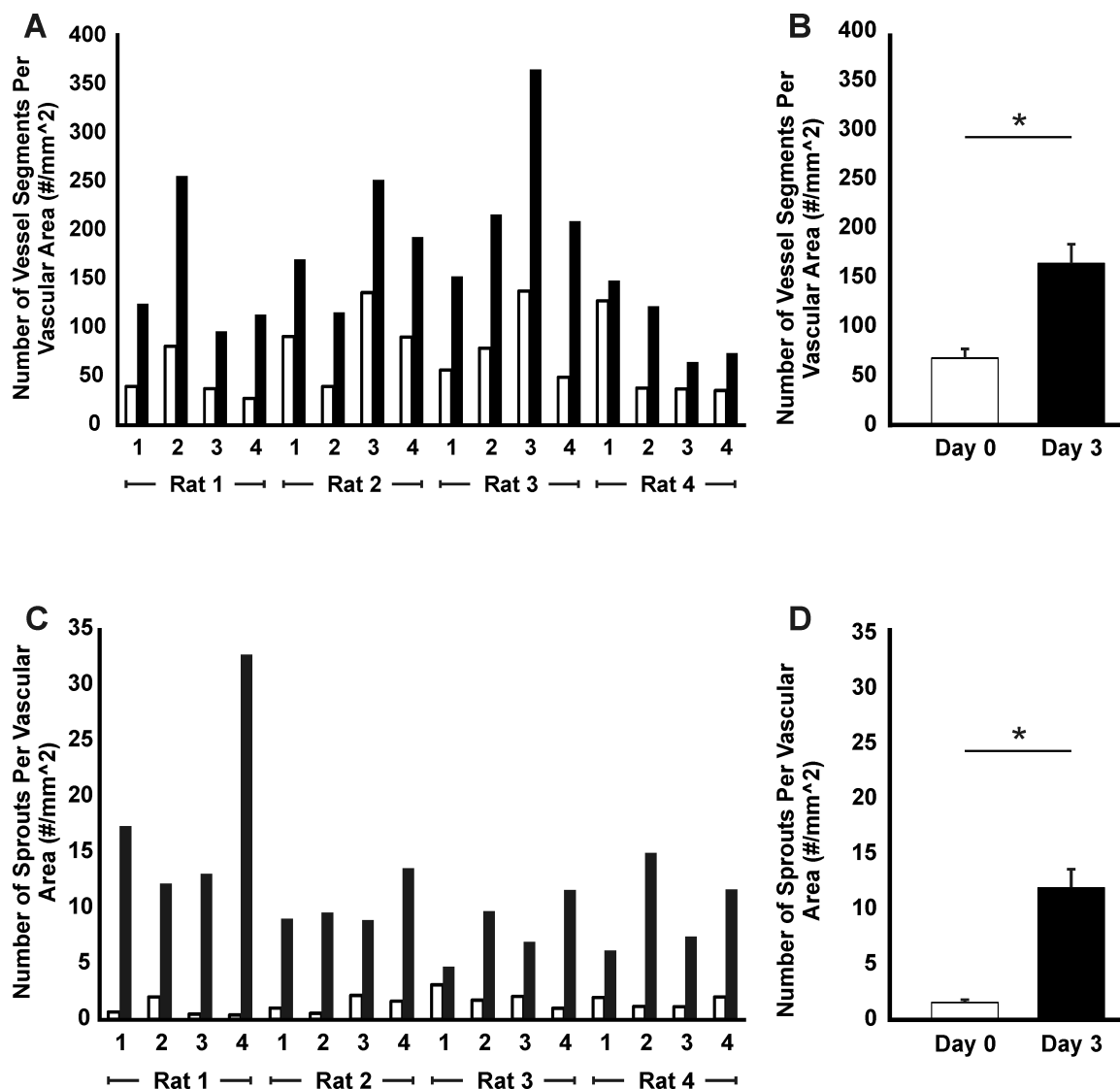


Figure 2.3 Angiogenic response in rat mesentery tissues following stimulation. Vessel density (A, B) and number of capillary sprouts (C, D) per vascular area were quantified before and after stimulation with 10% serum. An increase in both metrics occurred for each tissue. Comparison between day 0 and day 3 confirmed a significant difference in both the average number of vessel segments ($p < 0.001$) and the average number of sprouts ($p < 0.001$) per vascular area. White bars represent day 0 (before) and black bars represent day 3 (after). Values are averages \pm SEM.

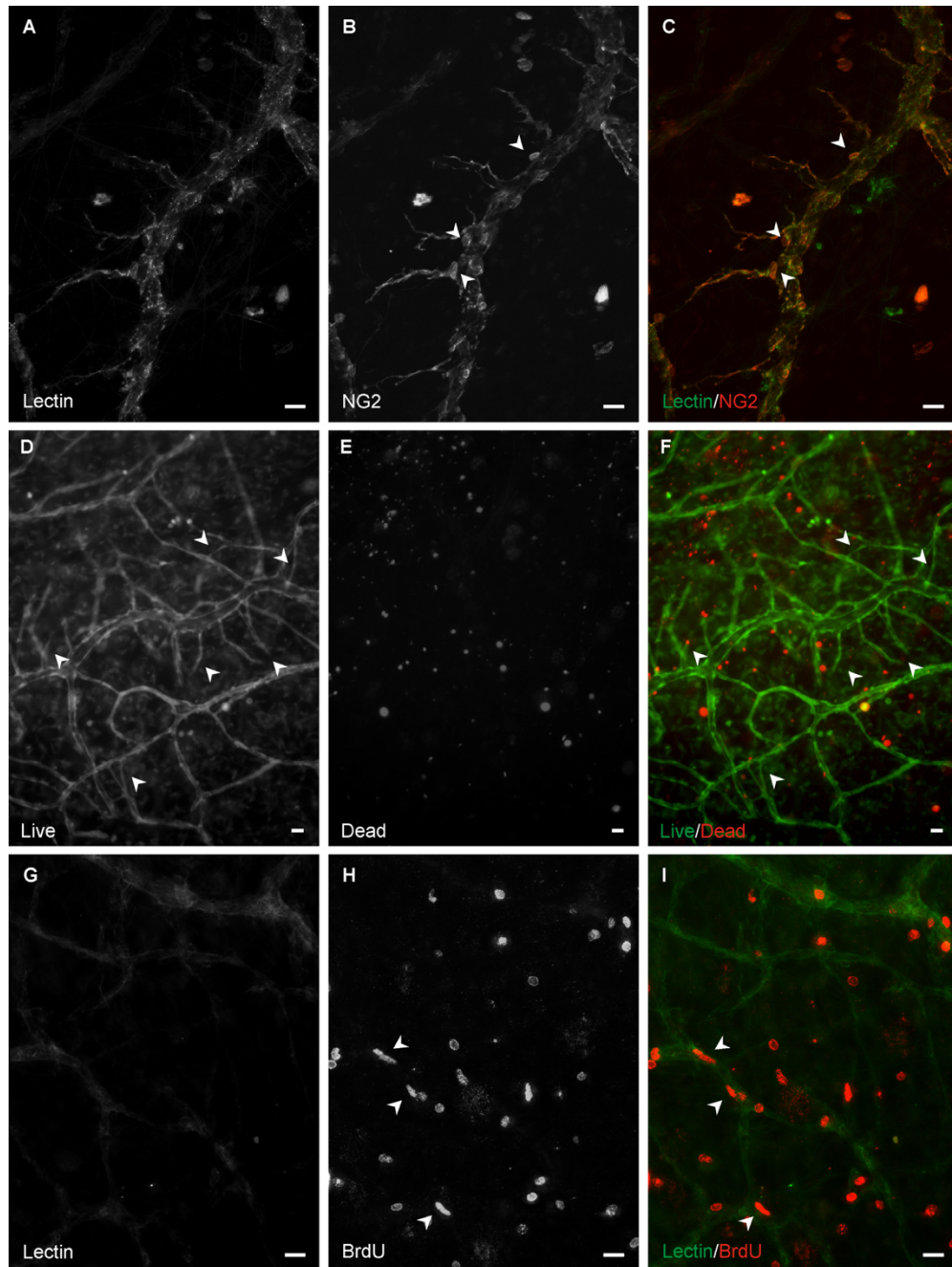


Figure 2.4 Presence of vascular pericytes, viable cells, and proliferative cells in angiogenic microvascular networks in the rat mesentery culture model. A-C) NG2 positive pericytes along BSI-lectin positive microvessels on day 3 post culture with 10% serum. Arrowheads show NG2+ pericytes. D-F) Live/Dead labeling of microvessels on day 3 post culture with 10% serum. Live and dead cells were identified by positive Calcein-AM and Eth-D labeling, respectively. Arrowheads indicate the Calcein-AM+ newly formed sprouts and connections within the network. G-I) BrdU positive cells along BSI-lectin positive microvessels on day 3 post culture with 10% serum. Proliferation of endothelial cells is supported by the observation of elongated nuclei within the lectin positive vessels (arrowheads). Scale bars = 20 μ m.

2.3.2. Time-Lapse Imaging Enables Lineage Studies for Vascular Island Incorporation During Angiogenesis

Comparative analysis of images at different time points during microvascular growth allowed for the lineage tracking of vascular islands, defined as endothelial segments disconnected from nearby networks over multiple time points. On day 3 post-stimulation with serum, 35% of the vascular islands were found to be connected to a nearby blood microvascular network. On day 5 post-stimulation, 42% of the islands had connected (Fig. 2.5). Vascular islands were commonly observed to undergo elongation and branching. While the origin of these disconnected endothelial cell segments remains unclear, previous work by our laboratory suggests that their number increases with vascular regression in the rat mesentery [17]. Using our culture model, we confirmed that vascular islands originating from vascular regressions are also able to connect to their nearby networks when the networks are stimulated with 10% serum to undergo re-growth (data not shown). Vascular island incorporation was also observed in microvascular networks stimulated with bFGF and with the combination of VEGF and PDGF (Fig. 2.6).

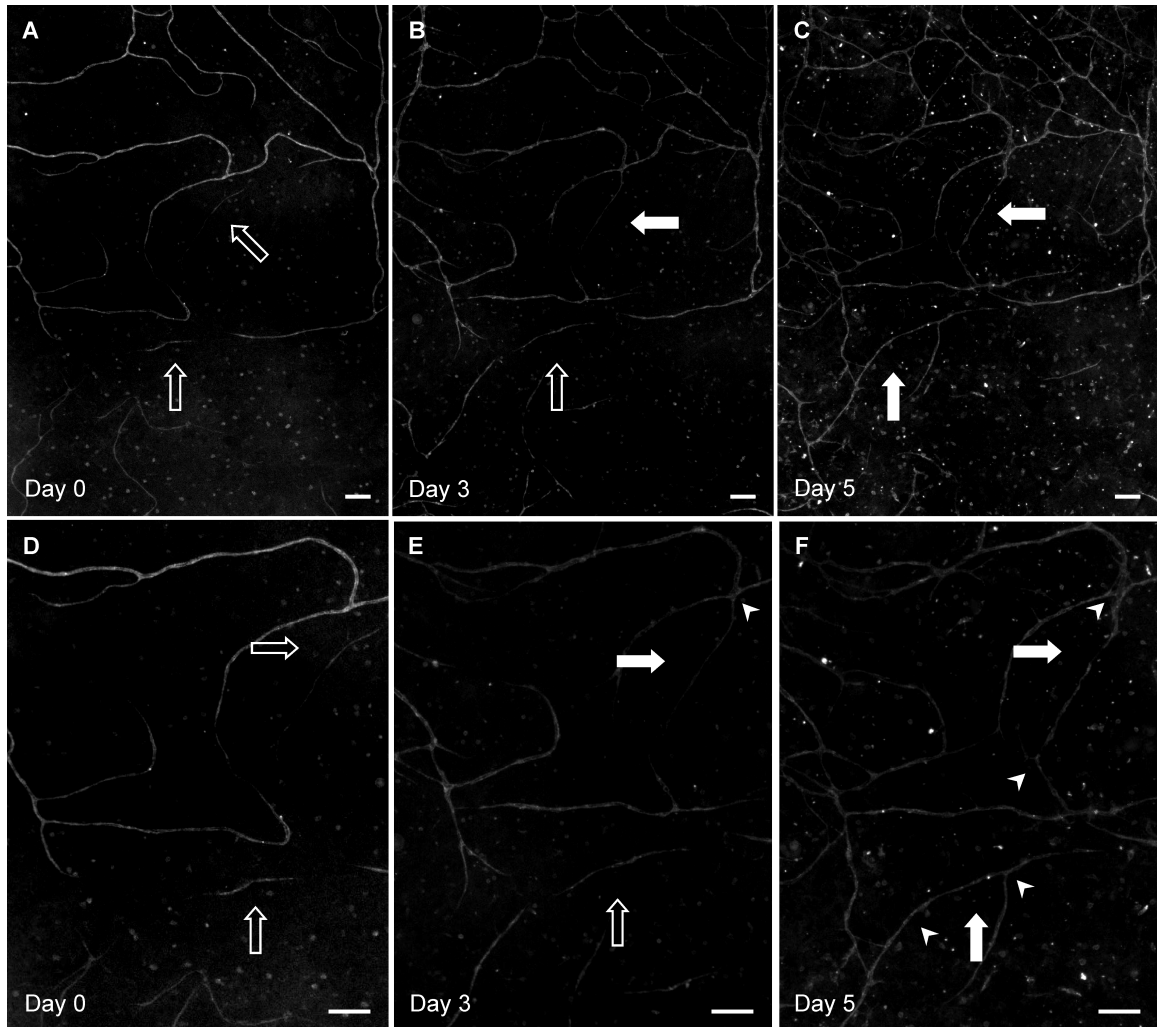


Figure 2.5 Tracking endothelial cell segments during angiogenesis. Comparison of lectin positive vessels taken at Day 0 (A, D), Day 3 (B, E) and Day 5 (C, F) provide examples of vascular island incorporation to nearby networks during angiogenesis with 10% serum. Vascular islands, defined as segments disconnected from nearby networks (open arrows) in the Day 0 images connected to the nearby network (closed arrows). Arrowheads indicate the locations of connection between a vascular island and the nearby network. Scale bars = 100 μm .

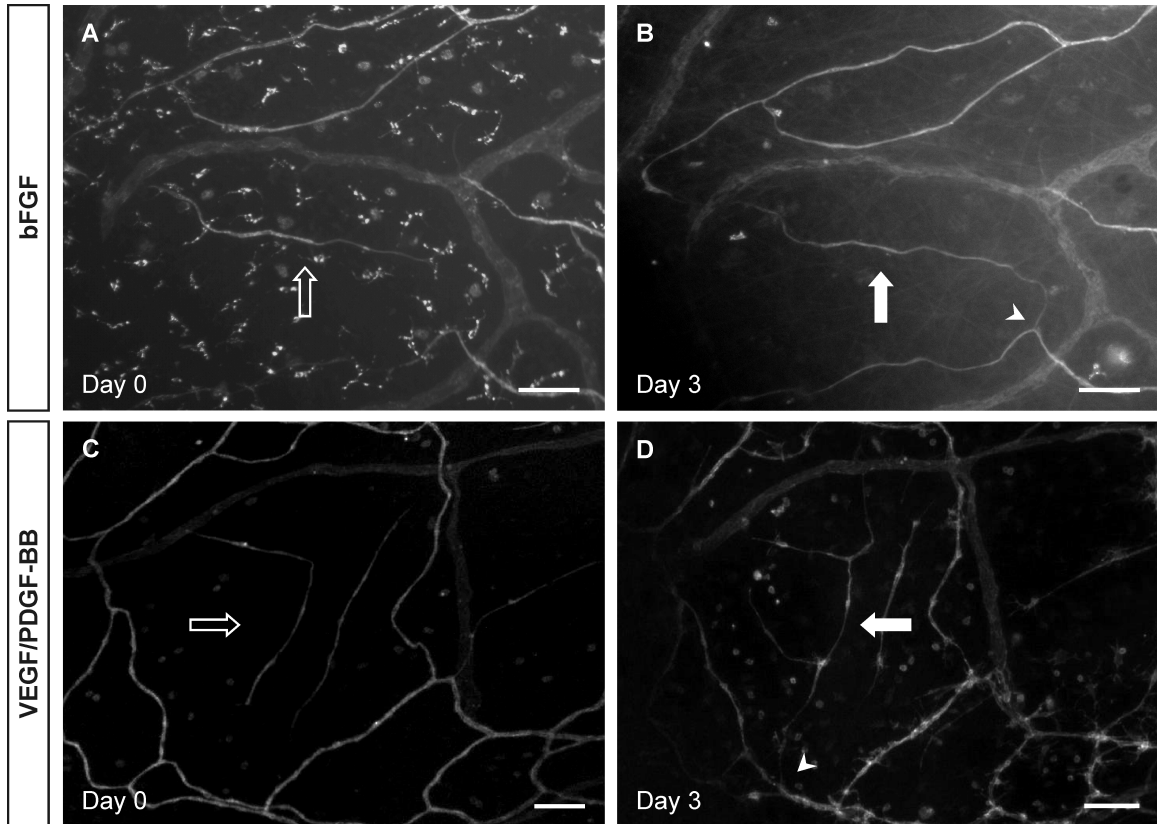


Figure 2.6 Vascular island incorporation occurs during growth factor stimulation. A, B) Day 0 (before) and Day 3 (after) images for tissues stimulated with bFGF. C, D) Day 0 (before) and Day 3 (after) images for tissues stimulated with VEGF/PDGF. Vascular islands (open arrows) were identified at Day 0 and observed to be connected to their nearby networks by Day 3 (closed arrows). Arrowheads indicate the locations of connection between a vascular island and the nearby network. Scale bars = 100 μ m.

2.3.3. Time-Lapse Imaging Enables Tracking of Blood and Lymphatic Vessel Remodeling

Lectin labeling at different time points identified blood and lymphatic vessel remodeling in rat mesenteric microvascular networks due to 10% serum stimulation (Fig. 2.7). As expected, mesenteric tissues stimulated in culture for 5 days with 10% serum displayed dramatic increases in microvascular network growth (Fig. 2.7 A, B). Examples of connections between lymphatic vessels and blood vessels were identified over 120 hours using time-lapse imaging (Fig. 2.7 C-L).

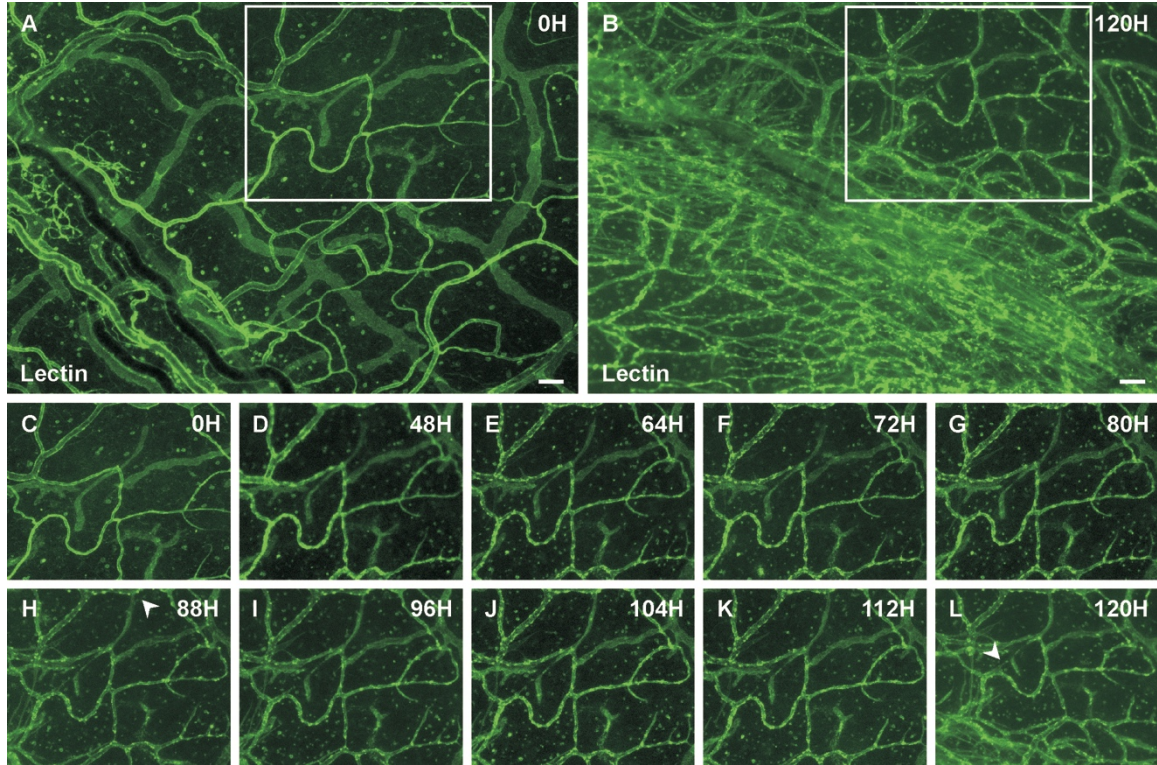


Figure 2.7 Time-lapse imaging of blood and lymphatic vessel remodeling following stimulation by serum. A, B) Comparison of the same network labeled with BSI-lectin on hour 0 and hour 120 after 10% serum stimulation identifies new connections between lymphatic vessel and blood vessel networks. C-L) Higher magnification images of the outlined region in A and B over time. The lymphatic vessel segment forms connections with blood vessels at hour 88 and hour 120, marked by arrowheads. Increased blood vessel density is evident by day 5. Scale bars = 100 μ m.

2.3.4. Lymphatic Endothelial Switch Phenotype Under Serum Stimulation

Labeling against lymphatic markers confirmed mis-patterning in lymphatic endothelial cells (Fig. 2.8 and 2.9). When compared to day 0, a subset of lymphatic endothelial cells stop expressing LYVE-1 markers after 5 days of serum stimulation (Fig. 2.9 B, E) Other lymphatic markers, such as Podoplanin also showed coverage gaps on lymphatic vessels (Data not shown). To confirm the lymphatic-to-blood endothelial cell phenotypic switch, a comparison was made between LYVE-1 coverage on lymphatic vessels between day 0 and day 5 (Fig. 2.10). While lymphatic vessels on day 0 showed almost no gaps in LYVE-1 coverage, every tissue stimulated with 10% serum for 5 days displayed gaps in LYVE-1 coverage. The mean coverage of LYVE-1 on day 0 and day 5 were 100% and 67.8%, respectively. Statistical analysis confirmed a significant difference between the two groups ($p < 0.0005$).

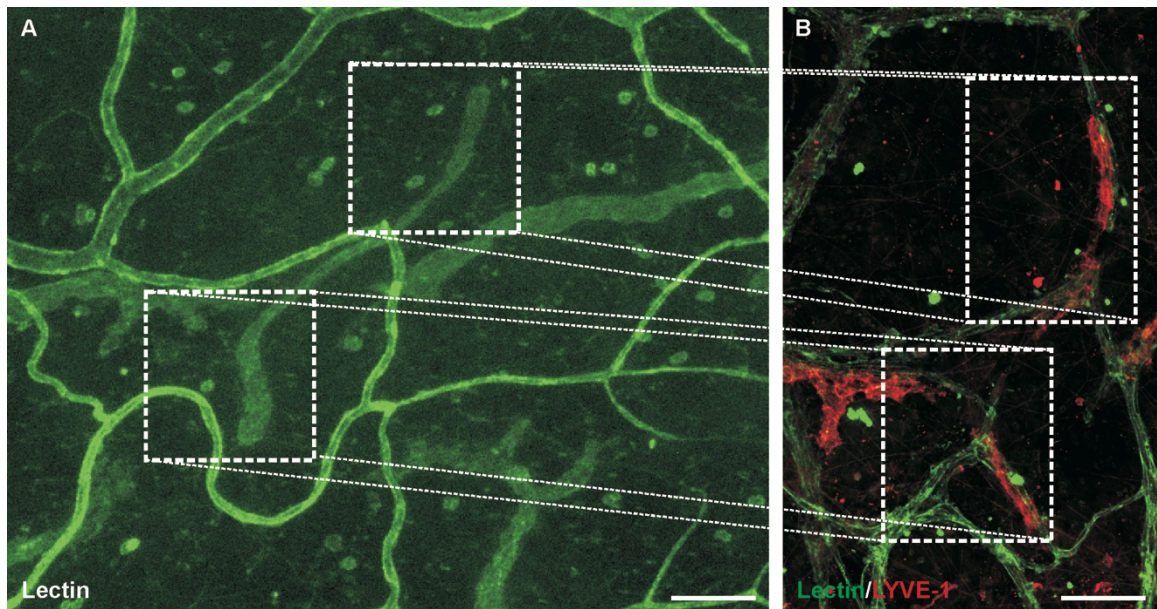


Figure 2.8 Lymphatic endothelial cell mis-patterning by serum stimulation. Blood and lymphatic vessels were identified based on morphology on day 0 by BSI-lectin labeling (A). The same spot was labeled against LYVE-1, a lymphatic marker, and imaged on day 5 (B). Boxes show segments of lymphatic vessels that partially maintained their lymphatic identity and were connected to blood vessels after 5 days of serum stimulation. Scale bars = 100 μm .

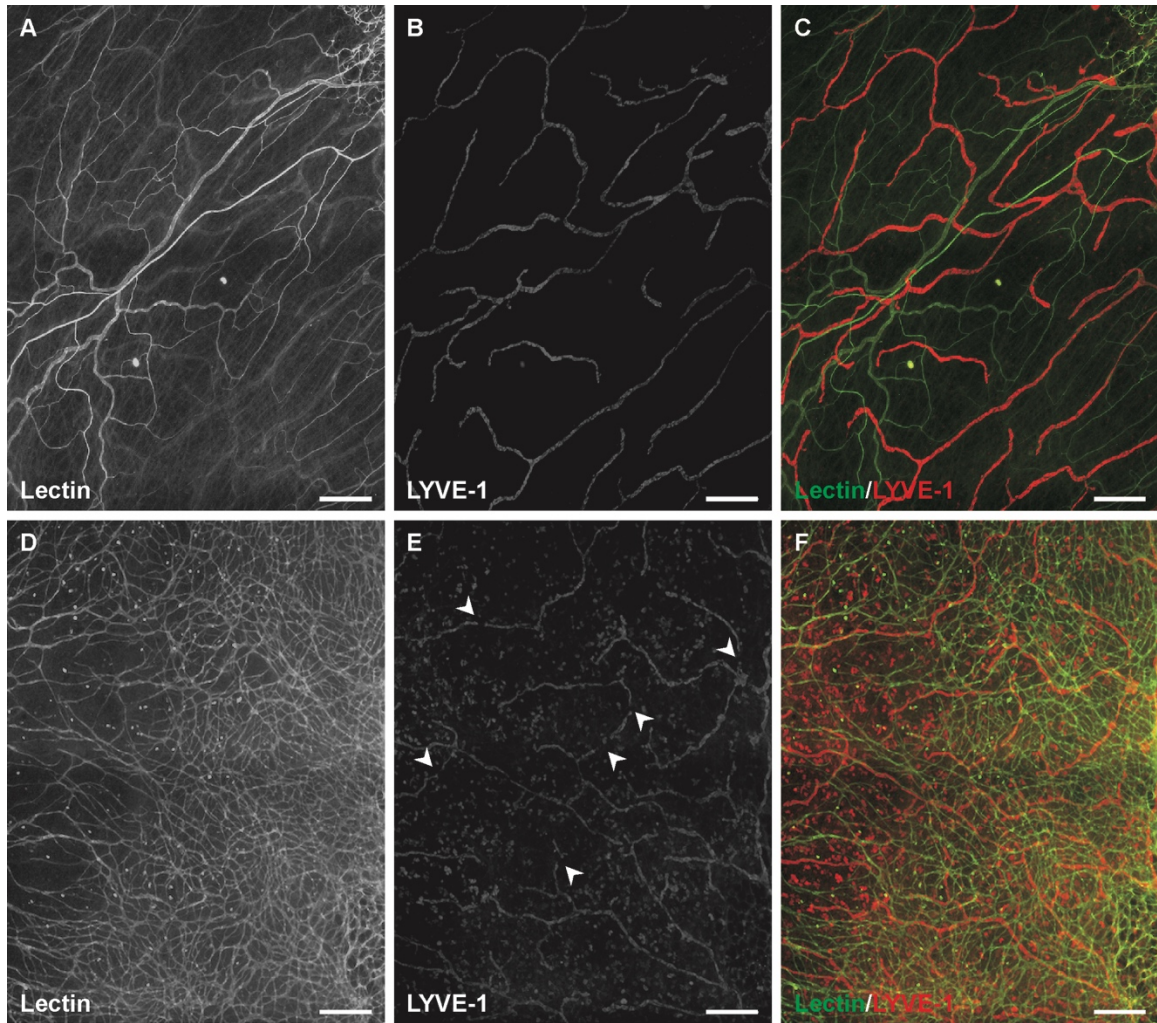


Figure 2.9 Loss in LYVE-1 coverage of lymphatic vessels after 5 days. A-C) LYVE-1 positive lymphatic vessels and BSI-lectin positive blood vessels on day 0. There is almost no gap in lymphatic LYVE-1 coverage. D-F) LYVE-1 positive lymphatic vessels and BSI-lectin positive blood vessels after 5 days of serum stimulation. Arrowheads point to examples of the gaps in lymphatic LYVE-1 coverage. Scale bars = 100 μ m.

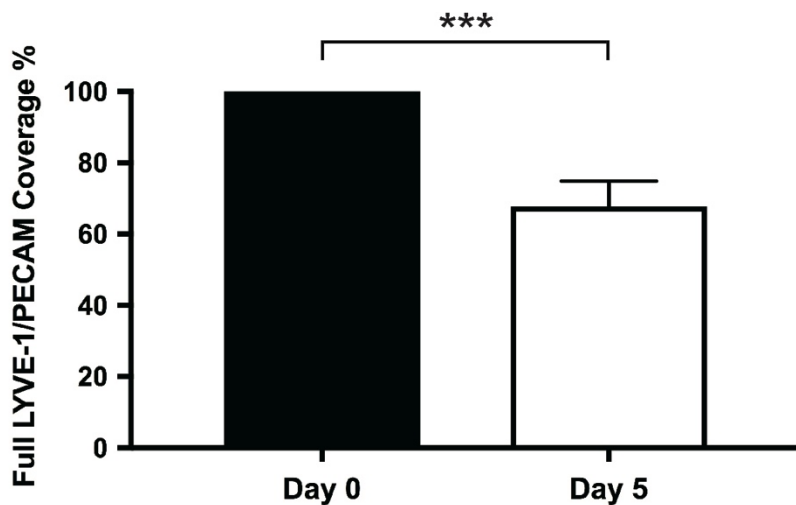


Figure 2.10 Quantification of lymphatic-to-blood endothelial cell phenotype switch by serum stimulation. The effect of serum treatment for 5 days on endothelial cell identity was quantified based on the percentage of lymphatic vessels fully covered with LYVE-1 marker. *** represents a significant difference between day 0 and day 5 groups ($p < 0.0005$) by two-tailed Student's t-test. Values are averages \pm SEM

2.4. DISCUSSION

The results of this aim establish the rat mesentery culture model as an *ex vivo* tool for time-lapse imaging of microvascular network growth. Our laboratory's initial introduction of the rat mesentery culture model established that it could be used for probing pericyte-endothelial cell interactions during angiogenesis [58]. We also provided an example of a network before and after angiogenesis stimulated by 20% serum. Our current study expands upon our previous work and supports imaging in the rat mesentery culture model at multiple time points as a method for 1) the quantification of tissue-specific growth responses, 2) the tracking of cell-cell interactions during various angiogenic stimuli, and 3) investigation of blood/lymphatic vessel mis-patterning dynamics. The observation of pericytes associating with the vascular cells and increased proliferation of endothelial cells during angiogenesis is consistent with our previous characterization of the model [58], and supports that microvascular growth associated with angiogenesis in cultured rat mesenteric tissues involves dynamic interactions between multiple cell types.

Compared to commonly used tissue culture models and *in vitro* cell culture systems, our rat mesentery culture model is unique because growth occurs within an intact, real microvascular network. *Ex vivo* tissue explants have proven extremely useful for studying angiogenesis. Nicosia et al. first introduced the aortic ring model as an assay to investigate angiogenic sprouting from aortic segments in a collagen gel [49]. While sprouting in the aortic ring involves multiple cell types, a limitation is that the sprouting occurs from macrovessels, atypical of the *in vivo* process. More recently, retina culture model has been introduced in which angiogenesis does occur from intact microvascular

networks [50,51]. For these models, culturing tissues harvested from GFP-transgenic mice stains offers the ability for observing endothelial sprouting over time.

Unfortunately, the mouse mesentery is avascular [44], eliminating the substitution for GFP-transgenic mice tissue for rat mesentery, as utilized in our model. Furthermore, we show that a simple lectin labeling of the rat mesentery culture is sufficient to determine network growth at different time points, and in comparison to the *ex vivo* models, our rat mesentery culture model allows for simultaneous observation of both blood and lymphatic endothelial cells.

The comparison of images before and after treatment reduces issues of variability that might influence non-paired statistical analysis. While both vessel and capillary sprout density metrics increased post-stimulation with 10% serum, the explant specific responses varied from 16% to 320% increases in vessel density and from 50% to 8000% increases in sprout density. The specific causes for this variation remain unknown, but the ability to quantify growth in the same tissue provides definitive evidence of whether a response occurred and enables the application of appropriate analytical methods to account for random variation among samples.

We acknowledge that similar to other *ex vivo* culture systems, a limitation of the rat mesentery culture model is that it lacks the presence of blood flow and related effects of shear stress, which have been shown to influence angiogenesis *in vivo* [63,64]. The recent development of microfluidic based assays has emphasized the importance of including shear stress in *in vitro* models [47,56,65]. While the rat mesentery culture lacks flow parameters, we feel that the top-down approach to maintain the multi-cell and multi-system complexity of a real microvascular network enables unique applications

exemplified by our drug testing results. Furthermore, the observation of vascular island incorporation and the observation of potential lymphatic/blood plasticity during angiogenesis underscore the importance of this model.

Tracking the fate of vascular islands at multiple time points was motivated by our laboratory's discovery that vascular islands undergo proliferation and extension during angiogenesis [16]. In our initial description of the rat mesentery culture model, we provided examples of microvascular network images on day 0 and after 3 days of culture with 20% serum and demonstrated that vascular islands can connect to nearby networks 34. The example of vascular island incorporation implicated a new mode for endothelial cell dynamics in angiogenesis. In the current study, we quantified the occurrence of vascular island incorporation (Fig. 2.5) at 3 and 5 days post-stimulation and showed that incorporation can occur in growth factor-induced angiogenesis scenarios. The observation of island connection to nearby networks at day 5 versus day 3 further suggests that islands at day 5 might still be able to connect at later time points. The morphology of the vascular islands was similar to blood capillary sprouts. Interestingly, however, apparent blood vascular islands were also observed to connect to nearby lymphatic vessels (data not shown). These observations support the use of the rat mesentery culture model for investigating lymphatic/blood endothelial cell plasticity.

Even though the blood endothelial cells give rise to lymphatic endothelial cells [66], the concept of endothelial cell plasticity was mainly believed to be limited to the developmental stages. For example, *slp76*-deficient embryonic mice exhibited blood filled lymphatics, a sign of lymphatic mis-identity [67]. Johnson et al. showed that downregulation of *Prox1* in adult mice can reverse the lymphatic identity of endothelial

cells back to a blood phenotype [68]. Another study showed that deletion of Rac1 causes mis-patterning in lymphatic vessels in embryonic mice [69]. These studies have all been done using transgenic mice models in developmental stages. However, the idea that endothelial cell plasticity can be replicated only by transgenic models has been challenged in recent years. Lin et al. showed that Lysophosphatidic acid (LPA) can upregulate the expression of lymphatic markers in human umbilical vascular endothelial cells (HUVECs) [70]. A combination of serum, VEGF, and FGF-2 have also been reported to promote lymphatic identity in endothelial cell culture [71]. Still, we don't know of any studies investigating endothelial cell plasticity in a setting that mimics the complexity of an adult microvascular network scenario. Previous work by our lab investigated endothelial cell plasticity in cultured mesentery tissues, but could not replicate the reported results by either LPA or serum alone [72].

In summary, this study introduces a novel *ex vivo* method for time-lapse investigation of angiogenesis in an intact microvascular network, and suggests the vascular island incorporation as a potential new mode of angiogenesis. This study also provides evidence for endothelial cell plasticity in an adult tissue. Our recent findings support a lymphatic-to-blood phenotypic switch in adult lymphatic endothelial cells by serum stimulation. To the best of our knowledge, this is the first time endothelial cell plasticity has been reported and confirmed in adult tissues.

2.5. FUTURE STUDIES

While we preferred the use of BSI-lectin in this study to visualize blood and lymphatic vessels, we recognize the limitations brought by its use. Lectin labeling fades quickly, and is not visible on new capillary sprouts, so it requires re-labeling at later time points. Nevertheless, lectin labeling was selected for this study because it is relatively fast, cost effective, and has minimal effects on cell survival. Future work will be needed to develop cell-targeted transfection methods that will allow for real-time tracking of endothelial and other cell types.

As it was mentioned before, the mouse mesentery is avascular, which prevents the substitution for already available GFP-transgenic mice tissue for rat mesentery. However, ongoing research in our lab is aimed at stimulating the peripheral blood vessel networks around the mouse mesentery by tamoxifen injections to create an angiogenic response, and induce microvascular coverage inside the mouse mesentery. This could lead to adopting the mouse mesentery into our model, thus eliminating the need for lectin labeling.

In the context of our study, since the aim was to validate our model's capability to investigate angiogenesis, the use of serum was justified because, based on our previous studies, it causes a robust angiogenic response in rat mesentery tissue [58]. However, serum is a mixture of different proteins with different levels of angiogenic stimulations. Alternatively, angiogenic factors that target one or a few receptors, e.g. growth factors, can be used to investigate the function of specific receptors, cell signaling pathways, etc.

Our study served to showcase the possibility of endothelial cell plasticity in adult tissues. This emphasizes the need to investigate how and why lymphatic/blood patterning can go wrong in adult tissues.

CHAPTER 3: VALIDATING THE RAT MESENTERY CULTURE MODEL FOR ANTI-ANGIOGENIC DRUG TESTING

(Published: Azimi, et al., PLOS ONE, 2015,10(3):e0119227)

3.1. INTRODUCTION

Recent advances in the field of medicine specifically in the post-genome era, have enabled researchers to identify and discover a myriad of new therapeutic targets in hopes of finding the best methods to combat disorders with ineffective or unavailable treatments, which has led to a significant hike in developing new drug formulations or new molecular entities. This, combined with more rigorous safety regulations imposed by the Food and Drug Administration (FDA) in recent years, has increased the research and development costs for the pharmaceutical companies and created a challenging trend. Although there are a great number of potential targets being identified and tested, the reality is, based on statistics, only a few will show promising results. It is estimated that out of five thousand new discoveries that enter the R&D pipeline, only one eventually gets to the market. This has led to a sharp increase in pharmaceutical companies' R&D expenses within the last fifteen years. Based on a report published by Tufts Center for the Study of Drug Development (CSDD) in 2014, the cost of developing a single drug that makes it to the market stands at \$2.6 billion, showing a whopping 145% increase compared to the inflation-adjusted estimates in 2003 [73]. The same report differentiates between the cost associated with the pre-clinical studies versus clinical studies and

reports that \$1.1 billion is dedicated to pre-clinical studies. Another factor adding to the challenges faced by drug developing companies is the amount of time required for discovery, development, as well as pre-clinical and clinical testing. The studies show that it takes more than 10 years for a formulation to go through the pipeline from the discovery phase to the FDA approval. The estimates for discovery and pre-clinical phases are anywhere from 5 to 7 years of which 2 to 3 years is dedicated to the pre-clinical phase. This presents a big opportunity for developing novel realistic tissue-on-a-chip models to replace the costly and time-consuming pre-clinical testing with a more cost-efficient and less costly alternative.

Tumor growth and metastasis depend on angiogenesis triggered by chemical signals from tumor cells. A challenge in evaluating anti-tumor therapies is the inability to decouple treatment effects on cancer cells versus the microvascular network. Therefore, a simple and reproducible *ex vivo* assay to measure the effects of possible anti-angiogenic agents would be beneficial. Furthermore, since a number of approved agents can manifest deleterious effects on normal angiogenesis, a relevant *ex vivo* system to measure side effects of drugs would be clinically applicable as well.

This served as the motivation to take advantage of the model previously introduced and examine its efficacy as a simple and reproducible *ex vivo* assay for anti-angiogenic drug screening studies. To validate the model, we took advantage of two well-known anti-angiogenic drugs: Sunitinib, which is a tyrosine kinase inhibitor targeting VEGFR-2 [74], and bevacizumab, a known VEGF-A inhibitor that was approved by the FDA in 2004 under the name Avastin for combined use with chemotherapy in colon cancer treatment [75]. After validation, the model was used in a drug repositioning study

to determine anti-angiogenic effects of different combinations of nelfinavir/curcumin. Nelfinavir and curcumin were selected for the study because nelfinavir causes endothelial dysfunction [76,77] and curcumin, an anti-oxidant and NF- κ B inhibitory dietary supplement, is known to have anti-angiogenic effects [78]. Also, preliminary studies suggested that the combination of nelfinavir and curcumin can produce synergistic anti-cancer effects [79]. However, the effects of this combination on angiogenesis remain unknown.

Our results suggest that the rat mesentery culture model offers a pre-clinical drug-screening platform that enables observation of drug effects within an intact microvascular network with an innate hierarchical pattern.

3.2. MATERIALS AND METHODS

3.2.1 Rat Mesentery Culture Model

All animal experiments were approved by Tulane University's Institutional Animal and Care Use Committee. Rat mesenteric tissues were harvested and cultured according to our previous description [58]. Adult male Wistar rats (325 - 349 g) were anesthetized via intramuscular injection with ketamine (80 mg/kg body weight) and xylazine (8 mg/kg body weight). The mesentery was aseptically exteriorized [59] and rats were euthanized by intracardiac injection of 0.2 ml Beuthanasia. Then, mesenteric windows, defined as the thin, translucent connective tissues found between artery/vein pairs feeding the small intestine, were harvested, starting from the ileum section. Tissues were immediately rinsed in sterile PBS (Gibco) with CaCl_2 and MgCl_2 at 37 °C, and immersed in sterile MEM (Gibco) containing 1% PenStrep (Gibco). They were then transferred to individual wells in a 6-well culture plate. For drug studies, each tissue was quickly spread out on the bottom of a well and secured in place with a commercially available insert with polycarbonate filter and covered with 3 ml of MEM containing 1% PenStrep. Tissues were cultured in standard incubator conditions (5% CO_2).

3.2.2 Drug Testing Studies

To validate the ability of the time-lapse imaging method for evaluating the anti-angiogenic effects for a given drug treatment, two drug studies were conducted. In the first study, mesenteric tissues were cultured for 3 days according to the two experimental groups: 1) 10% serum (n= 8 tissues from 4 rats), and 2) 10% serum + sunitinib (5 μM ; Cayman Chemical Company; San Diego, CA) (n= 8 tissues from 4 rats). Sunitinib was

selected because it is a multi-targeted receptor tyrosine kinase inhibitor and has commonly been used to inhibit endothelial cell dynamics associated with angiogenesis in both *in vitro* and *in vivo* assays [10,74,80]. The concentration for sunitinib was selected based on previously published *in vitro* studies [81,82].

For the second drug exposure study, the same harvesting and culture procedure was followed for two experimental groups: 1) 10% serum (n= 8 tissues from 4 rats), and 2) 10% serum + bevacizumab (10 µg/ml; n= 8 tissues from 4 rats). Bevacizumab, commercially known as Avastin, was a gift from Genentech (San Francisco, CA). The bevacizumab was selected for this study for its well-known anti-VEGF properties [75]. The number of vessel segments per vascular area and the number of capillary sprouts per vascular area were quantified per tissue from 4x images of randomly selected network regions per tissue. To eliminate any false negative drug responses in drug treated tissues, tissues were analyzed only when correspondent tissues from the same rat showed growth caused by serum treatment. After drug testing validation, the model was used to investigate the anti-angiogenic effects of a given drug treatment. Nelfinavir and curcumin were selected for the study. Nelfinavir-mesyate powder was extracted and purified from Viracept tablets (Agouron pharmaceuticals; San Diego, CA) and curcumin was obtained from Acros Organics (Fair Lawn, NJ). For these drug exposure studies, mesenteric windows were harvested following the same procedure and cultured for 3 days according to the three experimental groups: 1) Control (n= 8 tissues from 4 rats), 2) Low Dose (1.5 µM nelfinavir + 4.5 µM curcumin; n= 7 tissues from 4 rats), and 3) High Dose (4.5 µM nelfinavir + 4.5 µM curcumin; n= 8 tissues from 4 rats). The number of vessels per

vascular area and the number of capillary sprouts per vascular area were quantified per tissue from 4x images of randomly selected network regions per tissue.

3.2.3. Image Acquisition

Images were acquired using 4x (dry, NA = 0.1), 10x (dry, NA = 0.3), and 20x (oil, NA = 0.8) objectives on an inverted microscope (Olympus IX70) coupled with a Photometrics CoolSNAP EZ camera.

3.2.4 Statistical Analysis

Data was analyzed in terms of change in number of vessel segments and number of capillary sprouts between day 0 and day 3. Mixed model regression methods were used to determine whether the change from day 0 to day 3 was significant and whether the amount of change was significantly different between drug dosages. Mixed model methods were used to control the non-independence of change scores measured on the same subject; reported means are adjusted for this correlation. Where possible, alternative nonparametric analyses were used to confirm the findings. All analyses were conducted using SAS version 9.3.

3.3. RESULTS

3.3.1 Time-Lapse Imaging Enables Evaluation of Anti-Angiogenic Drugs

To validate the efficacy of the rat mesentery culture model for drug evaluation, we tested a known receptor tyrosine kinase inhibitor, sunitinib, and a well-known anti-VEGF drug, bevacizumab. Comparison of microvascular networks before (Day 0) and after (Day 3) enabled identification of tissue specific responses. VEGFR-2 blockage via sunitinib treatment inhibited any angiogenic response (Fig. 3.1 and 3.2). 7 out of 8 control tissues displayed a dramatic increase in vascular density and capillary sprouting post-stimulation with 10% FBS. The presence of sunitinib in each of the treated tissues inhibited these responses. The mean increase in vascular density in control tissue was 92.1 vessel segments per area compared to 1.0 for the sunitinib treated group ($p < 0.05$). The mean increase in number of capillary sprouts per area was 13.8 vs 0.1 for control and treated tissues respectively ($p < 0.01$).

Bevacizumab treatment also served to inhibit the serum induced angiogenesis in cultured rat mesenteric microvascular networks. In this separate study, 8 out of 8 control tissues displayed a dramatic increase in vascular density and capillary sprouting post stimulation with 10% FBS (Fig. 3.3 and 3.4). Media supplementation with bevacizumab inhibited both the vascular density and sprouting responses (Figure 3.4). The mean increase in vascular density in the control tissue was 53.9 vessel segments per area compared to 5.0 for the bevacizumab treated group ($p < 0.05$). The mean increase in number of capillary sprouts per area was 16.9 vs 4.4 for control angiogenic and treated tissues respectively ($p < 0.05$).

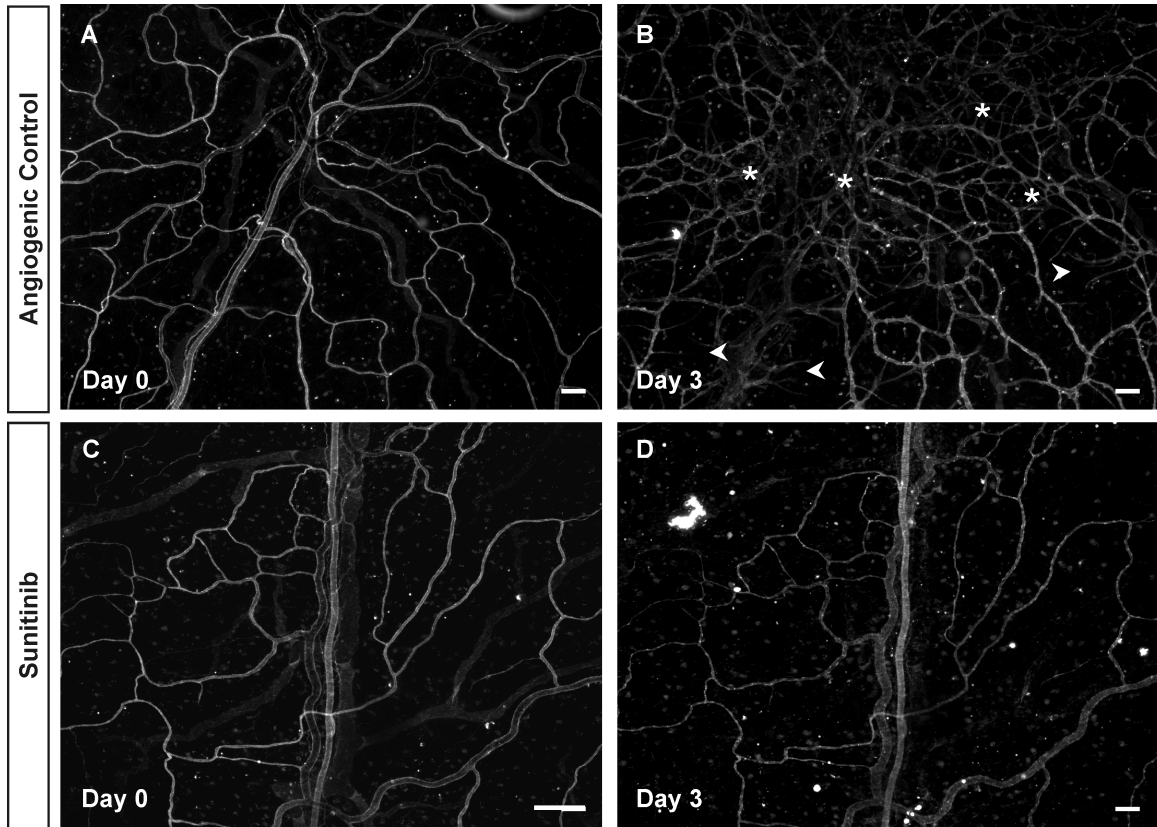


Figure 3.1 Inhibition of angiogenic response in microvascular networks by sunitinib. Examples of mesentery tissues stimulated with 10 % serum for 3 days with or without sunitinib treatment. A, B) Comparison of the same network labeled with BSI-lectin on day 0 and day 3 post-stimulation with 10% serum confirms a robust angiogenic response. Asterisks represent the regions with a higher vessel density, and arrowheads point to newly formed sprouts. C, D) Comparison of another network treated with sunitinib and labeled with BSI-lectin on day 0 and day 3 post-stimulation with 10% serum. The angiogenic response observed in the control group is inhibited with sunitinib treatment. Scale bars = 100 μ m.

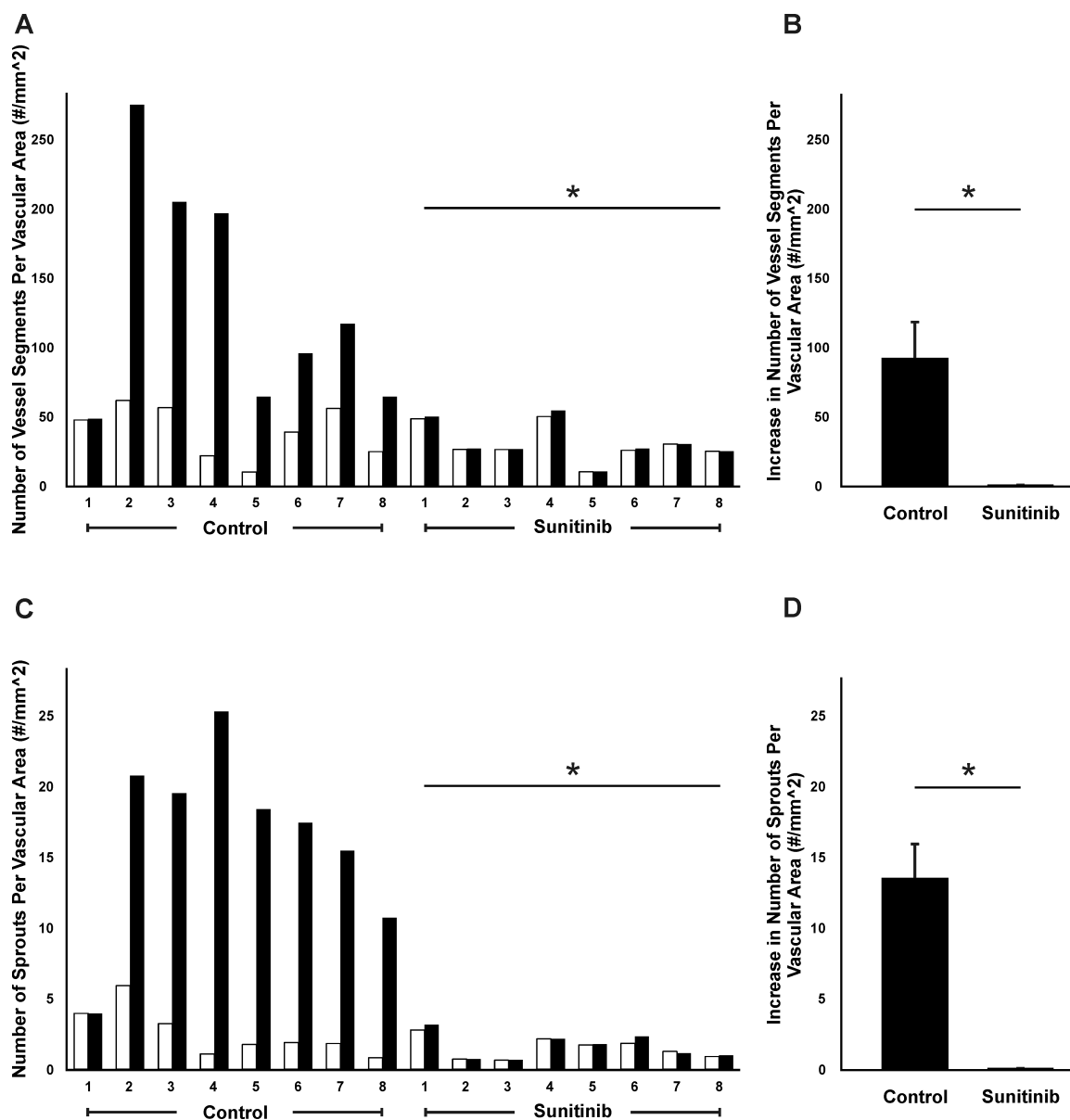


Figure 3.2 Quantification of angiogenesis inhibition following sunitinib treatment. The effect of 3-day exposure to sunitinib on 10% serum growth was evaluated based on two angiogenic metrics: Vessel density (A, B), and number of capillary sprouts (C, D) per vascular area. Control tissues were stimulated with 10% serum only. A, C) Each pair of bars represents a tissue. The average increase in vessel segments (B) and capillary sprouts (D) per area in control group is plotted against the sunitinib-treated group. * represents a significant difference between control and sunitinib groups ($p < 0.05$ for vessel segments and $p < 0.01$ for capillary sprouts). White bars represent day 0 (before) and black bars represent day 3 (after). Values are averages \pm SEM.

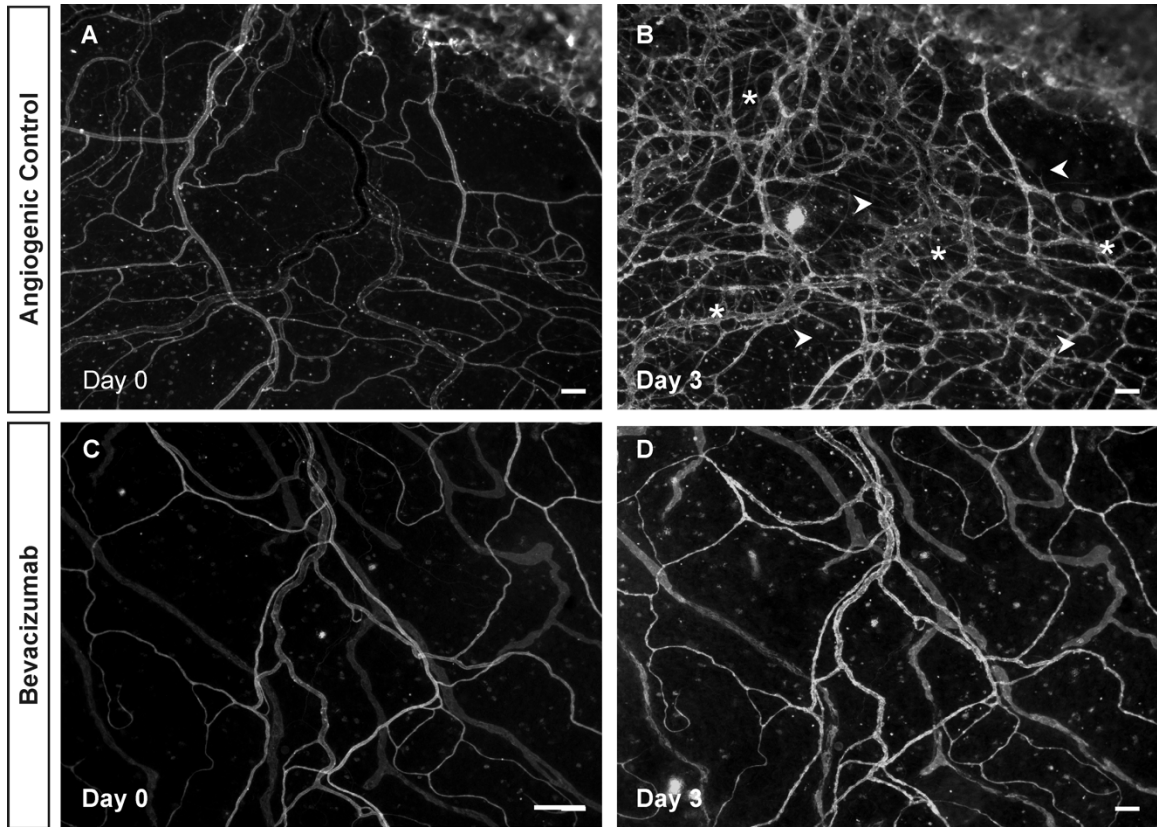


Figure 3.3 Inhibition of angiogenic response in microvascular networks by bevacizumab. Examples of mesentery tissues stimulated with 10 % serum for 3 days with or without bevacizumab treatment. A, B) Comparison of the same network labeled with BSI-lectin on day 0 and day 3 post-stimulation with 10% serum confirms a robust angiogenic response. Asterisks represent the regions with a higher vessel density, and arrowheads point to newly formed sprouts. C, D) Comparison of another network treated with bevacizumab and labeled with BSI-lectin on day 0 and day 3 post-stimulation with 10% serum. The angiogenic response observed in the control group is inhibited with sunitinib treatment. Scale bars = 100 μ m.

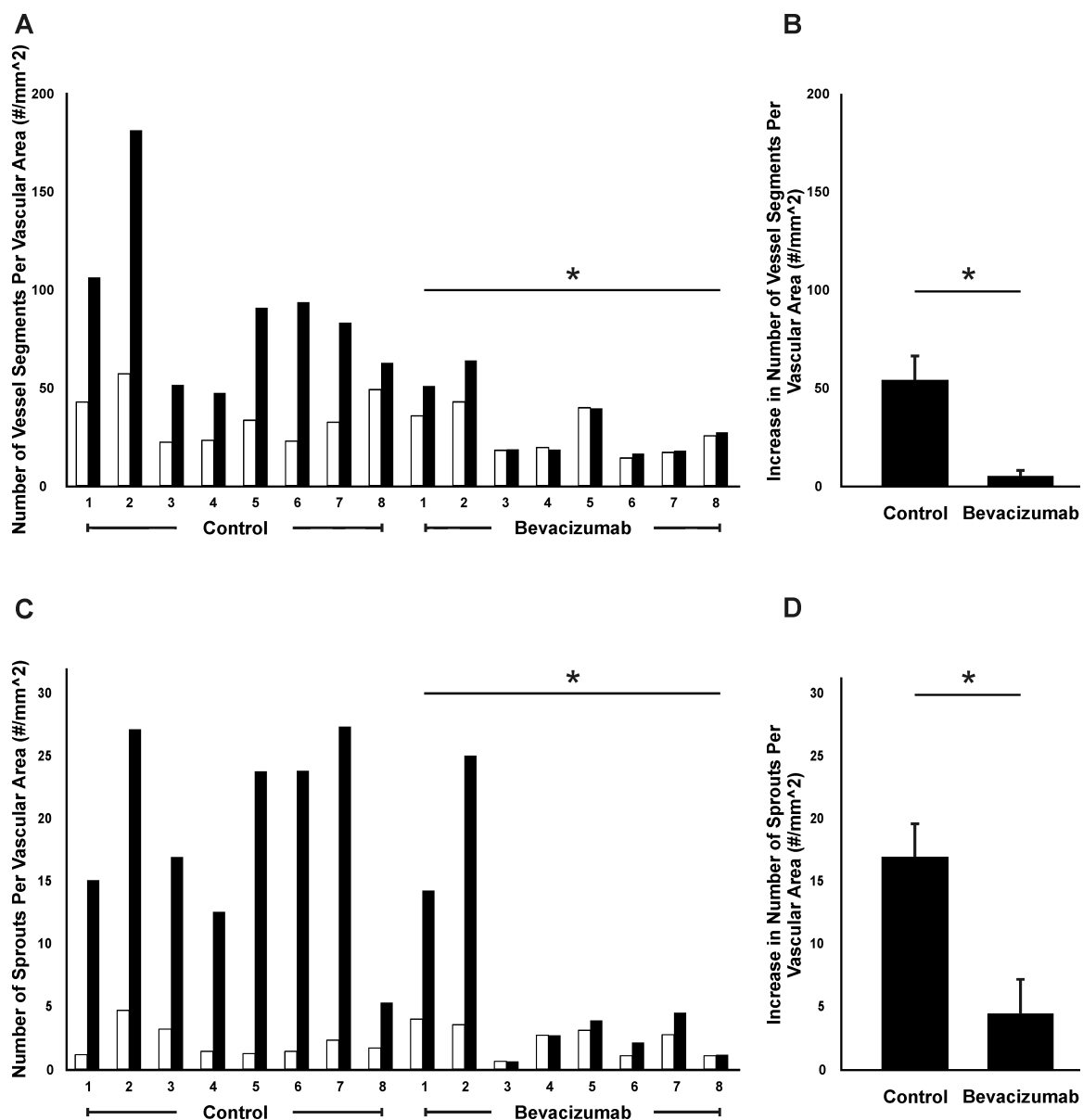


Figure 3.4 Quantification of angiogenesis inhibition following bevacizumab treatment. The effect of 3-day exposure to bevacizumab on angiogenic growth caused by 10% serum was evaluated by two angiogenic metrics: Vessel density (A, B), and number of capillary sprouts (C, D) per vascular area. Control tissues were stimulated with 10% serum only. A, C) Each pair of bars represents a tissue. The percentage of increase in vessel segments (B) and capillary sprouts (D) per area in control group is plotted against the bevacizumab-treated group. * represents a significant difference between control and bevacizumab groups ($p < 0.05$ for vessel segments and $p < 0.05$ for capillary sprouts). White bars represent day 0 (before) and black bars represent day 3 (after).

3.3.2 Time-Lapse Imaging Enables Kinetic Evaluation of Anti-angiogenic Drugs

Nelfinavir and curcumin were selected for this study, since nelfinavir is known to cause endothelial dysfunctions by suppressing PI3K/Akt signaling and nitric oxide (NO) production by endothelial cells [83], and curcumin is a potent anti-oxidant and NF- κ B inhibitory dietary supplement, known for its anti-angiogenic effects in tumor models *in vivo* [84]. Preliminary studies also suggest that the combination of nelfinavir and curcumin produce synergistic anti-cancer effects. To demonstrate the use of time-lapse imaging in our rat mesenteric culture model for identifying anti-angiogenic agents, we exposed the tissues to curcumin (4.5 μ M) in the presence of a low dose (1.5 μ M) or high dose (4.5 μ M) of nelfinavir for 3 days. Each tissue in the Control group (10% serum only) experienced a dramatic increase in angiogenesis (Figures 3.5 and 3.6). Increases in both vessel density and number of capillary sprouts per tissue were significantly diminished in the High Dose group compared to those in the Control group ($p < 0.001$), and the response was also attenuated in the High Dose group relative to the Low Dose group for both capillary sprouts ($p = 0.002$) and vessel density ($p < 0.001$). Differences between the Control and the Low Dose groups were not statistically significant.

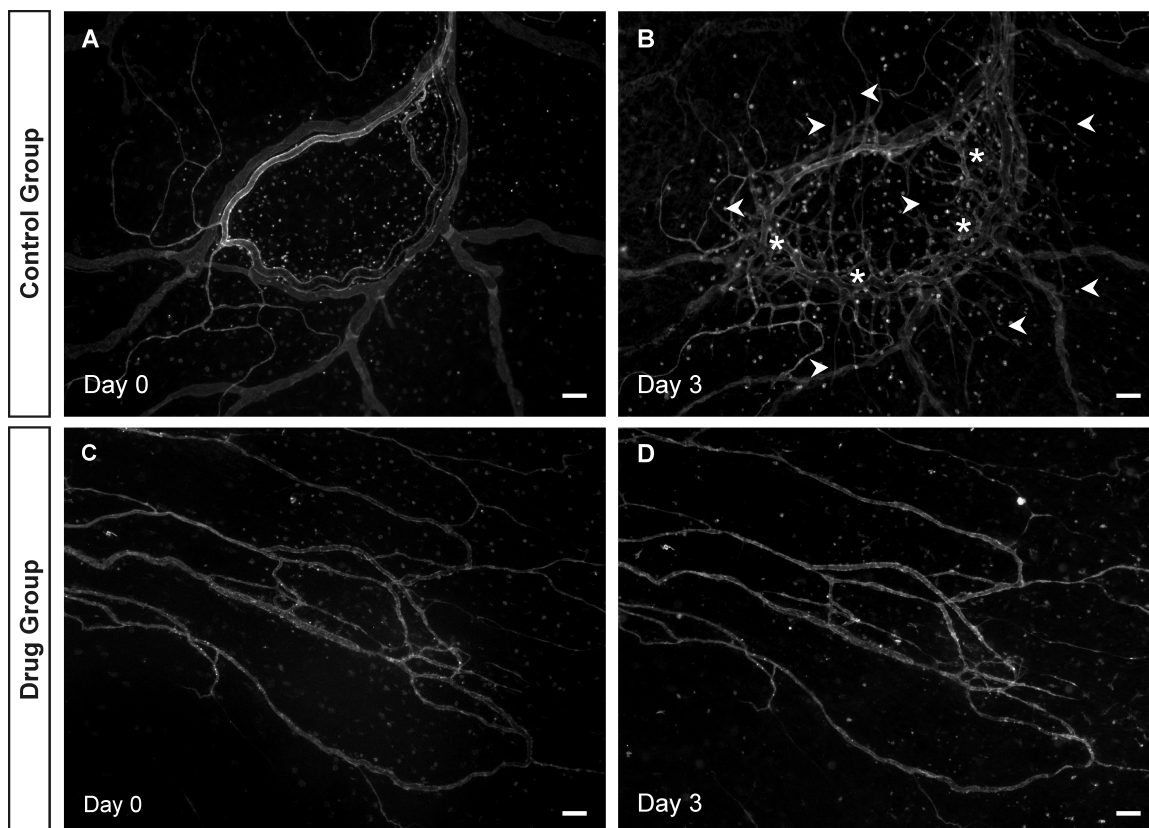


Figure 3.5 Time-lapse imaging of rat mesentery culture for drug testing combination of Nelfinavir/curcumin. A, B) Day 0 (before) and Day 3 (after) images for tissues stimulated with 10% serum (Control). Arrowheads indicate the newly formed sprouts caused by the stimulation. Asterisks show the regions with high vascular density. C, D) Day 0 (before) and Day 3 (after) images for tissues stimulated with 10% serum + 4.5 μ M nelfinavir + 4.5 μ M curcumin (High Dose) drug treatment. The capillary sprouting observed in the Control group is inhibited with drug treatment. Scale bars = 100 μ m.

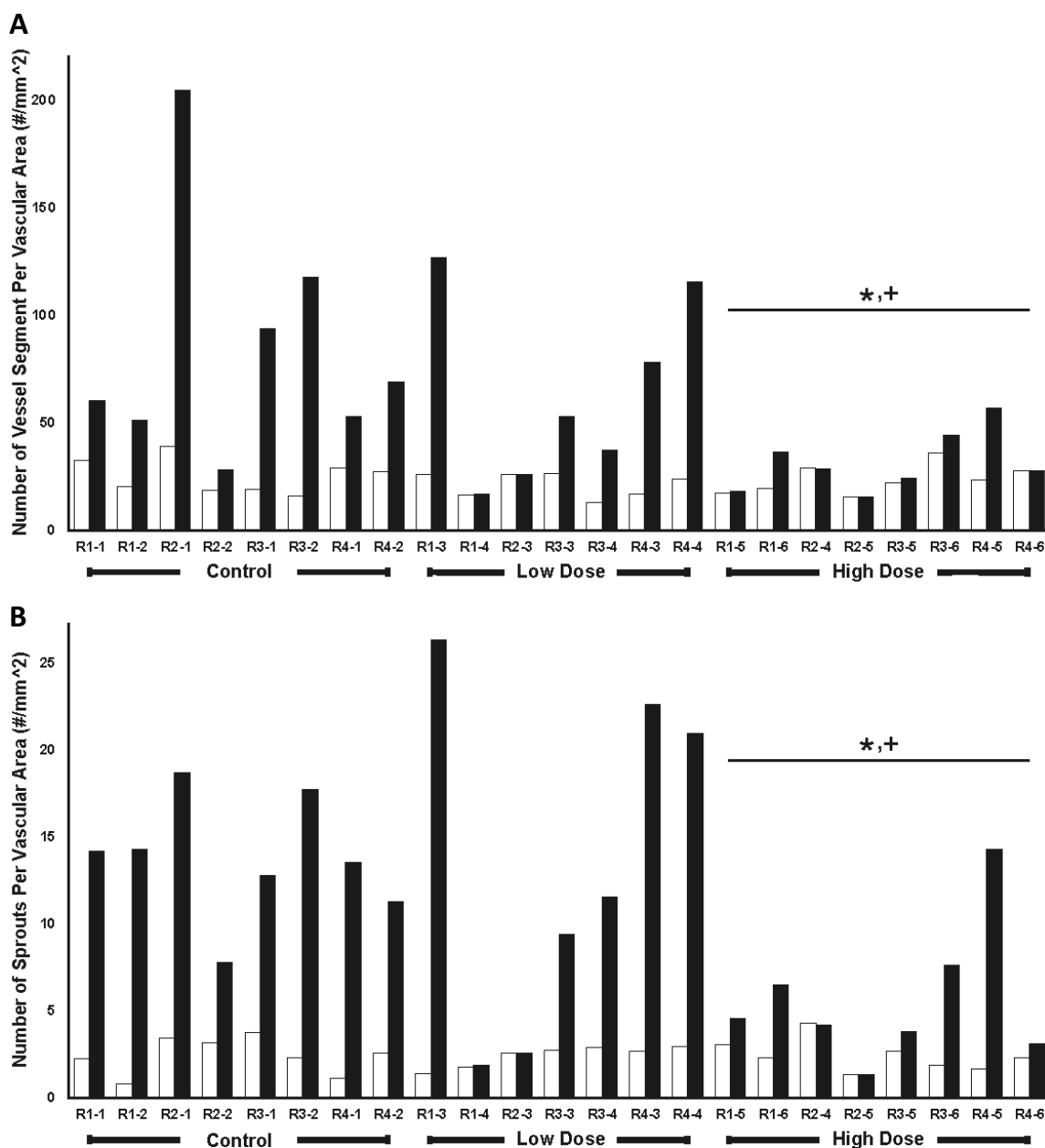


Figure 3.6 Quantification of angiogenesis for the drug testing study in untreated (Control), Low Dose and High Dose experimental groups. The effect of 3-day exposure to these drugs on 10% serum growth was evaluated for by vessel density (A), and the number of capillary sprouts per vascular area (B). White bars represent Day 0 (before). Black bars represent Day 3 (after). * and + represent statistical differences ($p < 0.05$ for both).

3.4 DISCUSSION

The results of this study support the use of the rat mesentery culture model as an *ex vivo* tool for anti-angiogenic drug evaluation on intact microvascular networks based on time-lapse imaging. Our initial introduction of the rat mesentery culture model for angiogenesis research established that it could be used for probing pericyte-endothelial cell interactions. Our current study expands upon our previous work and supports imaging in the rat mesentery culture model at multiple time points as a method for quantification of tissue-specific growth responses to different drug combinations.

The value of the rat mesentery for chemotherapy and anti-angiogenic drug testing is validated by numerous chronic *in vivo* animal studies [85,86]. Our study serves to expand the usefulness of this tissue by demonstrating the ability to evaluate drugs in an *ex vivo* scenario, which is more applicable for high content pre-clinical screening. Both bevacizumab and sunitinib are accepted anti-angiogenic drugs that target VEGF receptors on endothelial cells. Our results show that these agents are successful in overall inhibiting angiogenesis within our cultured networks. The variability in the responses to both drug treatments highlights the potential tissue-specific responses, which were discussed in the previous chapter in the context of the angiogenesis response to serum. Angiogenesis in local regions of a network is consistent with our previous report, and from a drug testing perspective, we speculate it would be useful to know where angiogenesis is stimulated within a network.

Similar to other *ex vivo* culture systems, a limitation of the rat mesentery culture model is that it lacks the presence of blood flow and related effects of shear stress, which had been shown to influence angiogenesis *in vivo* [63,64]. The recent development of

microfluidic-based assays has emphasized the importance of including shear stress in *in vitro* models [47,65,87]. While the rat mesentery culture lacks flow parameters, we feel that the top-down approach to maintain the multi-cell and multi-system complexity of a real microvascular network enables unique applications exemplified by our drug testing results.

Our drug treatment results support the use of the rat mesentery culture model for drug testing. For these studies, serum stimulated tissues were used as our control group because we were interested in showing the anti-angiogenic effect of drugs, and based on our previous report, 10% FBS stimulation causes robust microvascular growth compared to tissues cultured for 3 days in serum-free media. As an indicator of model robustness, 31 out of 32 serum-stimulated tissues from the three separate studies displayed a dramatic response. Moreover, the comparison of images before and after treatment reduces issues of variability that might influence non-paired statistical analysis. The explant specific responses to serum induced angiogenesis varied from 16% to 320% increases in vessel density and from 50% to 8000% increases in sprout density. Although the low number of existing sprouts in tissues before stimulation could be an explanation for some of the more drastic increases in the number of sprouts, the specific causes for this variation remain unknown. Nevertheless, the ability to quantify growth in the same tissue provides definitive evidence of whether a response occurred and enables the application of appropriate analytical methods to account for random variation among samples. Tissue specific responses were also present in our angiogenesis control groups for the sunitinib and bevacizumab studies. While an explanation of occasional lack of responses is

unclear, the concept of non-responders is consistent with other *ex vivo* models [88,89], and we speculate it might be associated with starting network size.

The anti-HIV agent, nelfinavir (viracept), which is being repositioned as an anti-cancer agent [90], is known to have anti-angiogenic effects as well [83]. In addition, the phytochemical curcumin (*Curcuma Longa*), with its known anti-cancer effects, is also known to inhibit angiogenesis [84]. Also, our preliminary studies suggest synergistic anti-cancer effects *in vivo* [79]. However, effects of nelfinavir/curcumin combination on angiogenesis remain unknown. This served as a motivation for investigating the anti-angiogenic effects of nelfinavir/curcumin combination. For both the Low Dose and High Dose drug treatment groups, the concentration of curcumin was 4.5 μM and the concentration of nelfinavir varied at 1.5 μM and 4.5 μM , respectively. The inhibitory effects on angiogenesis were different for these two groups, suggesting a more potent inhibition by nelfinavir than curcumin. The combined treatment with the high doses of drugs was able to suppress increases in both vascular density and capillary sprouting.

In summary, this study, for the first time, introduces a novel *ex vivo* method to evaluate an anti-angiogenic drug based on time-lapse imaging on an intact microvascular network. A challenge in evaluating angiogenesis therapies is the lack of realistic *in vitro* models. Our results meet this challenge and offer a simple and reproducible *ex vivo* assay to measure the effects of possible anti-angiogenic agents on vessel density and capillary sprouting across the hierarchy of networks. We also envision the use of tissues harvested from pathological rat strains will enable the investigation of how anti-angiogenic therapies are influenced by disease states.

3.5 FUTURE STUDIES

There are many *in vitro* and *in vivo* studies that examine the anti-angiogenic properties of drugs. However, often the drug dosage used in the studies are vastly different from each other. The difference can be contributed primarily to the disparity in the experimental setting. The fact that in most of the *in vivo* experiments, the drugs are administered systemically requires a high dose of active ingredients, whereas the *in vitro* experiments target a much smaller number of cells, and thus require a lower dose of the drug. This proves challenging when attempting to replicate these studies in *ex vivo* settings. Therefore, it's imperative to investigate how the variability and dose sensitivity for the rat mesentery culture model compares to these other angiogenesis assays.

Future studies will be needed to test the effects of curcumin and nelfinavir alone, and at different dose combinations. These studies may enable the delineation of mechanisms of action for each of these drugs, and may elucidate their side-effects profile and potential as anti-angiogenic agents.

Future work is also required to determine how long the mesenteric tissues remain viable in the current model. As mentioned in section 2.4.1., we demonstrated that post-angiogenesis images can be obtained out to 5 days with minimal cell death. Our observations revealed that even though the tissue remains mostly alive after 7 days, microvascular networks start to lose their structural hierarchy. This could be contributed mainly to the lack of shear stress derived from the blood flow present in *in vivo* scenarios. To overcome this limitation, a new project is currently underway in our lab to cannulate the mesenteric vessels and introduce flow to the system. This would offer an excellent opportunity to conduct long-term studies on of the microvascular dynamics, as well as the

effects of anti-angiogenic drugs. Building upon that, the potential drug compounds could be added to the intraluminal solution, instead of the surrounding media, to better analyze the effects of the new drugs in a more physiologically relevant framework.

CHAPTER 4: INVESTIGATING STEM CELL FATE USING RAT MESENTERY CULTURE MODEL

4.1. INTRODUCTION

The use of stem cells to manipulate microvascular networks offers a promising approach for targeting angiogenesis and cells present in microvasculature, to treat pathological conditions such as infarctions, cancers, retinopathy of immaturity (ROP), diabetic retinopathy, etc. [91-94,33]. In the traditional method of therapies, small molecules, larger biomolecules, or proteins are used to impact cells and signaling pathways to stimulate or inhibit angiogenesis. These treatments are often limited to one or a few molecules and the effects of the drug on the microvascular environment is one-way. In comparison, cell-based therapies deliver stem cells exogenously to the site of the injury and interact with the microvascular environment. These interactions influence the migration preference, cell-to-cell signaling, and cytokine secretion by both stem cells and resident cells, just to name a few. Another advantage is the fact that the stem cells are continually in communication with the environment, so their effects and incorporation patterns are dynamically tuned by local chemical and mechanical cues they receive from surrounding cells and extracellular matrix.

Aging can be defined as gradual loss of competency of cells and their functions in the body over time. This is usually accompanied by a risk increase in pathological conditions such as cancer [95], and cardiovascular diseases [72], and adverse effects on

regenerative processes such as wound healing [96]. One of the hallmarks of aging is stem cell exhaustion which can manifest itself in a decline in the number of stem cells, as well as the regeneration capabilities of the tissues [97]. For example, studies have reported that aged Bone-Marrow derived Stem Cells (BMSCs) show a decline in proliferation and differentiation potential, and exhibited a higher expression of p53 and p21, both indicative of cellular senescence [98,99]. More studies are needed about the effects of aging on stem cells to answer questions about differentiation capabilities and cell dynamics of stem cells in microvascular settings.

Mesenchymal Stem Cells (MSCs) are resident stem cells that can be found in and isolated from many sources such as bone marrow, adipose tissue, and blood [100]. These multi-potent cells have been used in recent years to promote angiogenesis by cytokine signaling, as well as differentiation into endothelial and perivascular cells [101-103,33].

While MSCs derived from bone marrow and adipose tissue have been shown to enhance angiogenesis via paracrine signaling and direct cell incorporation [104,42], our understanding of how to manipulate them or target where they go within a tissue remains relatively unclear. Previous studies have shown the incorporation of Adipose-derived Stem Cells (ASCs) into the retinal microvascular network as new pericytes [33], but choosing the best candidate requires screening different cell types, preferably in the presence of a microvascular network. New models can help answer those questions and add to our knowledge about the cell fate and its function within intact microvascular networks.

As previously described in Chapter two, our lab has recently developed the rat mesentery culture model for studying endothelial cell dynamics in an *ex vivo* scenario.

Taking advantage of the model, we delivered stem cells to the microvascular networks using two methods: cell seeding and cell printing via laser-direct write method. In both methods, MSCs were labeled with cell tracker DiI, delivered, and cultured with mesentery tissues for up to 5 days. Data from cell printing proved that the protocol enables the stem cells to adhere to the tissue and migrate from the original spots. The same result was observed in cells seeded onto the mesentery tissues. The effects of aging and the stem cell type on differentiation of cells into pericytes were investigated using ASCs and BMSCs. Blood vessels were visualized and imaged and the percentage of stem cells differentiated to pericytes was quantified in each tissue. The angiogenic effect of the stem cells was also measured after 5 days in select groups.

This aim validated the rat mesentery culture model as a platform to track stem cells and study their differentiation fate in a microvascular setting. The results confirmed that MSCs can be seeded onto the mesentery tissue and cultured for up to 7 days. The stem cells remained viable, penetrated the mesentery, and started migrating within the tissues as soon as day 1. After 5 days, a subset of seeded cells got incorporated into the microvascular networks in pericyte locations expressing pericyte markers with morphologies resembling pericytes, at a rate consistent with other studies. This study highlights the importance of donor selection and the variability between individual donors, and sheds light on the effects of stem cells on angiogenesis.

4.2. MATERIALS AND METHODS

4.2.1. Rat Mesentery Culture Model

All animal experiments were approved by Tulane University's Institutional Animal and Care Use Committee. Adult male Wistar rats (325-349 g) were anesthetized via intramuscular injection with ketamine (80 mg/kg body weight) and xylazine (8 mg/kg body weight). The mesentery was aseptically exteriorized and rats were euthanized by intracardiac injection of 0.2 ml Beuthanasia. The mesenteric windows, defined as the thin, translucent connective tissues found between artery/vein pairs feeding the small intestine, were harvested, starting from the ileum section. Tissues were immediately rinsed in sterile PBS (Gibco) with CaCl_2 and MgCl_2 at 37 °C, and immersed in sterile MEM (Gibco) containing 1% PenStrep (Gibco). Each tissue was quickly spread out on a commercially available insert (Sigma-Aldrich) with polycarbonate filter.

4.2.2. Stem Cell Isolation and Expansion

4.2.2.1. ASCs Preparation

Human ASCs were obtained from 16 donors (2 groups, 8 donors per group) undergoing elective liposuction procedures, as previously described [105]. All protocols were reviewed and approved by the Pennington Biomedical Research Center Institutional Review Board, and all human participants provided written informed consent. Briefly, ASCs were isolated from processed liposuction aspirates from the subcutaneous abdominal adipose tissue of adult (29.3 ± 6.4 years) or aged (62.5 ± 6.6 years) patients. Liposuction aspirates were incubated in 0.1 % type I collagenase (Sigma-Aldrich) and 1 % BSA (Sigma-Aldrich) dissolved in 100 ml of PBS (Gibco) supplemented with 2 mM

calcium chloride. The mixture was placed in a 37 °C shaking water-bath or incubator at 75 rpm for 60 min and then centrifuged to remove oil, fat, primary adipocytes, collagenase solution and cellular debris. The resulting cell pellet was re-suspended in stromal medium, which consisted of Dulbecco's Modified Eagle Medium F-12 (DMEM/F12; Hyclone; Logan, UT), 10 % FBS (Hyclone), 1 % antibiotic/antimycotic (Fisher Scientific; Houston, TX), and plated at 100-200 cells per cm². Fresh stromal medium was added every 2 to 3 days until cells achieved 70-80% confluence, at which time cells were harvested with 0.25 % trypsin/1 mM Ethylenediaminetetraacetic acid (trypsin/EDTA; Gibco) and cryopreserved prior to experimental use.

4.2.2.2. BMSCs Preparation

Primary human BMSCs were obtained from 16 healthy consenting Caucasian female donors under protocols approved by Tulane University Institutional Review Board and the Partners Human Research Committee. Younger donors were an average age of 25.9 ± 5.5 years, while older donors were an average of 55.9 ± 6.1 years. Donors in the two groups differed in age but had no other significant demographic differences including BMI. The cells were prepared from bone marrow aspirates taken from the iliac crest. Briefly, bone marrow aspirates were isolated from the iliac crest of normal adult donors using a density gradient (Ficol-Paque; Amersham Pharmacia Biotech; Milwaukee, WI) and cultured in complete culture media (CCM), which consisted of α -MEM (Gibco), 20% serum (FBS; Atlanta Biologicals; Lawrenceville, GA), 1% PenStrep (Gibco), and 2 mM L-glutamine (Gibco). Fresh CCM was added every 2-3 days until cells reached 70% confluence. When the cells were confluent, cells were washed with PBS (Gibco),

harvested with 0.25% trypsin/1 mM EDTA (Gibco), and cryopreserved prior to experimental use.

4.2.2.3. Cell Culture

Frozen vials of ASCs and BMSCs were thawed and cultured in complete culture medium and incubated at 37 °C with 5% humidified CO₂. After 24 hours, medium was removed and adherent, viable cells were washed with PBS, harvested with 0.25% trypsin/1 mM EDTA (Gibco), and re-plated at 10 cells/cm², 50 cells/cm², 100 cells/cm², and 1,000 cells/cm² on 60-cm² dishes. Medium was replaced every 3–4 days.

4.2.3. Stem Cell Seeding on Mesentery Tissues

Stem cells were suspended in media at a 1 million cell/ml concentration, mixed with 5 µl/ml cell tracker CM-DiI or DiO (both Molecular Probes; Eugene, OR), and incubated at 37 °C for 30 min. The cell suspension was centrifuged at 1000 rpm for 5 min and the media was replaced with fresh media. Cell were then resuspended in the media again, and washed for two more times. The cell suspension concentration was then brought down to 500 thousand cells/ml and 100-200 µl was placed on top of the mesentery tissue, based on our preliminary trials (data not shown). The co-culture was placed in incubator for 20 min to give the stem cells enough time to adhere to the mesentery tissue. After that, the supernatant was aspirated, and the co-culture was transferred to a well in a non-tissue culture treated 6-well plate. The insert was then covered with 4 ml of media supplemented with 1% serum and cultured for up to 5 days (Fig. 4.1).

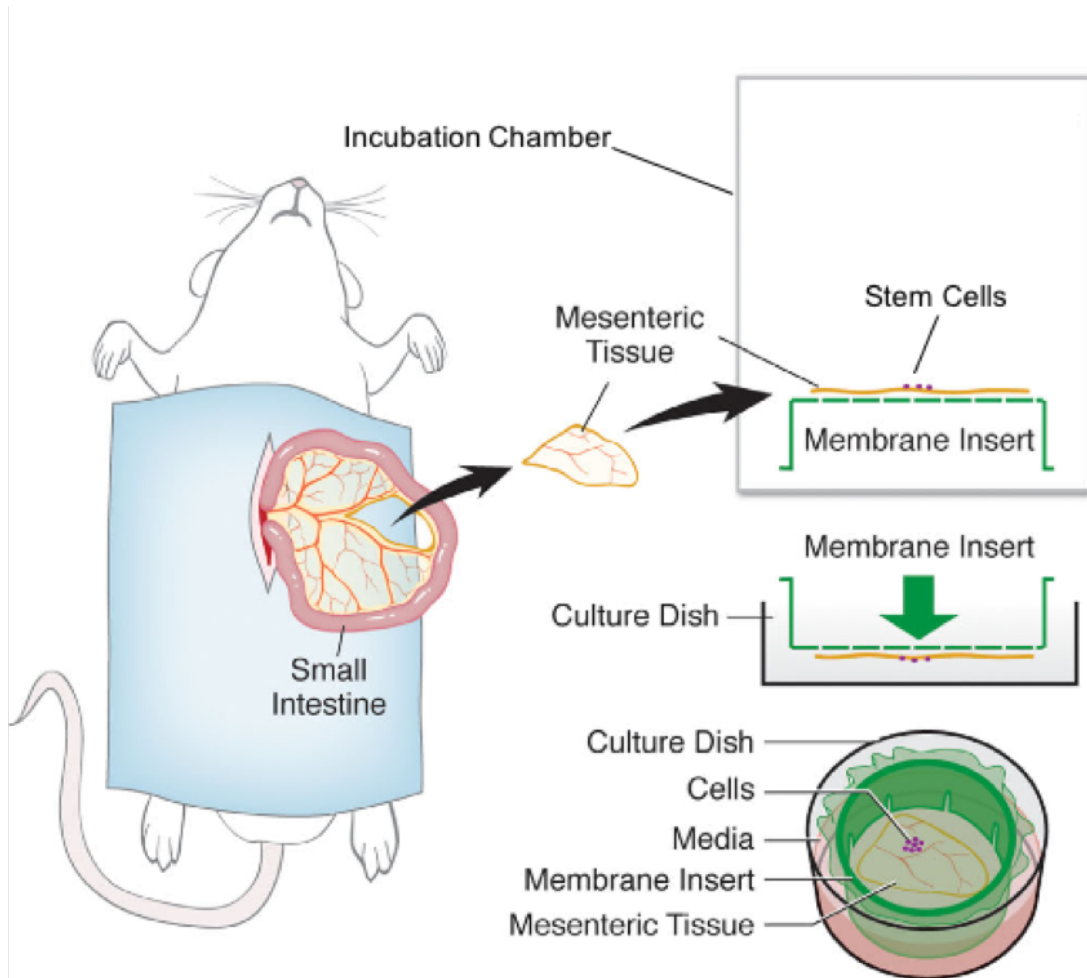


Figure 4.1 Schematic of stem cell seeding on mesentery tissue. Mesenteric tissue is harvested following the protocol described in 4.2.1. and cells are seeded on top of the mesentery tissue based on 4.2.3.

4.2.4. Printing Stem Cells by Laser-Direct Write Method (LDW)

MSCs were printed onto the mesentery tissues as previously described [106,107]. Briefly, UV-transparent quartz disk, or ribbon, was spin-coated at 2,000 rpm to generate a ~ 30 μm thick layer of liquefied 20% w/v gelatin (Type A porcine, 300 Bloom; Sigma Aldrich). A 1-ml suspension of trypsinized RFP-positive or DiI-labeled ASCs at 2 million cells/ml was pipetted onto the coated ribbon surface. The ribbon was placed in an incubator for 7 min followed by 5 min of incubation at room temperature to partially embed cells in the liquefied gelatin layer and solidify the gelatin, respectively. Excess media was blotted prior to cell printing. Ribbons were then inverted to face the flattened mesentery tissues for cell transfer. Both the ribbon and cell insert supports were loaded onto parallel holders with independently-motorized XY translation for computer-aided design/manufacturing ability. The working space environmental conditions were set at 21 $^{\circ}\text{C}$ and 45% relative humidity. A single pulse of 193 nm ArF excimer laser (near-Gaussian distribution, pulse width = ~ 8 ns, fluence = 0.42 ± 0.01 J/cm^2 ; Precision Microfab, Curtis Bay, MD) interacted with the sacrificial gelatin layer on the ribbon, forming a local vapor pocket that ejected a single droplet of cell suspension onto the tissue. Subsequent groups of cells, targeted in real-time with the aid of an *in situ* camera, were additively deposited into computer-programmable positions to complete the array patterns. Following the printing procedure, the cells were placed in a standard incubated for 12 min to initialize cell attachment to the tissue. Afterwards, 50 μl of media supplemented with 10% FBS (Gibco) was pipetted onto the tissues and incubated for another 20 min to further cell attachment. Finally, the cell crown was inverted and

inserted into a 6-well plate, such that the tissues were wedged between the membrane and well bottom and cultured (Fig. 4.2).

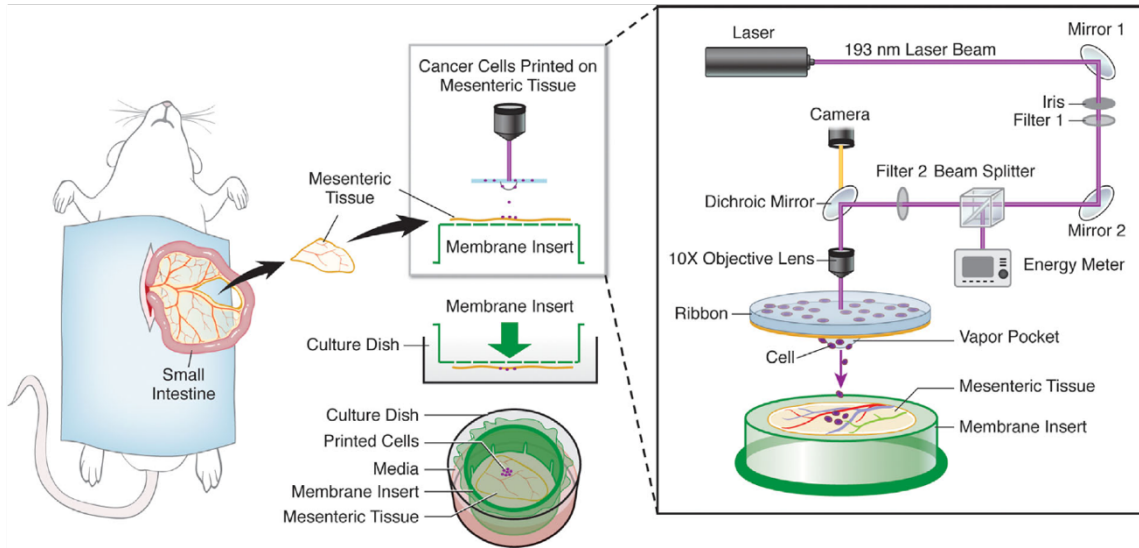


Figure 4.2 Schematic of stem cell printing on mesentery tissue using laser-direct write (LDW) method. Mesentery tissue is harvested following the protocol described in 4.2.1. and cells are printed on top of the mesentery tissue based on 4.2.4. Adopted from [122].

4.2.5. Stem Cell Location Investigation

Mesentery tissues were labeled with BSI-lectin to visualize blood and lymphatic vessels. To accomplish that, the culture media was supplemented with BSI-lectin conjugated to FITC (1:40; Sigma-Aldrich). Tissues were then incubated for 30 min under standard culture conditions. After the incubation, the lectin-supplemented media was removed, and tissues were washed with lectin-free media. Labeling with BSI-lectin identified all blood and lymphatic vessels in green and blood vessels were identified from lymphatics based on their morphology, network structure, and the intensity of lectin labeling. The culture plates were then placed into a culture chamber mounted on the microscope stage to ensure maintaining the temperature at 37 °C. Two to four microvascular networks were imaged per tissue using an inverted epifluorescent microscope. Stem cells were also imaged in red, and the two channels were superimposed to get the final image, showing stem cells within the microvascular network. Based on the experiment, the co-culture was imaged at different time points up to day 5. For tracking stem cells, the coordinates of the motorized microscope stage were recorded and used to ensure that the same microvascular network region was re-imaged. After day 5, tissues were labeled for perivascular markers.

4.2.6. Immunohistochemistry

Cultured tissues were fixed in methanol-free 4% formaldehyde solution for 10 min at room temperature. The formaldehyde solution was made by making a 1:3 solution of Pierce 16% formaldehyde (Thermo Scientific; Waltham, MA) with PBS. Tissues

where then rinsed in PBS three times for 10 min each, mounted on glass slides, and labeled against endothelia and pericyte markers.

PECAM/NG2: 1) 1:200 mouse biotinylated monoclonal PECAM antibody (BD Pharmingen) + 1:100 rabbit polyclonal NG2 antibody (Millipore); 2) 1:500 Strep-CY2 (Jackson ImmunoResearch Laboratories) + 1:100 GAR-CY3 (Jackson ImmunoResearch Laboratories) + 5% NGS (Jackson ImmunoResearch Laboratories).

Lectin/SMA: 1) 1:80 biotinylated BSI-lectin (Sigma-Aldrich) + 1:200 CY3-conjugated mouse monoclonal alpha-smooth muscle actin (alpha-SMA) (Sigma Aldrich); 2) 1:80 Alexa Fluor-350 Streptavidin secondary (Molecular Probes).

All antibodies were diluted in PBS + 2% BSA (Jackson ImmunoResearch Laboratories), and placed on tissues for 1 hour at room temperature unless specified otherwise. Between each step, tissues were rinsed with PBS for 10 min three times.

4.2.7. Quantification of Angiogenesis

To assess the angiogenic effect of stem cells on microvascular networks, tissues from 8 donors were randomly selected for angiogenesis quantification. Labeling with BSI-lectin identified all blood and lymphatic vessels and blood vessels were identified from lymphatics based on their morphology and network structure. The number of vessels per vascular area and the number of capillary sprouts per vascular area were quantified per tissue from 4x images of randomly selected network regions per tissue. Two to four fields of view were arbitrarily selected from the vascularized area to be representative of the microvascular networks. Blood vessel segments were defined as

lectin-positive blood endothelial cell segments present between two branch points and capillary sprouts were defined as blind ended segments originating from a host vessel.

4.2.8. Image Acquisition

Images were acquired using 4x (dry, NA = 0.1), 10x (dry, NA = 0.3), 20x (oil, NA = 0.8), and 60x (oil, NA = 1.4) objectives on an inverted microscope (Olympus IX70) coupled with a Photometrics CoolSNAP EZ camera. Image analysis and quantification were done using ImageJ 2.0.0-rc-54 (U.S. National Institutes of Health, Bethesda, MD). Confocal microscopy images were captured with a 40x objective (NA = 1.3) on a Nikon A1 confocal microscope equipped with 405, 488, and 561 nm diode laser lines, coupled with an ECLIPSE Ti Nikon inverted microscope.

4.2.9. Statistical Analysis

Comparison between experimental groups were made using two-tailed Student's t-test, and one-way ANOVA with Tukey's multiple comparisons post-hoc tests, when appropriate. Results were considered statistically significant when $P < 0.05$. Pearson's correlation coefficient (r) was calculated for linear correlation studies between angiogenic metrics and the percentage of stem cells in pericyte locations. The strength of correlation was considered weak if $0.1 \leq r < 0.30$, moderate if $0.30 \leq r < 0.50$, and strong if $0.50 \leq r$, based on conventions set by Cohen [108]. Statistical analysis was performed using Prism version 7 (Graphpad Software). Values are presented as mean \pm SEM.

4.3. RESULTS

4.3.1. Rat Mesentery Culture Model Enables Tracking of MSCs

BSI-lectin labeling visualized the microvascular structures within the mesentery tissue, and helped to identify the location of DiI-labeled stem cells in relationship to microvascular structures. Imaging after the initial seeding confirmed the presence of MSCs in the co-culture. Cells were found on the same focal plane as microvascular networks, and they began to spread out and adopt a spindle-like morphology, typical of MSCs, as soon as day 1 (data not shown). The movement of cells was tracked over the 5 days of culture (Fig. 4.3). Live-dead assay on day 5 confirmed that a significant number of cells stay alive up to 5 days (data not shown). Cell migration was confirmed both in seeded and printed cells. Images on day 0 from the cell printed using the LDW method showed distinct cell spots, but after 2 days, the initial spots disappeared and were replaced with a more uniform collection of cells. This confirmed the movement of cells away from the original spots and across the mesentery tissue (Fig. 4.4)

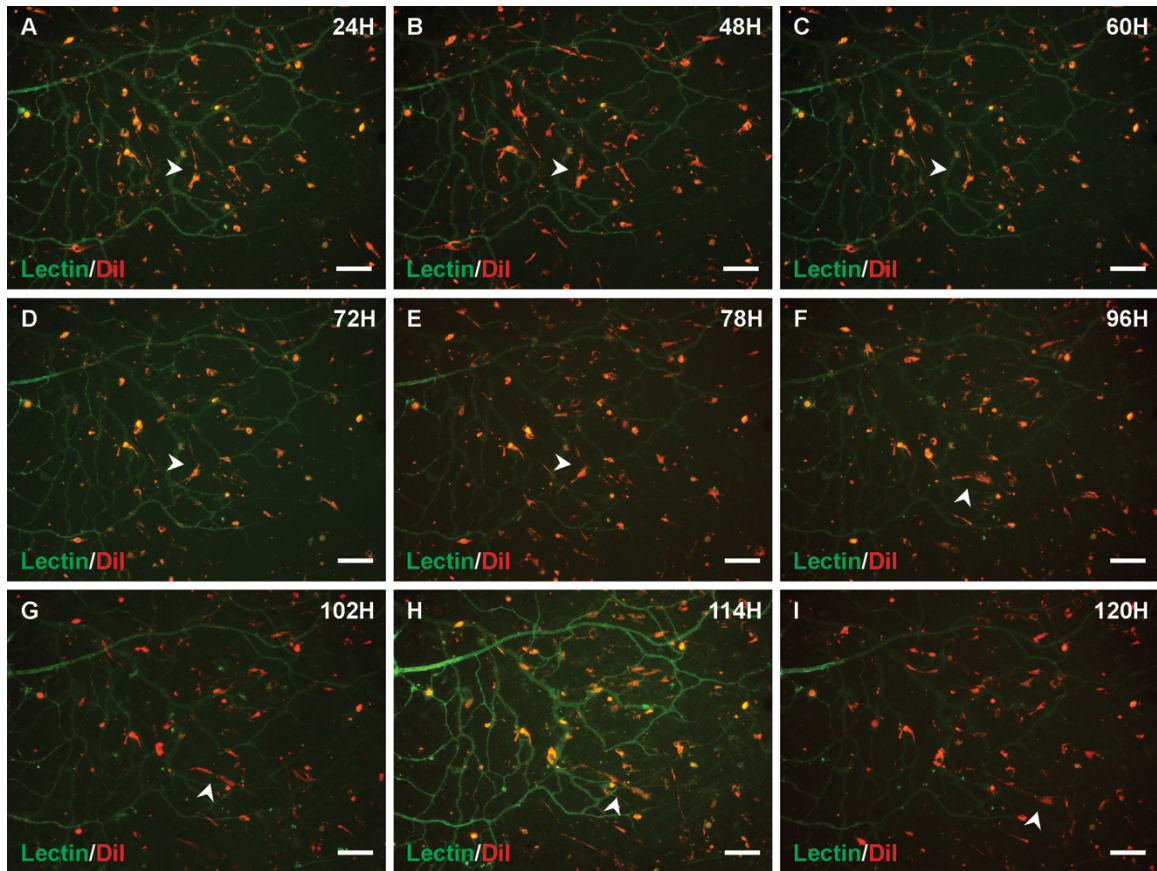


Figure 4.3 Tracking seeded MSCs within mesentery tissue for 5 days. The DiI-labeled MSCs spread out and start migration after 34 hours (A). The arrowhead points to an example of MSCs, and tracks the cell from day 1 to day 5 (A-I). Scale bar = 100 μ m.

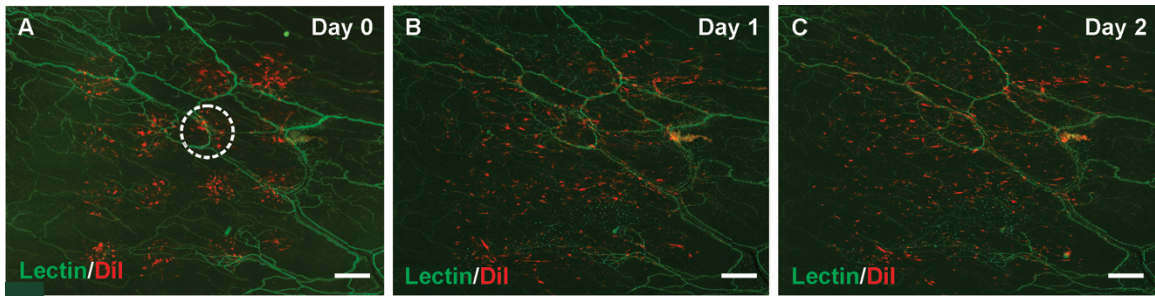


Figure 4.4 Tracking printed MSCs within mesentery tissue for 3 days. The DiI-labeled MSCs were printed onto 16 distinct spots using LDW method. Cells attached to the mesentery in their patterned spots on day 0 (A), but by day 2, time lapse imaging confirms cell migration away from the initial position (C). The circle outlines one of the spots as an example. Scale bar =500 μ m.

4.3.2. MSCs Can Differentiate into Pericytes After 5 Days in Rat Mesentery Culture Model

After 5 days of culture, a subset of stem cells was found in locations typical of vascular pericytes (Fig. 4.5). The pericyte identity was confirmed with the morphology acquired after 5 days. Stem cells wrapped around the capillaries and displayed pericyte morphology, an indicator of differentiation into vascular pericytes. Furthermore, immunolabeling revealed pericyte markers expression, such as NG2 and alpha-SMA in the cells present in perivascular locations (Fig. 4.6 and 4.7).

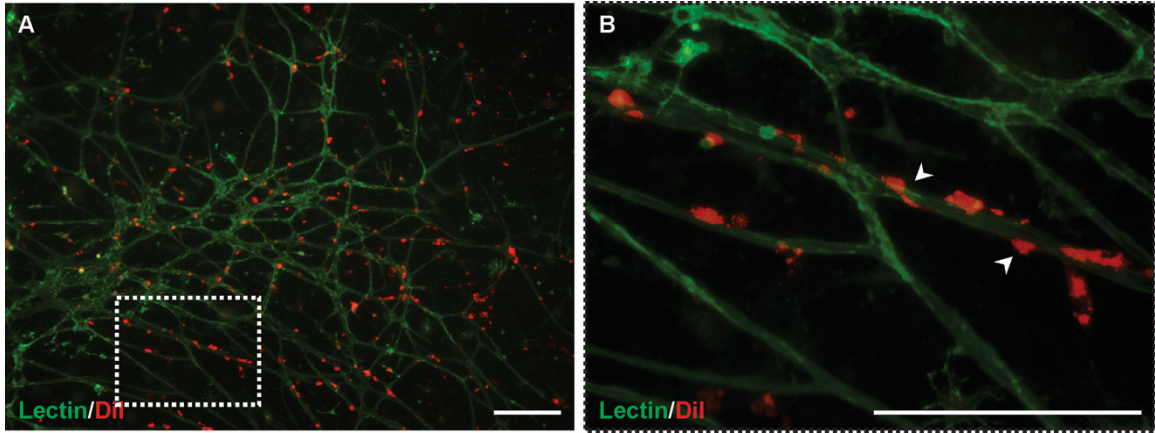


Figure 4.5 MSCs differentiation into vascular pericytes. (A) A subset of MSCs displayed pericyte location and morphology after 5 days. The outlined region was selected and higher magnification imaging was performed (B). The arrowheads point to examples of newly differentiated pericyte cells on lectin-positive capillaries. Scale bar =100 μm .

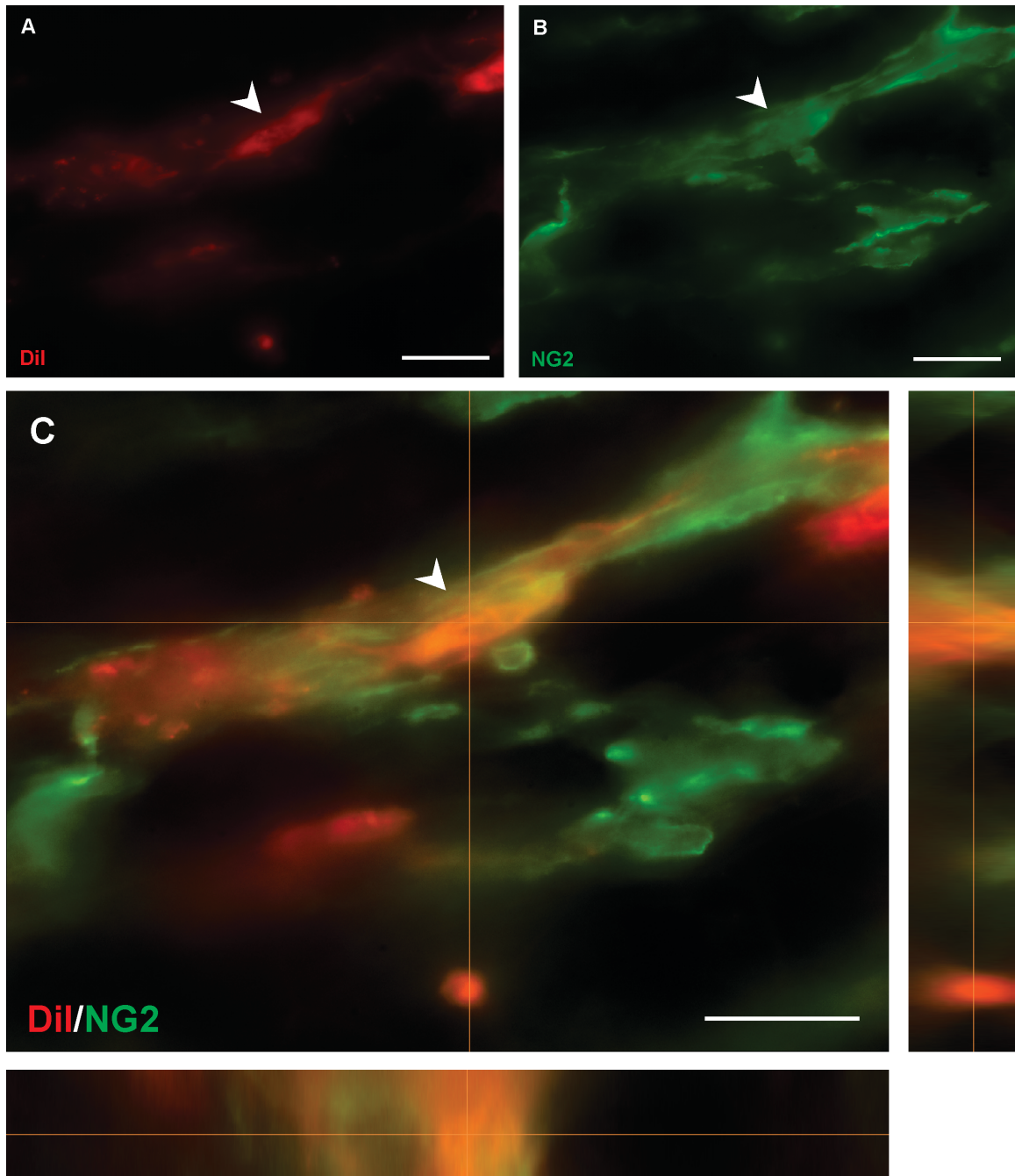


Figure 4.6 NG2 expression of MSCs in vascular pericyte locations. The Dil-positive MSCs in pericyte locations (A) expressing NG2 marker (B), a common pericyte marker. The arrowhead points to the cell and Z-stack imaging shows Dil and NG2 co-labeling on the cell (C). Scale bar =10 μm .

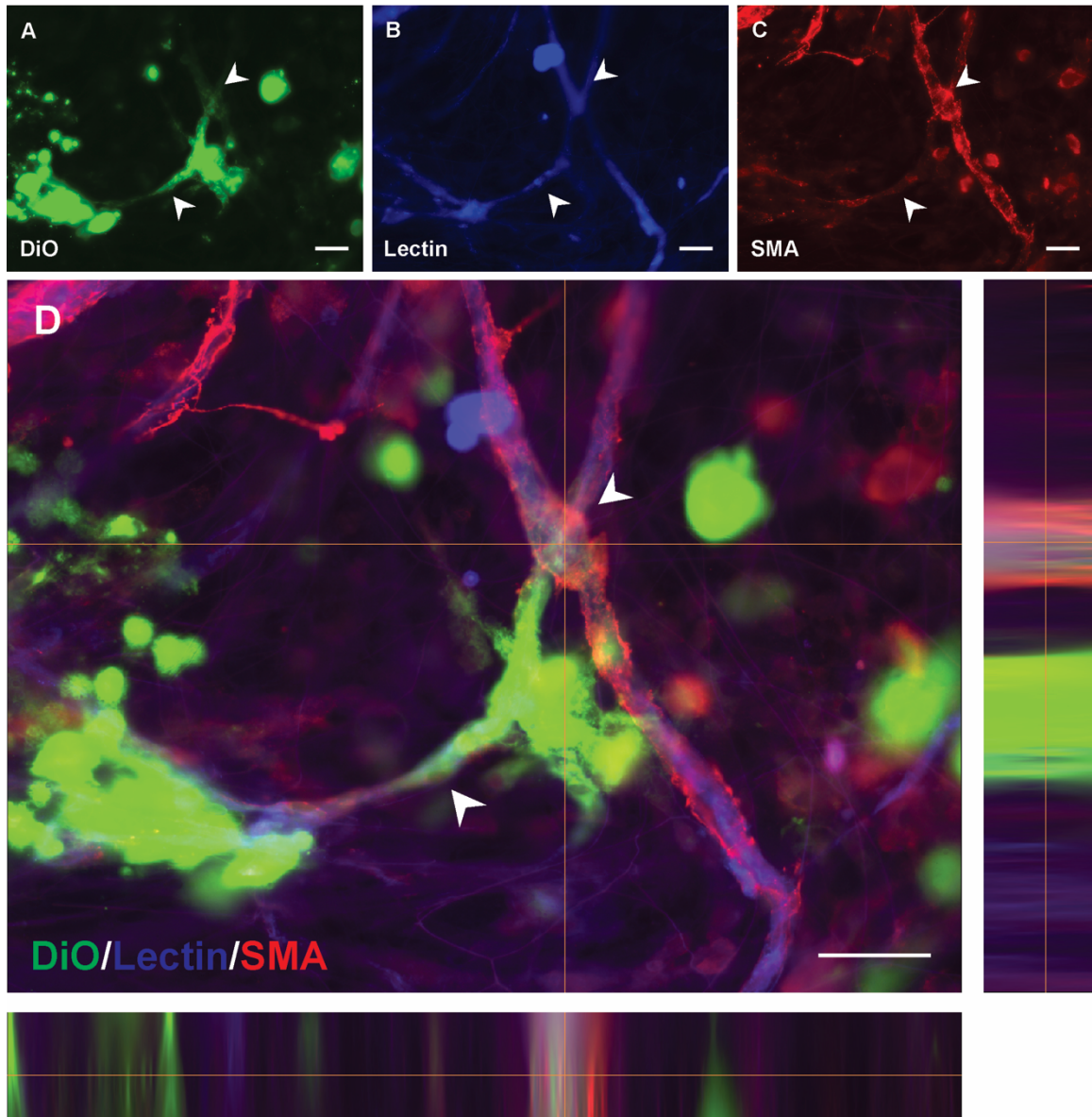


Figure 4.7 Alpha-SMA expression of MSCs in vascular pericyte locations. The DiO-positive MSCs (A) in pericyte locations (B), expressing alpha-SMA marker (C), another common pericyte marker. The arrowheads point to the cells and Z-stack imaging shows Lectin, DiO, and alpha-SMA co-labeling on the cell (D). Scale bar =20 μ m.

4.3.3. Age or Type Is Not a Deciding Factor in MSCs Differentiation to Vascular Pericytes

Our extensive donor studies showed no significant difference in pericyte differentiation rate between aged and adult stem cells. The source of the stem cells used in this study, adipose-derived vs bone marrow-derived, also did not make a significant difference in pericyte differentiation rate (Fig. 4.8). Significant differences were observed between individual donors, but the average pericyte differentiation rate remained close across different groups ($7.04 \pm 0.71\%$ for Adult ASCs, $5.87 \pm 0.60\%$ for Aged ASCs, $5.82 \pm 0.61\%$ for Adult BMSCs, $7.70 \pm 0.91\%$ for Aged BMSCs) (Fig. 4.9). The highest rate of cell incorporation belonged to our 1st old BMSC donor with $16.8 \pm 2.95\%$ and the lowest rate was $0.84 \pm 0.33\%$ in our 6th Adult ASC donor.

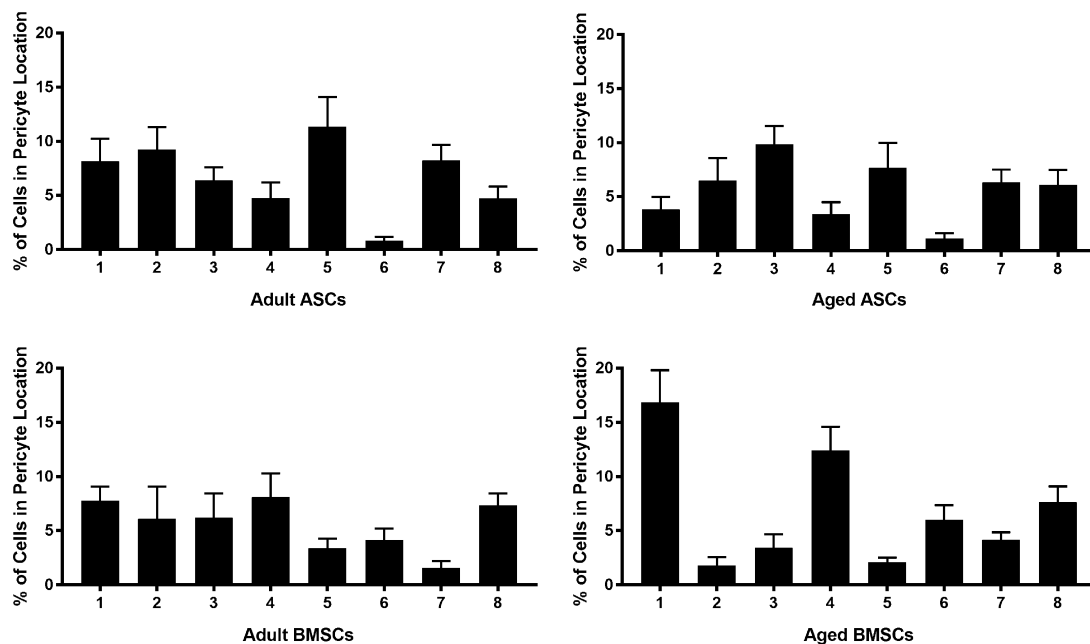


Figure 4.8 Incorporation of stem cells from different donors into microvascular networks. A subset of MSCs migrate towards the microvascular structures, and become pericytes. One-way ANOVA did not show a significant difference between adult ASC, aged ASC, adult BMSC, and aged BMSC groups. Each bar represents data from a donor. The highest rate of cell incorporation belonged to 1st aged BMSC donor with $16.8 \pm 2.95\%$ and the lowest rate was $0.84 \pm 0.33\%$ in 6th Adult ASC donor. Values are averages \pm SEM.

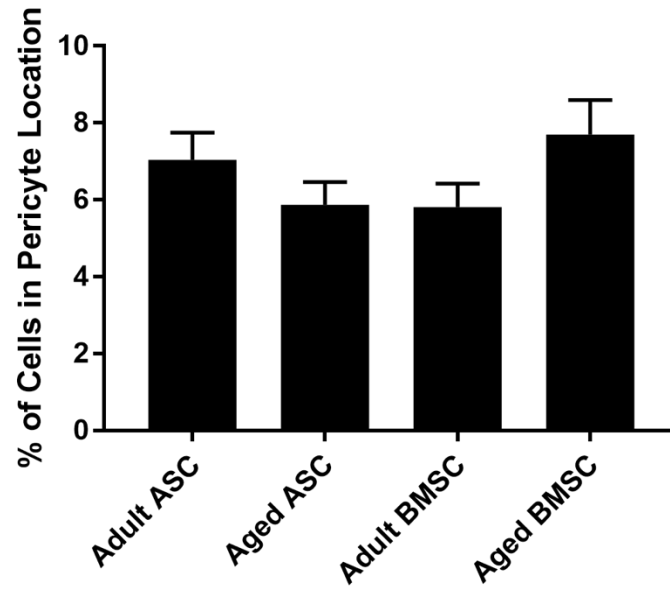


Figure 4.9 Average percent incorporation of stem cells from experimental groups into microvascular networks. One-way ANOVA did not show a significant difference between adult ASC, aged ASC, adult BMSC, and aged BMSC groups. The average pericyte differentiation rate remained close across different groups ($7.04 \pm 0.71\%$ for Adult ASCs, $5.87 \pm 0.60\%$ for Aged ASCs, $5.82 \pm 0.61\%$ for Adult BMSCs, $7.70 \pm 0.91\%$ for Aged BMSCs). Values are averages \pm SEM.

4.3.4. Angiogenic Response to MSCs

FITC-lectin labeling visualized the microvascular structures within the mesentery tissue on day 5. The correlation studies showed a positive moderate ($r = 0.40$) relationship between the number of capillary sprouts after co-culture with the number of stem cell incorporated into the networks in pericyte locations. However, the number of vessel segments had a weak positive relationship with the number of stem cell incorporated into the networks in pericyte locations ($r = 0.29$) (Fig. 4.10). Additional tests were carried out to learn more about the relationship between angiogenesis and stem cell incorporation. The capillary sprout dataset was divided into two categories based on whether the incorporation rate was above 15% or not. Additional tests revealed a strong positive relationship between the number of capillary sprouts after co-culture with stem cell incorporation when the incorporation rate is below 15% ($r = 0.56$), and a strong negative relationship between the number of capillary sprouts and stem cell incorporation when the incorporation rate is above 15% ($r = -0.50$).

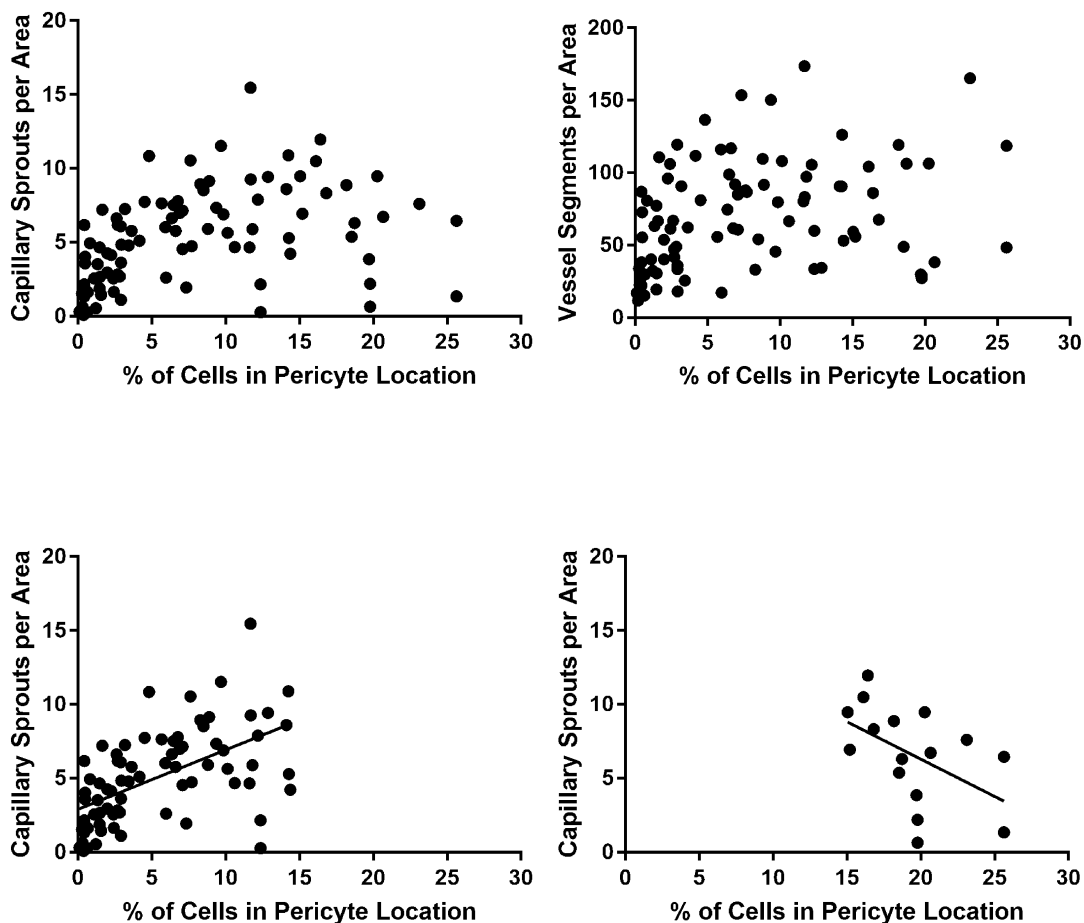


Figure 4.10 Angiogenic response to presence of stem cells. For angiogenesis studies, the number of capillary sprouts per area and the number of vessel segments per area were quantified in each tissue and plotted against the percent incorporation rate from the same tissue. The Person's correlation coefficient was calculated for linear correlation studies between angiogenic metrics and percent incorporation rate. For capillary sprouts (A), a positive moderate ($r = 0.40$) relationship was detected, but for vessel segments, the relationship was weak ($r = 0.29$, B). Based on the data distribution for capillary sprouts, additional tests were carried out for incorporation rates below and above 15%. The analysis showed a strong positive relationship ($r = 0.56$) for incorporation rates below 15%, and a strong negative relationship for incorporation rates above 15% ($r = -0.50$, D). Values are averages per tissue.

4.4. DISCUSSION

Our third aim establishes the rat mesentery culture model as a new platform for studying stem cell fate in a microvascular setting. Taking advantage of the model introduced in aim one, we developed a model that can be used for studying stem cell migration within a microvascular network, stem cell differentiation into vascular cells such as pericytes, and the angiogenic effects of stem cells on mesentery tissue. This study also showed that this model can be used to examine the implications of using stem cells from different sources, donors, and age groups. Additionally, our findings highlight the importance of donor studies, especially in stem cell investigations, by showing the variability across different donors.

In our study, we used the rat mesentery tissue as a conducive environment for vascular differentiation. As it was mentioned in previous chapters, rat mesentery tissue is a very thin translucent tissue that contains different vascular cell types and systems. This gives us an excellent opportunity to study the interactions of stem cells with microvascular networks and the cellular dynamics present in an intact microvascular system. The time-lapse capability of our model also enables the tracking of the stem cells' movement over time (Fig. 4.3 and 4.4), which is not possible with *in vivo* models. *In vitro* models, on the other hand, while extremely valuable for studying signaling pathways [46], are not capable of replicating the complexities of a realistic microvascular environment. Attempts at mimicking the microvascular environment has led to developing other *ex vivo* models, but finding a suitable candidate with different systems and cell types present has been proven difficult. For example, aortic and lymphatic ring

assays do not allow for capillary sprouting and growth from an intact network [49,109], and retina does not contain lymphatics [110].

Stem cells from 32 donors were selected for this project and used to generate differentiation data. The concept of using multiple donors to investigate cellular responses is a common practice [111-113]. The stem cell differentiation studies often use stem cells from multiple donors, usually 3 to 5, and report the average differentiation values to eliminate the donor-specific cellular responses [114,115]. However, using 8 different donors per cell group was justified to create a bigger pool of donors, and thus normalize the donor-specific responses to a higher degree. Multiple cell donors can also be used when the number of cells isolated from one donor is not enough [116], but that was not a concern in this study.

To reduce the variability in stem cell response in different donors, recent work by Bodle et al. has proposed creating a superlot, a collection of stem cells from different donors mixed and cultured together, instead of selecting individual donors for stem cell isolation [117]. The results showed a normalization in cellular responses from the superlot cells compared to individual donors. Even though our study was not conducted following the method described, we suspect the high number of stem cell donors and reporting the average values of cellular responses, such as differentiation into pericytes or angiogenic effects, served as another way to dissociate the reported results from donor-specific responses.

There have been speculations about the identity link between MSCs and pericytes. In a paper published by Crisan et al., the link between MSCs and vascular pericytes was investigated and it was concluded that pericytes give rise to multipotent progenitor cells

similar to MSCs. Several tissues were harvested from human organs including skeletal muscle, pancreas, adipose tissue, fetal myocardium, and placenta, and pericytes were identified based on marker expressions. Pericyte marker expressions were observed after these pericytes were isolated and cultured for long term, but the cells also displayed all recognized markers of MSCs [118]. In another study, da Silva Meirelles et al. discussed the mutual expressed markers in pericyte and MSCs and showed evidence of perivascular location for MSCs, linking MSCs to pericytes [119]. These reports have compelled prominent researchers in the field to suggest that MSCs are pericytes [120]. Even though these accounts imply a common identity for pericytes and MSCs, none of these studies have been carried out in an *ex vivo* scenario, in which interactions between MSCs and microvascular networks are possible. Also, immunolabeling done in our study to identify pericyte markers, such as NG2 and alpha-SMA, revealed that not all MSCs, exogenously delivered to the co-cultures, express common pericyte markers. Moreover, the idea of a common identity in MSCs and pericytes has been challenged in recent years as it's been shown that the common MSC characteristics shown by pericytes are by-products of the *in vitro* culture environment. The same study provided evidence to show that even though pericytes behave as MSCs in *in vitro* scenarios, the resident pericytes in *in vivo* scenarios did not contribute to other cell lineages, so they cannot be considered as multipotent tissue-resident progenitor cells [121]. More genetic and functional studies are needed to provide a definitive answer to when and how MSCs exhibit pericyte characteristics and vice versa.

In this study, we did not detect a significant difference between adult and aged subpopulations of stem cells in differentiation to pericytes. Aging is a complex

phenomenon and the exact effects of aging on different tissue-resident stem cell populations is still a point of debate. As it was mentioned in 4.1., aging in stem cells is generally associated with upregulation of genes linked with senescence, but the lack of models that are capable of testing stem cells and their functions in appropriate settings has made it difficult to provide evidence for aging's direct influence on stem cell behaviors [122]. The comparisons between ASCs and BMSCs also showed no significant differences. However, the variance was higher in aged subpopulations compared to adult, with aged BMSCs being the highest (data not shown). The average rates for incorporation were all relatively close and between 5.82 to 7.07%. These reported pericyte incorporation rates are similar to the ones previously reported using *in vivo* models [33,37]. For example, in a study done using human ASCs, in which the cell suspension was injected into the vitreous of mice to investigate the incorporation of delivered stem cells into the retina, 3.08% of the initial cells were found engrafted into the retina after 8 weeks [33]. Our preliminary studies did not show any MSC differentiation into the pericyte by day 3. Our images also did not show stem cell incorporation into large arterioles, venules, or lymphatics (data not shown).

This study presents new insights into the relationship between angiogenesis and stem cell incorporation into the networks. A positive strong relationship between the number of capillary sprouts and incorporated cells below 15% was detected, but for cell incorporation above 15% the relationship turned negative. One explanation for this phenomenon could be the fact that pericytes could both promote angiogenesis and stabilize vessels. Pericyte incorporation at lower rates could be accompanied by stronger angiogenic cues via cell and cytokine signaling, whereas higher pericyte incorporation

could lead to a more stabilized state of the microvascular networks. Conversely, this could be caused by possible signals from highly angiogenic microvascular networks to the stem cells, stopping them from incorporating into these vessels and thus resolving the growth. This speculation is supported in our study by observation of regions of interest for stem cells within the microvascular networks. Figure 4.11 is an example of a region with high angiogenesis and low stem cell incorporation and displays an imaginary border between the angiogenic dense network with low cell count, and the non-angiogenic region with high cell count. Further studies, however, are needed to shed more lights on this matter and identify new trends in angiogenesis in the presence of stem cells.

In summary, this study establishes the rat mesentery tissue culture model as a platform for tracking stem cells in a microvascular setting for stem cell therapy applications. In addition to studying stem cell migration patterns using time-lapse imaging, this model offers an unmatched view of stem cell differentiation within a microvascular network. Taking advantage of this model, we confirmed the perivascular location, morphology, and phenotype in a subset of MSCs, and reported no significant differences in incorporation rate between our experimental groups. We also showed that the angiogenic effects of stem cells could be more nuanced than previously reported.

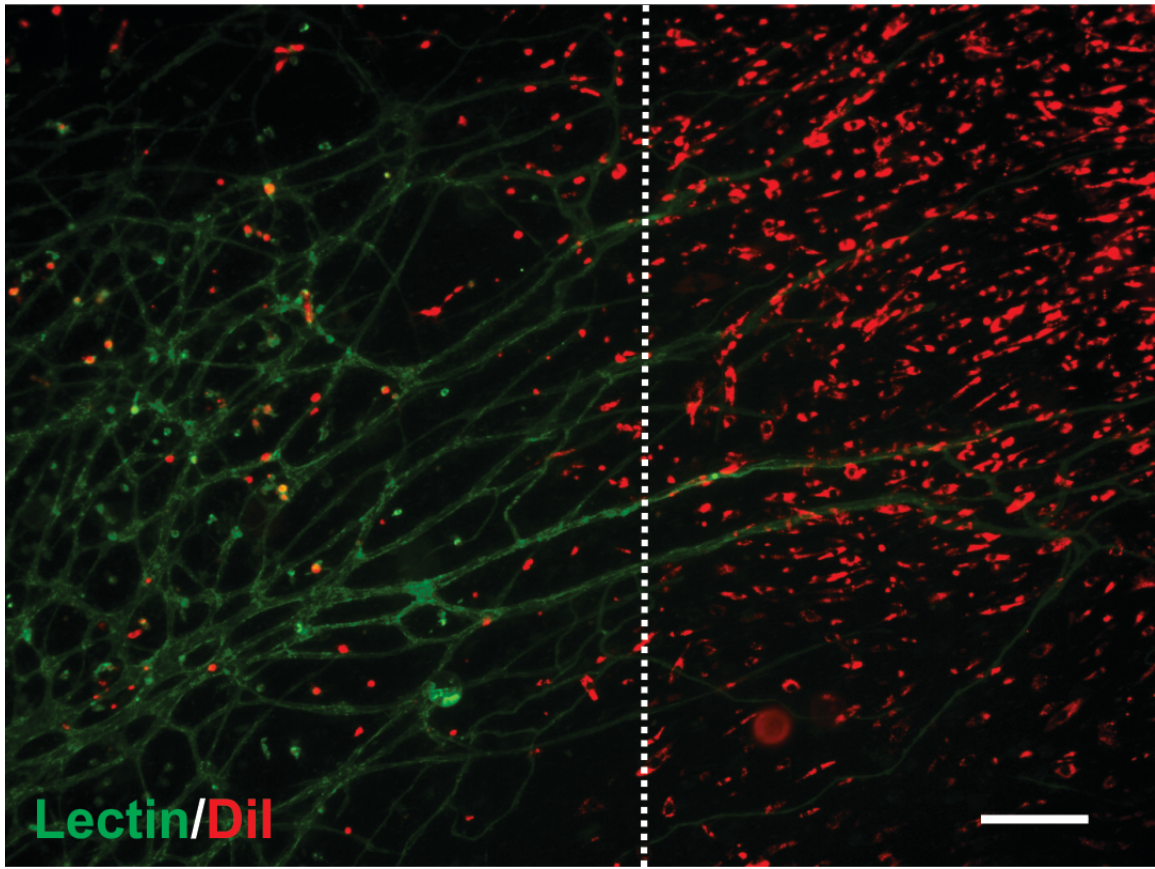


Figure 4.11 Regions of interest for MSCs in mesentery tissues. MSCs seeded on top of the mesentery are concentrated on the right side of the image. The dotted line highlights the border between the highly angiogenic region with few cells, and the non-angiogenic region with high density of MSCs. Scale bar =100 μm .

4.5. FUTURE STUDIES

As mentioned in Chapter 1, stem cell therapy applications served as a motivation for this study, because there is a need to find the stem cell type with the highest efficiency for various treatments, such as diabetic retinopathy. A proposed future study could be done following the protocol introduced in this study substituting the mesentery from healthy rats with mesentery from diseased rats, e.g. diabetic. This would create an environment closer to the real-life scenario and would provide valuable information about how a microvascular network in a diabetic tissue interacts with exogenously delivered MSCs.

The scope of our angiogenesis study was not as wide as our stem cell incorporation study. Future work with a larger sample size could be carried out to learn more about the relationship between stem cell differentiation into pericytes and angiogenesis, and the regions of interest for stem cell migration.

We recognize that cells from multiple donors do not interact with each other in our model, as they are co-cultured with mesentery tissue separately, thus eliminating the opportunity for them to establish intracellular dynamics with cells from other donors. This could serve as the motivation for future studies into creating an MSCs superlot instead of using cell individual donors. This will help identify the effects of superlot MSCs on pericyte differentiation rate in the rat mesentery culture model.

We have done preliminary experiments on the effects of stem cell pretreatment with pro-pericyte cytokines, such as TGF β . Further studies with pretreatment could help

us determine new ways to increase the pericyte differentiation rate of MSCs, which would be helpful for stem cell therapy applications.

CHAPTER 5: CONCLUSIONS

From regeneration of infarcted tissues and starving cancerous cells in malignant tumors, to creating new vascularized tissue constructs capable of growing and functioning independently, successfully manipulating the microvascular growth and remodeling represents an emerging therapeutic approach. To achieve this goal, it's imperative to study angiogenesis in a setting that matches the complexity and intricacies of the *in vivo* scenario. Endothelial cells, pericytes, smooth muscle cells, neurons, interstitial cells, resident progenitor cells, etc., all play important roles in microvascular homeostasis as well as growth, yet often existing angiogenesis models fall short of accounting for the contribution made by these cells to the remodeling of existing microvessel structures. This dissertation offers a novel experimental platform that incorporates this needed multi-cellular/system complexity and demonstrates its use for time-lapse observation and therapeutic evaluation.

This goal compelled us to carry out the first aim, and to develop a rat mesentery culture model with time-lapse imaging capability. We validated our model and showed that it can be used to study endothelial cell dynamics, such as vascular island incorporation, and endothelial cell plasticity. The complexity of a microvascular setting in our model coupled with time-lapse imaging, presented us a very powerful tool for better understanding the microvascular dynamics and how different cellular players

communicate with each other. The ability to study tissue-specific angiogenesis using a time-lapse method will provide us with a great opportunity to learn more about the interactions between different cells and vessels with each other, as well as with chemical and mechanical cues introduced in a microvascular setting. In this dissertation, we demonstrated the value of this capability by discovering two new endothelial cell dynamics in an adult setting: vascular island incorporation and lymphatic/blood endothelial cell plasticity. This manifested itself in our second aim where we used our model for anti-angiogenic drug testing and showed the capability to evaluate dose-dependent responses from microvascular networks. For our last aim, we modified our model to study stem cell fate and track exogenously delivered MSCs within a network. This third aim also demonstrated differentiation of stem cells into vascular pericytes, investigated the effects of stem cell incorporation on angiogenesis, and noted different patterns in stem cell migration.

Our findings introduce the rat mesentery culture model as a promising tool to study angiogenesis, microvascular dynamics, anti-cancer drugs, and stem cell fate within a microvascular network, and underscore the significance of more complex approaches to interpret and observe physiological phenomena in a microvascular setting. To our knowledge, we do not know of another *ex vivo* model that can match the advantages of our rat mesentery culture model. Thus, we foresee this dissertation as advancing the field of vascular biology and biomedical engineering.

LIST OF REFERENCES

1. Stapor PC, Murfee WL (2012) Spatiotemporal distribution of neurovascular alignment in remodeling adult rat mesentery microvascular networks. *J Vasc Res* 49 (4):299-308. doi:10.1159/000336714
2. Larrivee B, Freitas C, Suchting S, Brunet I, Eichmann A (2009) Guidance of vascular development: lessons from the nervous system. *Circ Res* 104 (4):428-441. doi:10.1161/CIRCRESAHA.108.188144
3. Carmeliet P, Tessier-Lavigne M (2005) Common mechanisms of nerve and blood vessel wiring. *Nature* 436 (7048):193-200. doi:10.1038/nature03875
4. Flamme I, Frolich T, Risau W (1997) Molecular mechanisms of vasculogenesis and embryonic angiogenesis. *J Cell Physiol* 173 (2):206-210. doi:10.1002/(SICI)1097-4652(199711)173:2<206::AID-JCP22>3.0.CO;2-C
5. Risau W (1997) Mechanisms of angiogenesis. *Nature* 386 (6626):671-674. doi:10.1038/386671a0
6. Tonnesen MG, Feng X, Clark RA (2000) Angiogenesis in wound healing. *J Investig Dermatol Symp Proc* 5 (1):40-46. doi:10.1046/j.1087-0024.2000.00014.x
7. Eming SA, Brachvogel B, Odorisio T, Koch M (2007) Regulation of angiogenesis: wound healing as a model. *Prog Histochem Cytochem* 42 (3):115-170. doi:10.1016/j.proghi.2007.06.001
8. Inoue M, Hager JH, Ferrara N, Gerber HP, Hanahan D (2002) VEGF-A has a critical, nonredundant role in angiogenic switching and pancreatic beta cell carcinogenesis. *Cancer Cell* 1 (2):193-202
9. Nagarsheth N, Wicha MS, Zou W (2017) Chemokines in the cancer microenvironment and their relevance in cancer immunotherapy. *Nat Rev Immunol*. doi:10.1038/nri.2017.49

10. Chung AS, Kowanetz M, Wu X, Zhuang G, Ngu H, Finkle D, Komuves L, Peale F, Ferrara N (2012) Differential drug class-specific metastatic effects following treatment with a panel of angiogenesis inhibitors. *J Pathol* 227 (4):404-416. doi:10.1002/path.4052
11. Chung AS, Lee J, Ferrara N (2010) Targeting the tumour vasculature: insights from physiological angiogenesis. *Nat Rev Cancer* 10 (7):505-514. doi:10.1038/nrc2868
12. Bergers G, Song S (2005) The role of pericytes in blood-vessel formation and maintenance. *Neuro Oncol* 7 (4):452-464. doi:10.1215/S1152851705000232
13. Huang FJ, You WK, Bonaldo P, Seyfried TN, Pasquale EB, Stallcup WB (2010) Pericyte deficiencies lead to aberrant tumor vascularization in the brain of the NG2 null mouse. *Dev Biol* 344 (2):1035-1046. doi:10.1016/j.ydbio.2010.06.023
14. Maniotis AJ, Folberg R, Hess A, Seftor EA, Gardner LM, Pe'er J, Trent JM, Meltzer PS, Hendrix MJ (1999) Vascular channel formation by human melanoma cells in vivo and in vitro: vasculogenic mimicry. *Am J Pathol* 155 (3):739-752. doi:10.1016/S0002-9440(10)65173-5
15. Ponce AM, Price RJ (2003) Angiogenic stimulus determines the positioning of pericytes within capillary sprouts in vivo. *Microvasc Res* 65 (1):45-48
16. Kelly-Goss MR, Winterer ER, Stapor PC, Yang M, Sweat RS, Stallcup WB, Schmid-Schonbein GW, Murfee WL (2012) Cell proliferation along vascular islands during microvascular network growth. *BMC Physiol* 12:7. doi:10.1186/1472-6793-12-7
17. Kelly-Goss MR, Sweat RS, Azimi MS, Murfee WL (2013) Vascular islands during microvascular regression and regrowth in adult networks. *Front Physiol* 4:108. doi:10.3389/fphys.2013.00108
18. Rossi A, Weber E, Sacchi G, Maestrini D, Di Cintio F, Gerli R (2007) Mechanotransduction in lymphatic endothelial cells. *Lymphology* 40 (3):102-113
19. Skobe M, Detmar M (2000) Structure, function, and molecular control of the skin lymphatic system. *J Invest Dermatol Symp Proc* 5 (1):14-19. doi:10.1046/j.1087-0024.2000.00001.x
20. Ji RC (2006) Lymphatic endothelial cells, lymphangiogenesis, and extracellular matrix. *Lymphat Res Biol* 4 (2):83-100. doi:10.1089/lrb.2006.4.83

21. Podgrabinska S, Braun P, Velasco P, Kloos B, Pepper MS, Skobe M (2002) Molecular characterization of lymphatic endothelial cells. *Proc Natl Acad Sci U S A* 99 (25):16069-16074. doi:10.1073/pnas.242401399
22. Dore-Duffy P (2008) Pericytes: pluripotent cells of the blood brain barrier. *Curr Pharm Des* 14 (16):1581-1593
23. Stratman AN, Davis GE (2012) Endothelial cell-pericyte interactions stimulate basement membrane matrix assembly: influence on vascular tube remodeling, maturation, and stabilization. *Microsc Microanal* 18 (1):68-80. doi:10.1017/S1431927611012402
24. Jain RK (2003) Molecular regulation of vessel maturation. *Nat Med* 9 (6):685-693. doi:10.1038/nm0603-685
25. Saunders WB, Bohnsack BL, Faske JB, Anthis NJ, Bayless KJ, Hirschi KK, Davis GE (2006) Coregulation of vascular tube stabilization by endothelial cell TIMP-2 and pericyte TIMP-3. *J Cell Biol* 175 (1):179-191. doi:10.1083/jcb.200603176
26. Hall CN, Reynell C, Gesslein B, Hamilton NB, Mishra A, Sutherland BA, O'Farrell FM, Buchan AM, Lauritzen M, Attwell D (2014) Capillary pericytes regulate cerebral blood flow in health and disease. *Nature* 508 (7494):55-60. doi:10.1038/nature13165
27. Hamilton NB, Attwell D, Hall CN (2010) Pericyte-mediated regulation of capillary diameter: a component of neurovascular coupling in health and disease. *Front Neuroenergetics* 2. doi:10.3389/fnene.2010.00005
28. Kelly-Goss MR, Sweat RS, Stapor PC, Peirce SM, Murfee WL (2014) Targeting pericytes for angiogenic therapies. *Microcirculation* 21 (4):345-357. doi:10.1111/micc.12107
29. Gerhardt H, Betsholtz C (2003) Endothelial-pericyte interactions in angiogenesis. *Cell Tissue Res* 314 (1):15-23. doi:10.1007/s00441-003-0745-x
30. Romeo G, Liu WH, Asnaghi V, Kern TS, Lorenzi M (2002) Activation of nuclear factor-kappaB induced by diabetes and high glucose regulates a proapoptotic program in retinal pericytes. *Diabetes* 51 (7):2241-2248
31. Ejaz S, Chekarova I, Ejaz A, Sohail A, Lim CW (2008) Importance of pericytes and mechanisms of pericyte loss during diabetes retinopathy. *Diabetes Obes Metab* 10 (1):53-63. doi:10.1111/j.1463-1326.2007.00795.x

32. Kramerov AA, Ljubimov AV (2016) Stem cell therapies in the treatment of diabetic retinopathy and keratopathy. *Exp Biol Med (Maywood)* 241 (6):559-568. doi:10.1177/1535370215609692
33. Mendel TA, Clabough EB, Kao DS, Demidova-Rice TN, Durham JT, Zotter BC, Seaman SA, Cronk SM, Rakoczy EP, Katz AJ, Herman IM, Peirce SM, Yates PA (2013) Pericytes derived from adipose-derived stem cells protect against retinal vasculopathy. *PLoS One* 8 (5):e65691. doi:10.1371/journal.pone.0065691
34. Fakhrejahani E, Toi M (2012) Tumor angiogenesis: pericytes and maturation are not to be ignored. *J Oncol* 2012:261750. doi:10.1155/2012/261750
35. Raza A, Franklin MJ, Dudek AZ (2010) Pericytes and vessel maturation during tumor angiogenesis and metastasis. *Am J Hematol* 85 (8):593-598. doi:10.1002/ajh.21745
36. Kalluri R (2003) Basement membranes: structure, assembly and role in tumour angiogenesis. *Nat Rev Cancer* 3 (6):422-433. doi:10.1038/nrc1094
37. Cronk SM, Kelly-Goss MR, Ray HC, Mendel TA, Hoehn KL, Bruce AC, Dey BK, Guendel AM, Tavakol DN, Herman IM, Peirce SM, Yates PA (2015) Adipose-derived stem cells from diabetic mice show impaired vascular stabilization in a murine model of diabetic retinopathy. *Stem Cells Transl Med* 4 (5):459-467. doi:10.5966/sctm.2014-0108
38. Fuchs S, Baffour R, Zhou YF, Shou M, Pierre A, Tio FO, Weissman NJ, Leon MB, Epstein SE, Kornowski R (2001) Transendocardial delivery of autologous bone marrow enhances collateral perfusion and regional function in pigs with chronic experimental myocardial ischemia. *J Am Coll Cardiol* 37 (6):1726-1732
39. Brown AB, Yang W, Schmidt NO, Carroll R, Leishear KK, Rainov NG, Black PM, Breakefield XO, Aboody KS (2003) Intravascular delivery of neural stem cell lines to target intracranial and extracranial tumors of neural and non-neural origin. *Hum Gene Ther* 14 (18):1777-1785. doi:10.1089/104303403322611782
40. Hao C, Shintani S, Shimizu Y, Kondo K, Ishii M, Wu H, Murohara T (2014) Therapeutic angiogenesis by autologous adipose-derived regenerative cells: comparison with bone marrow mononuclear cells. *Am J Physiol Heart Circ Physiol* 307 (6):H869-879. doi:10.1152/ajpheart.00310.2014
41. Yasuhara T, Matsukawa N, Hara K, Yu G, Xu L, Maki M, Kim SU, Borlongan CV (2006) Transplantation of human neural stem cells exerts neuroprotection

in a rat model of Parkinson's disease. *J Neurosci* 26 (48):12497-12511.
doi:10.1523/JNEUROSCI.3719-06.2006

42. Rajashekhar G (2014) Mesenchymal stem cells: new players in retinopathy therapy. *Front Endocrinol (Lausanne)* 5:59. doi:10.3389/fendo.2014.00059

43. Sengupta N, Caballero S, Mames RN, Butler JM, Scott EW, Grant MB (2003) The role of adult bone marrow-derived stem cells in choroidal neovascularization. *Invest Ophthalmol Vis Sci* 44 (11):4908-4913

44. Norrby K (2006) In vivo models of angiogenesis. *J Cell Mol Med* 10 (3):588-612

45. Staton CA, Stribbling SM, Tazzyman S, Hughes R, Brown NJ, Lewis CE (2004) Current methods for assaying angiogenesis in vitro and in vivo. *Int J Exp Pathol* 85 (5):233-248. doi:10.1111/j.0959-9673.2004.00396.x

46. Kaunas R, Kang H, Bayless KJ (2011) Synergistic Regulation of Angiogenic Sprouting by Biochemical Factors and Wall Shear Stress. *Cell Mol Bioeng* 4 (4):547-559. doi:10.1007/s12195-011-0208-5

47. Song JW, Munn LL (2011) Fluid forces control endothelial sprouting. *Proc Natl Acad Sci U S A* 108 (37):15342-15347. doi:10.1073/pnas.1105316108

48. Chen WC, Baily JE, Corselli M, Diaz ME, Sun B, Xiang G, Gray GA, Huard J, Peault B (2015) Human myocardial pericytes: multipotent mesodermal precursors exhibiting cardiac specificity. *Stem Cells* 33 (2):557-573. doi:10.1002/stem.1868

49. Nicosia RF, Ottinetti A (1990) Growth of microvessels in serum-free matrix culture of rat aorta. A quantitative assay of angiogenesis in vitro. *Lab Invest* 63 (1):115-122

50. Sawamiphak S, Ritter M, Acker-Palmer A (2010) Preparation of retinal explant cultures to study ex vivo tip endothelial cell responses. *Nat Protoc* 5 (10):1659-1665. doi:10.1038/nprot.2010.130

51. Unoki N, Murakami T, Ogino K, Nukada M, Yoshimura N (2010) Time-lapse imaging of retinal angiogenesis reveals decreased development and progression of neovascular sprouting by anecortave desacetate. *Invest Ophthalmol Vis Sci* 51 (5):2347-2355. doi:10.1167/iovs.09-4158

52. Aref AR, Huang RY, Yu W, Chua KN, Sun W, Tu TY, Bai J, Sim WJ, Zervantonakis IK, Thiery JP, Kamm RD (2013) Screening therapeutic EMT blocking agents in a three-dimensional microenvironment. *Integr Biol (Camb)* 5 (2):381-389. doi:10.1039/c2ib20209c
53. Carmeliet P (2005) Angiogenesis in life, disease and medicine. *Nature* 438 (7070):932-936. doi:10.1038/nature04478
54. Carmeliet P, Jain RK (2000) Angiogenesis in cancer and other diseases. *Nature* 407 (6801):249-257. doi:10.1038/35025220
55. Adams RH, Alitalo K (2007) Molecular regulation of angiogenesis and lymphangiogenesis. *Nat Rev Mol Cell Biol* 8 (6):464-478. doi:10.1038/nrm2183
56. Chan JM, Zervantonakis IK, Rimchala T, Polacheck WJ, Whisler J, Kamm RD (2012) Engineering of in vitro 3D capillary beds by self-directed angiogenic sprouting. *PLoS One* 7 (12):e50582. doi:10.1371/journal.pone.0050582
57. Peirce SM, Mac Gabhann F, Bautch VL (2012) Integration of experimental and computational approaches to sprouting angiogenesis. *Curr Opin Hematol* 19 (3):184-191. doi:10.1097/MOH.0b013e3283523ea6
58. Stapor PC, Azimi MS, Ahsan T, Murfee WL (2013) An angiogenesis model for investigating multicellular interactions across intact microvascular networks. *Am J Physiol Heart Circ Physiol* 304 (2):H235-245. doi:10.1152/ajpheart.00552.2012
59. Yang M, Stapor PC, Peirce SM, Betancourt AM, Murfee WL (2012) Rat mesentery exteriorization: a model for investigating the cellular dynamics involved in angiogenesis. *J Vis Exp* (63):e3954. doi:10.3791/3954
60. Robichaux JL, Tanno E, Rappleye JW, Ceballos M, Stallcup WB, Schmid-Schonbein GW, Murfee WL (2010) Lymphatic/Blood endothelial cell connections at the capillary level in adult rat mesentery. *Anat Rec (Hoboken)* 293 (10):1629-1638. doi:10.1002/ar.21195
61. Sweat RS, Stapor PC, Murfee WL (2012) Relationships between lymphangiogenesis and angiogenesis during inflammation in rat mesentery microvascular networks. *Lymphat Res Biol* 10 (4):198-207. doi:10.1089/lrb.2012.0014
62. Hao X, Silva EA, Mansson-Broberg A, Grinnemo KH, Siddiqui AJ, Dellgren G, Wardell E, Brodin LA, Mooney DJ, Sylven C (2007) Angiogenic effects of sequential

release of VEGF-A165 and PDGF-BB with alginate hydrogels after myocardial infarction. *Cardiovasc Res* 75 (1):178-185. doi:10.1016/j.cardiores.2007.03.028

63. Skalak TC, Price RJ (1996) The role of mechanical stresses in microvascular remodeling. *Microcirculation* 3 (2):143-165

64. Milkiewicz M, Brown MD, Egginton S, Hudlicka O (2001) Association between shear stress, angiogenesis, and VEGF in skeletal muscles in vivo. *Microcirculation* 8 (4):229-241. doi:10.1038/sj/mn/7800074

65. Hsu YH, Moya ML, Abiri P, Hughes CC, George SC, Lee AP (2013) Full range physiological mass transport control in 3D tissue cultures. *Lab Chip* 13 (1):81-89. doi:10.1039/c2lc40787f

66. Oliver G, Srinivasan RS (2010) Endothelial cell plasticity: how to become and remain a lymphatic endothelial cell. *Development* 137 (3):363-372. doi:10.1242/dev.035360

67. Abtahian F, Guerriero A, Sebzda E, Lu MM, Zhou R, Mocsai A, Myers EE, Huang B, Jackson DG, Ferrari VA, Tybulewicz V, Lowell CA, Lepore JJ, Koretzky GA, Kahn ML (2003) Regulation of blood and lymphatic vascular separation by signaling proteins SLP-76 and Syk. *Science* 299 (5604):247-251. doi:10.1126/science.1079477

68. Johnson NC, Dillard ME, Baluk P, McDonald DM, Harvey NL, Frase SL, Oliver G (2008) Lymphatic endothelial cell identity is reversible and its maintenance requires Prox1 activity. *Genes Dev* 22 (23):3282-3291. doi:10.1101/gad.1727208

69. D'Amico G, Jones DT, Nye E, Sapienza K, Ramjuan AR, Reynolds LE, Robinson SD, Kostourou V, Martinez D, Aubyn D, Grose R, Thomas GJ, Spencer-Dene B, Zicha D, Davies D, Tybulewicz V, Hodivala-Dilke KM (2009) Regulation of lymphatic-blood vessel separation by endothelial Rac1. *Development* 136 (23):4043-4053. doi:10.1242/dev.035014

70. Lin CI, Chen CN, Huang MT, Lee SJ, Lin CH, Chang CC, Lee H (2008) Lysophosphatidic acid up-regulates vascular endothelial growth factor-C and lymphatic marker expressions in human endothelial cells. *Cell Mol Life Sci* 65 (17):2740-2751. doi:10.1007/s00018-008-8314-9

71. Cooley LS, Handsley MM, Zhou Z, Lafleur MA, Pennington CJ, Thompson EW, Poschl E, Edwards DR (2010) Reversible transdifferentiation of blood vascular endothelial cells to a lymphatic-like phenotype in vitro. *J Cell Sci* 123 (Pt 21):3808-3816. doi:10.1242/jcs.064279

72. Sweat RS, Azimi MS, Suarez-Martinez AD, Katakam P, Murfee WL (2016) Lysophosphatidic acid does not cause blood/lymphatic vessel plasticity in the rat mesentery culture model. *Physiol Rep* 4 (13). doi:10.14814/phy2.12857
73. DiMasi JA, Grabowski HG, Hansen RW (2016) Innovation in the pharmaceutical industry: New estimates of R&D costs. *J Health Econ* 47:20-33. doi:10.1016/j.jhealeco.2016.01.012
74. O'Farrell AM, Abrams TJ, Yuen HA, Ngai TJ, Louie SG, Yee KW, Wong LM, Hong W, Lee LB, Town A, Smolich BD, Manning WC, Murray LJ, Heinrich MC, Cherrington JM (2003) SU11248 is a novel FLT3 tyrosine kinase inhibitor with potent activity in vitro and in vivo. *Blood* 101 (9):3597-3605. doi:10.1182/blood-2002-07-2307
75. Ferrara N, Hillan KJ, Novotny W (2005) Bevacizumab (Avastin), a humanized anti-VEGF monoclonal antibody for cancer therapy. *Biochem Biophys Res Commun* 333 (2):328-335. doi:10.1016/j.bbrc.2005.05.132
76. Mondal D, Pradhan L, Ali M, Agrawal KC (2004) HAART drugs induce oxidative stress in human endothelial cells and increase endothelial recruitment of mononuclear cells: exacerbation by inflammatory cytokines and amelioration by antioxidants. *Cardiovasc Toxicol* 4 (3):287-302
77. Mondal D, Liu K, Hamblin M, Lasky JA, Agrawal KC (2013) Nelfinavir suppresses insulin signaling and nitric oxide production by human aortic endothelial cells: protective effects of thiazolidinediones. *Ochsner J* 13 (1):76-90
78. Bhandarkar SS, Arbiser JL (2007) Curcumin as an inhibitor of angiogenesis. *Adv Exp Med Biol* 595:185-195. doi:10.1007/978-0-387-46401-5_7
79. Mathur A, Abd Elmageed ZY, Liu X, Kostochka ML, Zhang H, Abdel-Mageed AB, Mondal D (2014) Subverting ER-stress towards apoptosis by nelfinavir and curcumin coexposure augments docetaxel efficacy in castration resistant prostate cancer cells. *PLoS One* 9 (8):e103109. doi:10.1371/journal.pone.0103109
80. Tugues S, Fernandez-Varo G, Munoz-Luque J, Ros J, Arroyo V, Rodes J, Friedman SL, Carmeliet P, Jimenez W, Morales-Ruiz M (2007) Antiangiogenic treatment with sunitinib ameliorates inflammatory infiltrate, fibrosis, and portal pressure in cirrhotic rats. *Hepatology* 46 (6):1919-1926. doi:10.1002/hep.21921
81. Dib E, Maia M, Lima Ade S, de Paula Fiod Costa E, de Moraes-Filho MN, Rodrigues EB, Penha FM, Coppini LP, de Barros NM, Coimbra Rde C, Magalhaes Junior O, Guerra T, Furlani Bde A, Freymuller E, Farah ME (2012) In vivo, in vitro toxicity and

in vitro angiogenic inhibition of sunitinib malate. *Curr Eye Res* 37 (7):567-574. doi:10.3109/02713683.2011.635916

82. Osusky KL, Hallahan DE, Fu A, Ye F, Shyr Y, Geng L (2004) The receptor tyrosine kinase inhibitor SU11248 impedes endothelial cell migration, tubule formation, and blood vessel formation in vivo, but has little effect on existing tumor vessels. *Angiogenesis* 7 (3):225-233. doi:10.1007/s10456-004-3149-y

83. Pore N, Gupta AK, Cerniglia GJ, Jiang Z, Bernhard EJ, Evans SM, Koch CJ, Hahn SM, Maity A (2006) Nelfinavir down-regulates hypoxia-inducible factor 1alpha and VEGF expression and increases tumor oxygenation: implications for radiotherapy. *Cancer Res* 66 (18):9252-9259. doi:10.1158/0008-5472.CAN-06-1239

84. Bimonte S, Barbieri A, Palma G, Luciano A, Rea D, Arra C (2013) Curcumin inhibits tumor growth and angiogenesis in an orthotopic mouse model of human pancreatic cancer. *Biomed Res Int* 2013:810423. doi:10.1155/2013/810423

85. Lennernas B, Albertsson P, Damber JE, Norrby K (2004) Antiangiogenic effect of metronomic paclitaxel treatment in prostate cancer and non-tumor tissue in the same animals: a quantitative study. *APMIS* 112 (3):201-209. doi:10.1111/j.1600-0463.2004.apm1120306.x

86. Albertsson P, Lennernas B, Norrby K (2012) Low-dosage metronomic chemotherapy and angiogenesis: topoisomerase inhibitors irinotecan and mitoxantrone stimulate VEGF-A-mediated angiogenesis. *APMIS* 120 (2):147-156. doi:10.1111/j.1600-0463.2011.02830.x

87. Galie PA, Nguyen DH, Choi CK, Cohen DM, Janmey PA, Chen CS (2014) Fluid shear stress threshold regulates angiogenic sprouting. *Proc Natl Acad Sci U S A* 111 (22):7968-7973. doi:10.1073/pnas.1310842111

88. Wilting J, Christ B, Bokeloh M (1991) A modified chorioallantoic membrane (CAM) assay for qualitative and quantitative study of growth factors. Studies on the effects of carriers, PBS, angiogenin, and bFGF. *Anat Embryol (Berl)* 183 (3):259-271

89. Olivo M, Bhardwaj R, Schulze-Osthoff K, Sorg C, Jacob HJ, Flamme I (1992) A comparative study on the effects of tumor necrosis factor-alpha (TNF-alpha), human angiogenic factor (h-AF) and basic fibroblast growth factor (bFGF) on the chorioallantoic membrane of the chick embryo. *Anat Rec* 234 (1):105-115. doi:10.1002/ar.1092340112

90. Buijsen J, Lammering G, Jansen RL, Beets GL, Wals J, Sosef M, Den Boer MO, Leijtens J, Riedl RG, Theys J, Lambin P (2013) Phase I trial of the combination of

the Akt inhibitor nelfinavir and chemoradiation for locally advanced rectal cancer. *Radiother Oncol* 107 (2):184-188. doi:10.1016/j.radonc.2013.03.023

91. Fernandez-Aviles F, San Roman JA, Garcia-Frade J, Fernandez ME, Penarrubia MJ, de la Fuente L, Gomez-Bueno M, Cantalapiedra A, Fernandez J, Gutierrez O, Sanchez PL, Hernandez C, Sanz R, Garcia-Sancho J, Sanchez A (2004) Experimental and clinical regenerative capability of human bone marrow cells after myocardial infarction. *Circ Res* 95 (7):742-748. doi:10.1161/01.RES.0000144798.54040.ed

92. Rafii S, Lyden D (2003) Therapeutic stem and progenitor cell transplantation for organ vascularization and regeneration. *Nat Med* 9 (6):702-712. doi:10.1038/nm0603-702

93. Takahashi K, Tanabe K, Ohnuki M, Narita M, Ichisaka T, Tomoda K, Yamanaka S (2007) Induction of pluripotent stem cells from adult human fibroblasts by defined factors. *Cell* 131 (5):861-872. doi:10.1016/j.cell.2007.11.019

94. Loebinger MR, Eddaoudi A, Davies D, Janes SM (2009) Mesenchymal stem cell delivery of TRAIL can eliminate metastatic cancer. *Cancer Res* 69 (10):4134-4142. doi:10.1158/0008-5472.CAN-08-4698

95. Finkel T, Serrano M, Blasco MA (2007) The common biology of cancer and ageing. *Nature* 448 (7155):767-774. doi:10.1038/nature05985

96. Ashcroft GS, Horan MA, Ferguson MW (1997) The effects of ageing on wound healing: immunolocalisation of growth factors and their receptors in a murine incisional model. *J Anat* 190 (Pt 3):351-365

97. Lopez-Otin C, Blasco MA, Partridge L, Serrano M, Kroemer G (2013) The hallmarks of aging. *Cell* 153 (6):1194-1217. doi:10.1016/j.cell.2013.05.039

98. Yu JM, Wu X, Gimble JM, Guan X, Freitas MA, Bunnell BA (2011) Age-related changes in mesenchymal stem cells derived from rhesus macaque bone marrow. *Aging Cell* 10 (1):66-79. doi:10.1111/j.1474-9726.2010.00646.x

99. Zhou S, Greenberger JS, Epperly MW, Goff JP, Adler C, Leboff MS, Glowacki J (2008) Age-related intrinsic changes in human bone-marrow-derived mesenchymal stem cells and their differentiation to osteoblasts. *Aging Cell* 7 (3):335-343. doi:10.1111/j.1474-9726.2008.00377.x

100. Hou L, Kim JJ, Woo YJ, Huang NF (2016) Stem cell-based therapies to promote angiogenesis in ischemic cardiovascular disease. *Am J Physiol Heart Circ Physiol* 310 (4):H455-465. doi:10.1152/ajpheart.00726.2015
101. Kachgal S, Putnam AJ (2011) Mesenchymal stem cells from adipose and bone marrow promote angiogenesis via distinct cytokine and protease expression mechanisms. *Angiogenesis* 14 (1):47-59. doi:10.1007/s10456-010-9194-9
102. Rehman J, Traktuev D, Li J, Merfeld-Clauss S, Temm-Grove CJ, Bovenkerk JE, Pell CL, Johnstone BH, Considine RV, March KL (2004) Secretion of angiogenic and antiapoptotic factors by human adipose stromal cells. *Circulation* 109 (10):1292-1298. doi:10.1161/01.CIR.0000121425.42966.F1
103. Kondo K, Shintani S, Shibata R, Murakami H, Murakami R, Imaizumi M, Kitagawa Y, Murohara T (2009) Implantation of adipose-derived regenerative cells enhances ischemia-induced angiogenesis. *Arterioscler Thromb Vasc Biol* 29 (1):61-66. doi:10.1161/ATVBAHA.108.166496
104. Traktuev DO, Merfeld-Clauss S, Li J, Kolonin M, Arap W, Pasqualini R, Johnstone BH, March KL (2008) A population of multipotent CD34-positive adipose stromal cells share pericyte and mesenchymal surface markers, reside in a periendothelial location, and stabilize endothelial networks. *Circ Res* 102 (1):77-85. doi:10.1161/CIRCRESAHA.107.159475
105. Strong AL, Bowles AC, MacCrimmon CP, Frazier TP, Lee SJ, Wu X, Katz AJ, Gawronska-Kozak B, Bunnell BA, Gimble JM (2015) Adipose stromal cells repair pressure ulcers in both young and elderly mice: potential role of adipogenesis in skin repair. *Stem Cells Transl Med* 4 (6):632-642. doi:10.5966/sctm.2014-0235
106. Phamduy TB, Sweat RS, Azimi MS, Burow ME, Murfee WL, Chrisey DB (2015) Printing cancer cells into intact microvascular networks: a model for investigating cancer cell dynamics during angiogenesis. *Integr Biol (Camb)* 7 (9):1068-1078. doi:10.1039/c5ib00151j
107. Burks HE, Phamduy TB, Azimi MS, Saksena J, Burow ME, Collins-Burow BM, Chrisey DB, Murfee WL (2016) Laser Direct-Write Onto Live Tissues: A Novel Model for Studying Cancer Cell Migration. *J Cell Physiol* 231 (11):2333-2338. doi:10.1002/jcp.25363
108. Cohen J (1988) *Statistical power analysis for the behavioral sciences*. 2nd edn. L. Erlbaum Associates, Hillsdale, N.J.

109. Bruyere F, Noel A (2010) Lymphangiogenesis: in vitro and in vivo models. *FASEB J* 24 (1):8-21. doi:10.1096/fj.09-132852
110. Chen L (2009) Ocular lymphatics: state-of-the-art review. *Lymphology* 42 (2):66-76
111. Phinney DG, Kopen G, Righter W, Webster S, Tremain N, Prockop DJ (1999) Donor variation in the growth properties and osteogenic potential of human marrow stromal cells. *J Cell Biochem* 75 (3):424-436
112. Siddappa R, Licht R, van Blitterswijk C, de Boer J (2007) Donor variation and loss of multipotency during in vitro expansion of human mesenchymal stem cells for bone tissue engineering. *J Orthop Res* 25 (8):1029-1041. doi:10.1002/jor.20402
113. Sundelacruz S, Levin M, Kaplan DL (2015) Comparison of the depolarization response of human mesenchymal stem cells from different donors. *Sci Rep* 5:18279. doi:10.1038/srep18279
114. Krawiec JT, Weinbaum JS, Liao HT, Ramaswamy AK, Pezzone DJ, Josowitz AD, D'Amore A, Rubin JP, Wagner WR, Vorp DA (2016) In Vivo Functional Evaluation of Tissue-Engineered Vascular Grafts Fabricated Using Human Adipose-Derived Stem Cells from High Cardiovascular Risk Populations. *Tissue Eng Part A* 22 (9-10):765-775. doi:10.1089/ten.TEA.2015.0379
115. Maria AT, Toupet K, Maumus M, Fonteneau G, Le Quellec A, Jorgensen C, Guilpain P, Noel D (2016) Human adipose mesenchymal stem cells as potent anti-fibrosis therapy for systemic sclerosis. *J Autoimmun* 70:31-39. doi:10.1016/j.jaut.2016.03.013
116. Shapiro AM, Lakey JR, Ryan EA, Korbitt GS, Toth E, Warnock GL, Kneteman NM, Rajotte RV (2000) Islet transplantation in seven patients with type 1 diabetes mellitus using a glucocorticoid-free immunosuppressive regimen. *N Engl J Med* 343 (4):230-238. doi:10.1056/NEJM200007273430401
117. Bodle JC, Teeter SD, Hluck BH, Hardin JW, Bernacki SH, Lobo EG (2014) Age-related effects on the potency of human adipose-derived stem cells: creation and evaluation of superlots and implications for musculoskeletal tissue engineering applications. *Tissue Eng Part C Methods* 20 (12):972-983. doi:10.1089/ten.TEC.2013.0683
118. Crisan M, Yap S, Casteilla L, Chen CW, Corselli M, Park TS, Andriolo G, Sun B, Zheng B, Zhang L, Norotte C, Teng PN, Traas J, Schugar R, Deasy BM, Badylak

S, Buhring HJ, Giacobino JP, Lazzari L, Huard J, Peault B (2008) A perivascular origin for mesenchymal stem cells in multiple human organs. *Cell Stem Cell* 3 (3):301-313. doi:10.1016/j.stem.2008.07.003

119. da Silva Meirelles L, Caplan AI, Nardi NB (2008) In search of the in vivo identity of mesenchymal stem cells. *Stem Cells* 26 (9):2287-2299. doi:10.1634/stemcells.2007-1122

120. Caplan AI (2008) All MSCs are pericytes? *Cell Stem Cell* 3 (3):229-230. doi:10.1016/j.stem.2008.08.008

121. Guimaraes-Camboa N, Cattaneo P, Sun Y, Moore-Morris T, Gu Y, Dalton ND, Rockenstein E, Masliah E, Peterson KL, Stallcup WB, Chen J, Evans SM (2017) Pericytes of Multiple Organs Do Not Behave as Mesenchymal Stem Cells In Vivo. *Cell Stem Cell* 20 (3):345-359 e345. doi:10.1016/j.stem.2016.12.006

122. Sharpless NE, DePinho RA (2007) How stem cells age and why this makes us grow old. *Nat Rev Mol Cell Biol* 8 (9):703-713. doi:10.1038/nrm2241

BIOGRAPHY

Mohammad Sadegh Azimi was born on May 19th, 1986 in Tehran, Iran. He earned his Bachelor's degree in 2008, and his Master's degree in 2010, both in biomedical engineering at Amirkabir University of Technology (Tehran Polytechnic) in Iran. He joined the Microvascular Dynamics Laboratory at Tulane University in 2011 to pursue a PhD in biomedical engineering, under the supervision of Dr. Walter Lee Murfee. This dissertation highlights his contributions to the microvascular research field with a focus on microvascular model development, and its applications for drug testing and stem cell tracking.